Synthesis and antiplasmodial structure-activity relationships for some novel 4-aminoquinolines and 5-chlorobenzimidazoles

Master of Science

Johannes Dawid van der Merwe

2004

Supervised by

Professor R. Hunter and Associate Professor T.J. Egan

Department of Chemistry
P D Hahn Building
Upper Campus
University of Cape Town
Rondebosch
7701
South Africa

Abstract

Two novel 7-substituted 4-aminoalkylated quinolines, N^1,N^1-diethyl-N^2-(7-trifuoromethylthio-4-quinolinyl)-1,2-ethanediamine **11** and N^1,N^1-diethyl-N^2-(7-trifuoromethoxy-4-quinolinyl)-1,2-ethanediamine **12** were synthesized via a versatile 6-step route and their antiplasmodial activities against the chloroquine sensitive D10 strain of *Plasmodium falciparum* have been investigated in vitro. A quantitative structure activity analysis of these compounds showed an excellent correlation of log IC_{50}, corrected for vacuolar accumulation, with log β-haematin inhibitory activity when compared with known values for other analogues substituted at the 7-position. The correlation showed a low accumulation-normalised IC_{50} for **11**, which suggests that it is the most potent antimalarial at the site of action of all of the analogues of this type. **11** and **12** however had relatively high observed IC_{50} values compared to the other analogues, which can be attributed to their low pKa_1 values and subsequent low vacuolar accumulation in the parasite. In addition, the benzimidazole nucleus, which has similar dipolar character to 4-aminoquinoline nucleus, was investigated as alternative template for potential antimalarials. This involved the synthesis of the chloroquine-like analogues 2-(5-chlorobenzoimidazol-1-yl)-*N*-(2-diethylaminoethylethanamide **13**, *N*-[2-(5-chlorobenzoimidazol-1-yl)ethyl]-2-(4-methylpiperazin-1-yl)ethanamide **14** and *N*-[2-(5-chlorobenzoimidazol-1-yl)ethyl]-*N*-[2-(4-methylpiperazin-1-yl)ethyl]amine **15**. The latter two products were prepared by a regioselective route to 5-chlorobenzimidazoles. These compounds had poor activity against *P. falciparum* and none showed β-haematin inhibitory activity although their precursor, 5-chloro-1H-benzimidazole, had β-haematin inhibitory activity. Their poor activity was ascribed to this lack of β-haematin inhibitory activity as well as their low pK_a which would result in poor vacuolar accumulation. Finally, the novel side chain *N*-(2-aminoethyl)-2-(4-methylpiperazin-1-yl)ethanamide **14b** incorporated in **14** was coupled to a 7-chloroquinoline nucleus in order to compare the 4-amino-7-chloroquinoline nucleus directly with the 5-chlorobenzimidazole nucleus. Thus, the analogous 4-aminoquinoline *N*-[2-(7-chloro-4-quinolinyl)ethyl]-2-(4-methylpiperazin-1-yl)ethanamide **16** was synthesized. This compound retains anti-plasmodial activity, demonstrating that the lack of activity in **14** and **15** can be ascribed to the replacement of the quinoline nucleus with the benzimidazole nucleus and not to the side chain itself.

Acknowledgements

I want to acknowledge and thank the following people:

Associate Professor Timothy J. Egan for the opportunity to enter this study and for his supportive supervision throughout.

Professor Roger Hunter for his stimulating supervision and input to shape all his students into innovative and competent scientists.

Mr Kanyile Ncokazi for his kind assistance with the physical experimental methods and for the performance of the $BHIA_{50}$ assay.

Mr Donelly van Schalkwyk at the Department of Pharmacology for the IC_{50} assay he performed on numerous target compounds.

All previous and current students in the Organic and Inorganic research groups whom I worked with for their support and advice in the laboratory, which formed a central part of my research training.

Mr John Tsavimbi for his assistance with pKa determinations.

Mr. André de Jager for his quick assistance with alterations to glassware.

The Chemistry Department administration staff for their friendly assistance.

All other support staff at the NMR workstation, water distillation, document binding facilities, workshop and supplies store in the Chemistry Department.

The Department of Chemistry for financial support to attend the SACI 2002 conference in Port Elizabeth and the Frank Warren Organic chemistry conference in Grahamstown in 2003.

The NRF for the grandholders bursary I received for the duration of this study.

Abbreviations

π	lipophilicity constant
α	ratio of AR of compound relative to AR of chloroquine
σ_m	meta-Hammett constant
σ_p	para-Hammett constant
AR	ratio of vacuolar accumulation relative to extra-vacuolar accumulation
BHIA	β-haematin inhibitory activity
$BHIA_{50}$	activity of compound inhibiting 50% of β-haematin formation.
EMME	diethyl ethoxymethylnemalonate
IC_{50}	concentration of compound which kills 50% of a parasite culture
K	drug – haematin association constant
NMR	nucleur magnetic resonance
P. falciparum	*Plasmodium falciparum*
QSAR	quantitative structure-activity relationships
QSARs	quantitative structure-activity relationship studies
SAR	structure-activity relationships
SARs	structure-activity relationship studies
TLC	thin layer chromatography

1. Introduction

The aim of this project was to utilize the antiplasmodial structure activity relationships of 4-aminoquinolines identified by our laboratory in previous studies [1, 2] in the synthesis of novel 4-aminoquinolines. These novel analogues would then contribute further to our understanding of the mode of action of these compounds. The project also investigated an alternative template to the traditional 4-aminoquinoline nucleus, namely 6-chlorobenzimidazole.

1.1. The current malaria situation

Currently malaria places at risk at least 3 billion people globally and between 1 million and 1.5 million people die from the disease annually. Malaria is endemic in the tropics and extends to some part of the subtropics (Figure 1.1). The spread of malaria by humans traveling by air is now an important cause of malaria deaths in non-malarial areas. Fortunately the vector's flight range outside a viable habitat is a maximum of 2 miles, not taking prevailing winds into account.[3]

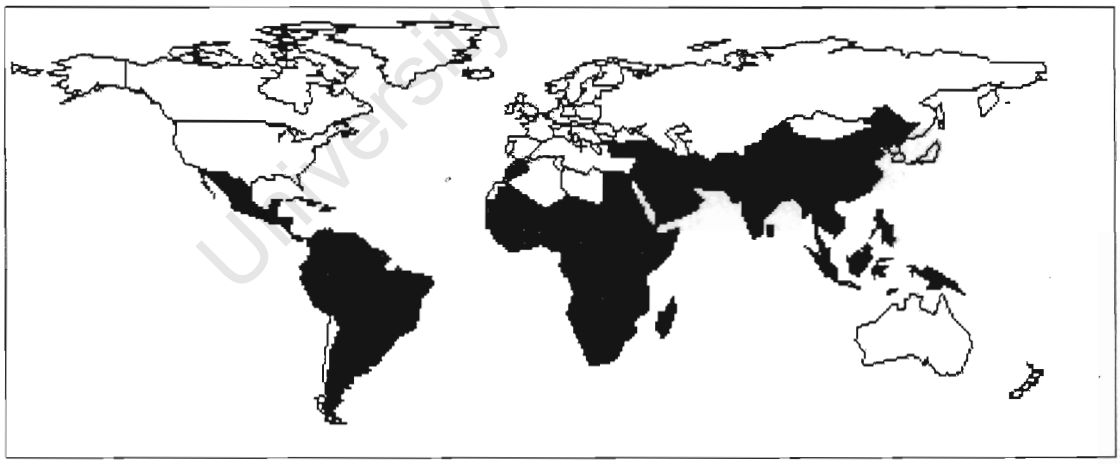

Figure 1.1. A map showing the countries currently affected by indigenous malaria.[3]

The African continent accounted for 80% of malaria cases in 1990 with the remainder clustered in nine countries namely India, Brazil, Afghanistan, Sri-Lanka, Thailand, Indonesia, Vietnam, Cambodia and China. *Plasmodium falciparum* is the predominant

species causing 120 million new cases annually and virtually all malaria deaths. *P. falciparum* has developed drug resistant strains starting in Asia [3] and is now almost universal.

Control and eradication of malaria has three main facets. These are: reducing vector mosquito numbers; protection of humans from vector mosquitoes and the treatment of malaria infected humans to prevent further transmission.

1.2. Biology of Plasmodium parasites and Anopheles Mosquitoes

Malaria is caused by the protozoal parasite *Plasmodium spp*. The life cycle of the Plasmodium genus is divided between a vertebrate host and an insect vector. The most common species are *P.falciparum*, *P.vivax*, *P.ovale* and *P.malariae* of which *P.malariae* is the only species that is not exclusively a parasite of the human. The female Anophelene mosquito is always the vector. Out of the 380 species of Anophelene mosquito, only 60 can be malaria transmitters.

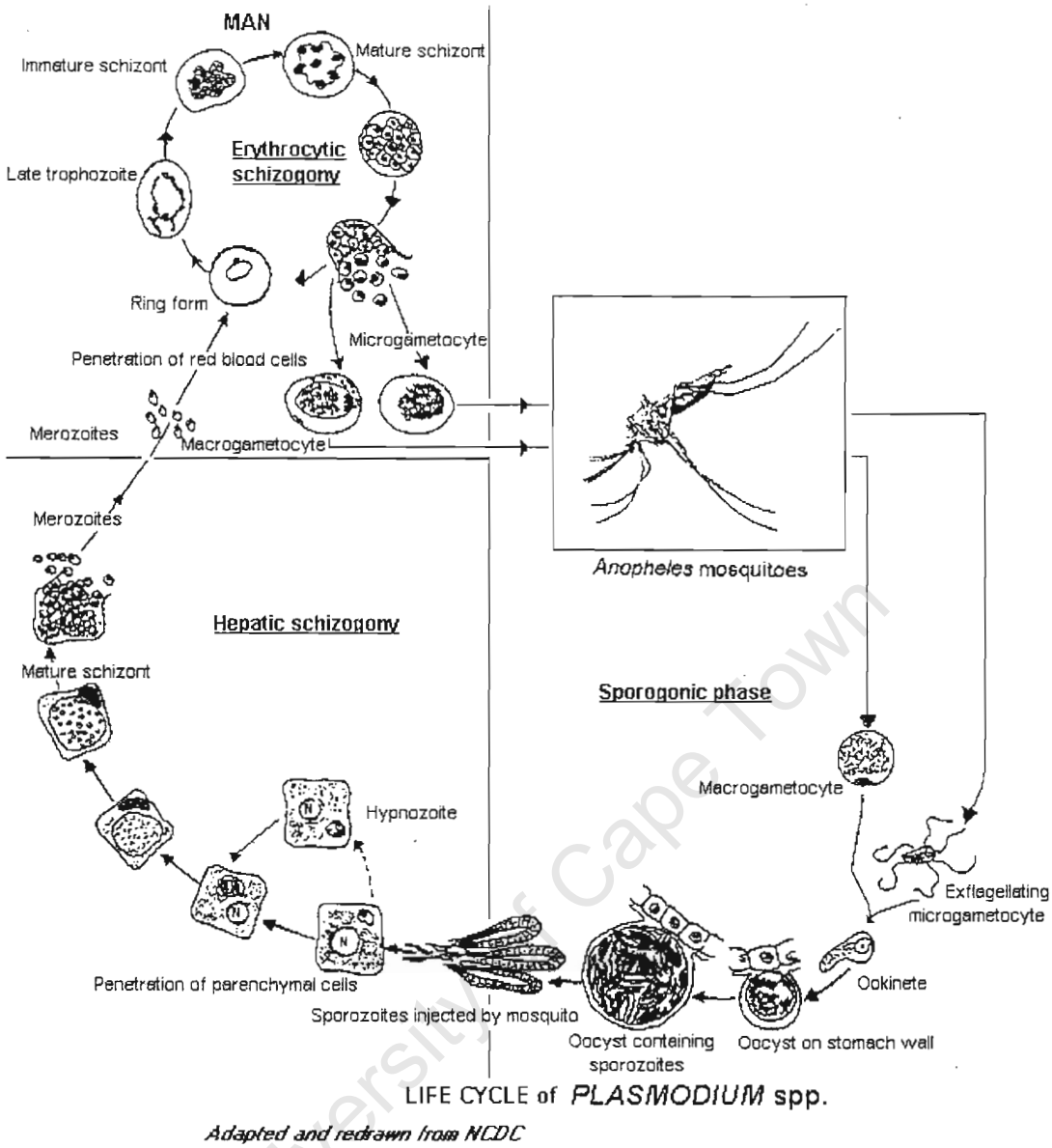

Figure 1.2. The life cycle of *Plasmodium spp* in the human host (hypnozoites do not occur in *P. falciparum*) .[4]

The mosquito injects anticoagulant from its salivary gland to ensure an even flowing blood meal from the host. Sporozoites in the salivary gland of the mosquito are then injected into the host. The sporozoites migrate to the liver and penetrate hepatocytes where during a period of 9-16 days they multiply and then migrate into the bloodstream and invade erythrocytes. Inside the erythrocyte the parasite either develops into merozoites which further reinfect erythrocytes or it develops into micro- and -macrogametocytes which have no further activity in the host. The macro- and microgametocytes can then be ingested by a mosquito. In the mosquito gut

microgametocytes exflagellate and macrogametocytes are fertilized to form ookinetes that penetrate the cell wall of the midgut and develop into oocysts. After sporogony of the oocyst, many sporozoites are formed. The sporozoites then migrate to the salivary gland of the mosquito where they can be injected into a host to complete the life cycle of the parasite (fig 1.2).[4]

1.3. Haem detoxification in *P. falciparum*.

All symptoms of malaria are associated with the blood stages of the parasite [5] and drugs must act strongly against these stages to be efficacious. During the three blood stages (ring, trophozoite and blood schizont) the parasite ingests haemoglobin from the host as a food source.[6] Inside the food vacuole (Figure 1.3.), an acidic compartment in the parasite, the haemoglobin is digested by the specialized enzymes plasmepsins I, II and IV, histo aspartic protease and falcipains I, II and III [7, 8] as well as falcilysin. Haem is released which is then autoxidised to haematin (aquaferriprotoporphyrin IX, H_2O-Fe(III)PPIX), a potential toxin to the parasite.[9, 10] Solubilised haematin is a cytotoxin which shows damaging effects to biological membranes [11] and inhibition of several enzymes.[12] The haematin is then converted to yield haemozoin/ malaria pigment which is an insoluble crystalline material.[5] β-haematin, the synthetic form of haemozoin consists of dimers of ferriprotoporphyrin IX which are reported to be linked through reciprocal iron-carboxylate bonds to one of the propionic side chains of each porphyrin. These dimers interact in the crystal via H-bonding involving the remaining propionic acid groups of each porphyrin.[13] The structure of β-haematin has been shown to be identical to that of haemozoin by x-ray diffraction.[14] It was also suggested that an enzyme was required, based on harsh conditions required for β-haematin formation synthetically and the observation that an extract from plasmodial membranes apparently catalyzes β-haematin formation, which was thought to be polymeric at the time [15]. Pre-formed β-haematin [16, 17] and lipids [17-19] however also have a similar function and heating the parasite extract to boiling point still retains the β-haematin promoting activity, arguing against the presence of an enzyme.[16] Later work suggested that histidine rich protein II (HRPII) secreted by Plasmodium, initiates or catalyzes haemozoin formation.[20-22] In a study of the kinetics of β-haematin formation in concentrated acetate solutions it was observed that haemozoin formation may be a unique biomineralization process which proceeds via a rapid precipitation of amorphous haematin, followed by a slow conversion to microcrystalline β-haematin.[23]

This view is further supported by a report that Plasmodial histidine rich protein II acts as a biomineralization template for haemozoin.[24] More research however is still required to clarify the mechanism of haemazoin formation.[25]

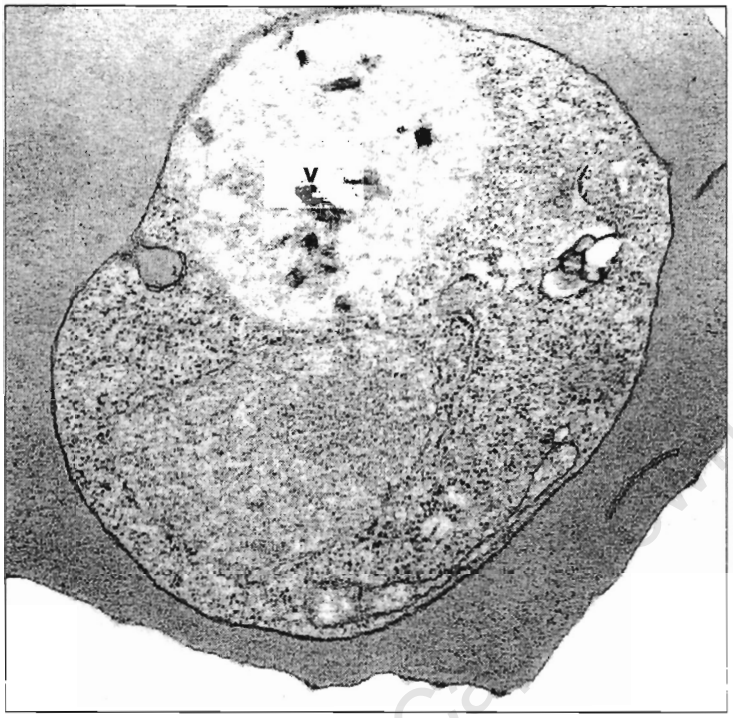

Figure 1.3. *P. falciparum* trophozoite with a forming food vacuole **v**.[3]

1.4. Quinoline anti-malarials

1.4.1. History

Until now the quinolines (Figure 1.4.) have dominated the therapeutic scene as antimalarials. Centuries ago, the native inhabitants of Peru already used the bark of *Cinchona ledgeriana*,[26] a local tree which contains the four alkaloids quinine and its isomers, quinidine, 9-epiquinine and 9-epiquinidine (collectively known as totaquine).[27] Of these four alkaloids only quinine and quinidine have strong antimalarial activity.[28, 29] These alkaloids only became known to Western medicine in 1640. In 1820 quinine was isolated from cinchona bark and in 1908 its structure was determined.[30]

The Germans started to investigate and synthesize synthetic antimalarials during World War I after their supply of natural quinine alkaloides were cut off by the allied blockade. This led to the first synthetic antimalarials, pamaquine (1932) and quinacrine (1933). Then in 1935 a German chemist at Bayer I.G. discovered sontoquine and resochin (later known as chloroquine). The Germans abandoned resochin because they considered it to be clinically too toxic.[30] At the beginning of World War II a stock of sontoquine (Fig. 1.4.) fell into US hands. This then started a dynamic search for analogous quinoline antimalarials, leading to the rediscovery of chloroquine in 1945 and subsequently to the synthesis of amodiaquine (1945) and primaquine (1950) (Fig. 1.4).[31] Chloroquine remained the first line prophylaxis and treatment for malaria for almost half a century. A new quinoline methanol antimalarial, mefloquine, was introduced clinically in 1984 as a result of ongoing research by the Walter Reed Army Institute of Research in the USA (Fig. 1.4). A related acridine, pyronaridine, was discovered by the Chinese recently and is under development (Fig. 1.4).[30]

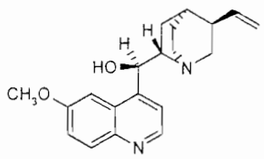

Quinine

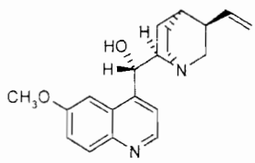

Quinidine

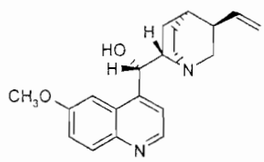

9-Epiquinine

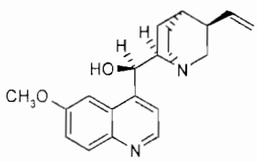

9-Epiquinidine

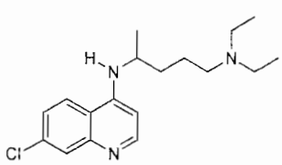

Chloroquine

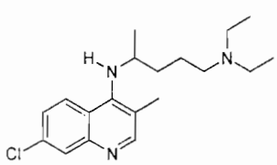

Sontoquine

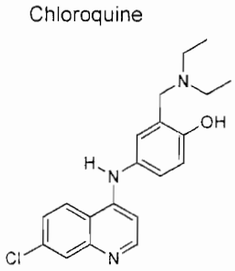

Amodiaquine

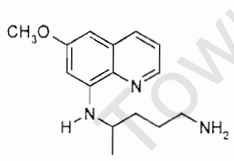

Primaquine

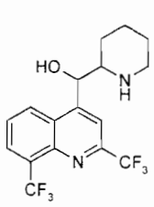

Mefloquine

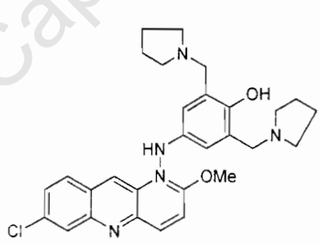

Pyronaridine

Figure 1.4. Structures of quinolines discussed in this section.

1.4.2. Mechanism of action

Many hypotheses have been proposed over the years to explain the activity of chloroquine. These can essentially be divided into two groups: those operating within the acidic food vacuole of the parasite and those operating in the parasite cytosol outside the food vacuole.

1.4.2.1. Extravacuolar mechanisms

1.4.2.1.1. DNA binding/intercalation

Evidence shows that chloroquine and quinine bind to DNA and that chloroquine exhibits antibacterial activity by inhibiting DNA and RNA synthesis.[32] The concentration however to accomplish this is 1000 times higher than the IC_{50} of chloroquine against *P. falciparum*. Mefloquine which is also active against the blood stage of malaria does not intercalate with DNA.[33]

1.4.2.1.2. Inhibition of protein synthesis

At 3μM concentrations, chloroquine is reported to inhibit protein synthesis in *P. falciparum*. These findings could not be reproduced by other studies [34-36] and concentrations in excess of the IC_{50} of chloroquine were required.

1.4.2.1.3. Inhibition of polyamine metabolism

Ornithine decarboxylase activity is reportedly inhibited by chloroquine and mefloquine in trophozoite extracts but this does not explain chloroquine's blood stage specificity [33] as this enzyme is likely to be active in the liver stage as well.[32]

1.4.2.2. Intravacuolar mechanism

The aminoalkyl side chain of chloroquine and analogues give these compounds weak base properties. The pKa's of chloroquine are 8.3 and 10.2.[37] The free base present in the general cytoplasm is sufficiently hydrophobic to cross the lipid bilayers of the

food vacuole . At pH 5.3 in the food vacuole the compound becomes protonated. This protonated charged form cannot cross the membrane and it is unable to easily diffuse out of the vacuole. This causes pH trapping. These factors cause up to 8000-fold concentration of the compound in the vacuole. Additional mechanisms appear to be responsible to an even greater extent for the accumulation.

1.4.2.2.1. Increased pH of food vacuole

It has been argued that chloroquine and analogues accumulate in the food vacuole due to their basic character and alter the pH.[37] However no changes [38] [39] or changes of less than 0.25 pH units [40] were observed and these changes are too small to account for their activity.[33]

1.4.2.2.2. Inhibition of vacuolar phosphilipase

Single membrane endocytic vesicles occur in the food vacuole during treatment with chloroquine. This could result from the general breakdown in lysosomal function or the inhibition of phospholipase enzymes by chloroquine. Once again this mechanism requires high concentration of chloroquine and is not blood stage specific.[33]

1.4.2.2.3. Inhibition of vacuolar protease

Aspartic proteases, which degrade haemoglobin, are partially inhibited by chloroquine ,[41] but only at concentrations higher than that of chloroquine occurring in the vacuole.[25]

1.4.2.2.4. Degradation of haem

In two recent studies it has been suggested that only 30% of haem is converted into haemozoin and that chloroquine and related compounds inhibit the degradation of most of the haem in the parasite. One study suggests that haem is degraded by glutathione and that chloroquine inhibits this process to cause the accumulation of toxic haem.[42] The other study suggests that hydrogen peroxide which is a by-product from the oxidation of ferroprotoporphyrin IX to ferriprotoporphyrin IX, degrades haem and that chloroquine targets this process to elevate toxic haem levels.[43] Using Mössbauer

spectroscopy, chemical analysis of the iron content of various cellular components and electron spectroscopic imaging, our laboratory has shown that most of the iron from haemoglobin is converted into haemozoin inside the parasitised erythrocyte [44] which suggests that the haem degradation is unlikely to be a significant target of these drugs.

1.4.2.2.5. Inhibition of haemozoin formation

It has been shown that chloroquine, amodiaquine and quinine directly inhibit the synthetic formation of β-haematin.[45] This suggests that the activity of these drugs in vivo which target the erythrocytic stage of malaria involves the inhibition of haemozoin formation as a result of direct interaction with Fe(III)PPIX. This hypothesis has also been supported by Dorn *et al.*[16, 17] Egan *et al.* have shown that compounds with a poor binding constant to haematin have weak antimalarial activity.[46] As further evidence another study has shown that the cellular uptake of chloroquine is dependent on binding to Fe(III)PPIX and that the addition of specific proteinase inhibitors to stop the generation of Fe(III)PPIX, inhibit chloroquine uptake and reduce its activity.[47] This supports the mechanism further, in that normally chloroquine would bind to Fe(III)PPIX in the food vacuole lowering the concentration of its free form and thereby increasing the influx of more chloroquine.

The above evidence strongly favors this mechanism and forms the basis on which this dissertation is approached.

1.5. Quinoline-Fe(III)PPIX interactions

Based on the inhibition of haemozoin formation hypothesis, the interaction of quinolines with haematin (figure 1.5.) is an important focus point for the development of new antimalarials.

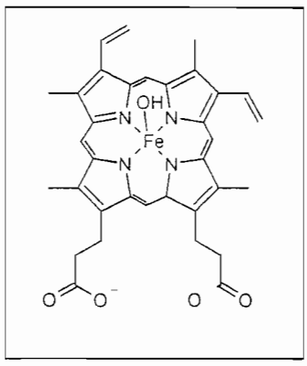

Figure 1.5. Structure of haematin.

The interaction of quinolines and Fe(III)PPIX has been studied in different solvents.[46, 48-52] In theory, haematin in solution can exist either as a monomer, μ-oxo-dimer or an aggregate of μ-oxo-dimers, depending on the concentration, pH and ionic strength.[53] Brown *et al.* made an extensive study on the state of haematin in aqueous solution and claimed that it extensively dimerised into an μ-oxo-dimer.[54]

Studies [46, 55] of the chloroquine-haematin interaction performed in the pH range of 5.6 to 9.0 have shown that the complex is virtually unchanged between pH 5.6 and 7.4. As interaction with the deprotonated form of the drug (which would be expected to favour any coordination with the iron that may occur) does not increase, it would appear that the protonation state of the drug and therefore metal-coordination is not important. The ability of chloroquine to form complexes with metal free porphyrins, protoporhyrin IX [56] and uroporphyrin I [57] with similar strength to corresponding metal porphyrin complexes is further evidence that the complexation does not involve metal-coordination. It is strongly suggested that the nature of the drug-Fe(III)PPIX association is based on co-planar π-π interactions between the aromatic ring system of chloroquine and the porphyrin.[46, 56-58] There are cases such as quinine where additional interactions may arise where the side chain hydroxyl group can bind to the iron center of the

porphyrin.[59] It is shown that the chloroquine-haematin complex formation is predominantly entropically driven based on thermodynamic parameters obtained while quinine-haematin complex formation is enthalpically driven.[46]

Dorn *et al.* have measured association constants in an aqueous environment using titration calorimetry where large haematin-drug stoichiometries are observed.[60] There is no evidence that the strength of drug-haematin binding is quantitatively related to antiplasmodial activity,[45, 60-62] although erythrocytic stage antimalarial compounds all form strong complexes with haematin.

1.6. Drug resistance mechanisms in *P. falciparum*

In this thesis only a short discussion will be made on the drug resistance phenomenon.

Resistance to chloroquine developed slowly and originated simultaneously in the 1960's in South East Asia and South America. This resistance then spread to all malaria endemic parts of the world.[63]

A number of theories exist on the resistance mechanism and they can be divided into two topics: (i) the parasite gene responsible for resistance and the protein products thereof and (ii) the physiological changes or mechanisms in the parasite associated with resistance.

1.6.1. Gene mutation/ changes in expression

Chloroquine resistance has been mapped to a 36 kb segment of chromosome 7 [64] and is related to complex polymorphisms. Candidate genes in this segment, *cg1* and *cg2*, have been identified but a recent study has indicated that they are not responsible for chloroquine resistance.[65] It was then suggested that a nearby gene is probably responsible, accounting for the strong linkage with *cg1* and *cg2*.[65] Indeed recent evidence shows that chloroquine resistance is a result of a gene, *pfcrt*, which appears to be a transmembrane protein consisting of 424 amino acids located close to the *cg1* and *cg2* genes. It is localized in the vacuolar membrane and it may be a transporter or channel. The evidence strongly indicates that this is the chloroquine resistance

mediator. Mutations observed from respectively the Western and Eastern Hemisphere are distinctly different which is in accord with the independent development of resistance in South America and South East Asia.

1.6.2. Physiological changes

A common feature of chloroquine resistance is that chloroquine resistant parasites accumulate less drug than their sensitive counterparts.[66-68]

Others then argued that chloroquine resistance is the result of an impaired amiloride-sensitive Na^+/H^+ exchanger (NHE) pump which inhibits chloroquine uptake into the parasite.[69, 70] Subsequent studies found no effect of amiloride analogues on chloroquine uptake and susceptibility of parasites and also no difference in NHE activity between sensitive and resistant strains.[71] The involvement of NHE in active transport would appear to have been conclusively discounted.

Geary *et al.* argued that reduced chloroquine accumulation in resistant parasites is the result of an increased vacuolar pH due to a weakened proton pump.[72] Krogstad *et al.* however found no significant differences in vacuolar pH between resistant and sensitive parasites.[40] Bray *et al.* concluded in their studies on the binding of chloroquine to haematin that the chloroquine resistance mechanism probably regulates the access to haematin, reducing the apparent binding affinity which can be reversed in the presence of verapamil.[47, 73] This is consistent with the resistance hypotheses arguing that prevention of chloroquine accumulation at the local site of action is the basis of the mechanism.

A few structural changes to the quinolines have been explored to circumvent resistance. Altering the number of carbon atoms between the two nitrogens in the lateral side chain of chloroquine has demonstrated that only aminoquinolines with side chains distinctly shorter or longer (ethyl, propyl, decyl or dodecyl) are also active against chloroquine resistant *P. falciparum*.[74] Vippagunta *et al.* tested thirteen chloroquine analogues and found that the diaminoalkyl side chain is an important structural determinant in chloroquine drug resistance.[61] Their study also showed that the analogue **1** of chloroquine where the tertiary nitrogen of the side chain was replaced with a carbon atom had a 4-fold decrease in activity against the sensitive strain and a 1.7 fold increase in activity against the resistant strain. This implies that the tertiary nitrogen in the side chain is a structural feature associated with parasite

drug resistance. Biot *et al.* synthesized and studied the effect of introducing a ferrocene group in the side chain of chloroquine analogues. One of these compounds, **2** was reported to be 22 times more active than chloroquine *in vitro* against resistant strains of *P. falciparum*.[75] Another group synthesized and tested a complex **3** of gold with chloroquine which they reported to be more active against chloroquine resistant strains than previously reported metal-chloroquine complexes.[76] The evidence above establishes that it is possible to produce aminoquinolines active against chloroquine resistant *P. falciparum* by modifying the aminoquinoline side chain.

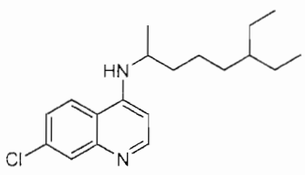

1

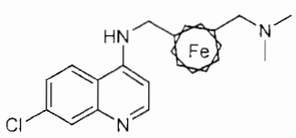

2

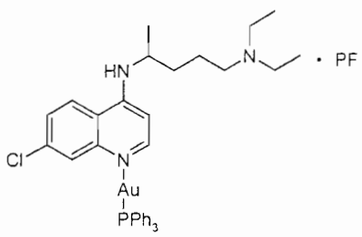

3

1.7. Structure-activity relationships of the aminoquinolines.

Studies of structure activity relationships and the quantification thereof plays an extremely important role in the approach to the design of novel therapeutic agents with a specific application such as activity against the erythrocytic stage of malaria in this case. A few comprehensive studies to define the pharmacophore of aminoquinoline antimalarials will be discussed here, which form the background for the synthetic approach of this thesis.

The results of most studies are compared with chloroquine. Chloroquine is a 4-aminoquinoline with an electron withdrawing chlorine in the 7 position. Its structure contains three nitrogens of which two are weakly basic: the quinoline nitrogen and the tertiary nitrogen in a *N,N*-diethylamino isopentyl side chain. The two nitrogens of the side chain are separated by four carbon atoms.

In a study [62] focused on circumventing the toxicity of tebuquine (an amodiaquine analogue) by replacing the 4-hydroxyl group with a fluorine and with a substituent in the

5 position (e.g. **4**) to prevent bioactivation to a toxic quinonimine, activities of some of the compounds were directly related to their cellular accumulation ratios. A study by Hawley *et al.* [77] also showed that some of these compounds and other quinolines which inhibit β-haematin formation indicate a correlation between IC_{50} values for inhibition of β-haematin formation and accumulation-normalised IC_{50} values against cultured parasites. The evidence above establishes that it is possible to produce aminoquinolines active against chloroquine resistant *P. falciparum* by modifying the aminoquinoline side chain.

Bisquinolines have also been the focus of a number of studies. These are compounds in which two quinoline rings are joined by a linker group. The 4-amino-7-chlorobisquinolines joined by a linear or cyclic alkane or heteroalkane group attached to the 4-amino groups of each of the two quinoline rings have been amongst the compounds studied. They showed all the characteristics of the monoquinolines and as expected associate with haematin,[60] inhibit β-haematin formation [17, 78, 79] and show strong activity. Bisquinolines based on 4,6- and 4,8-diaminoquinolines show much lower activity.[80] It appears therefore that the activity of most bisquinolines can be explained by the structure-activity relationships of the monoquinolines.

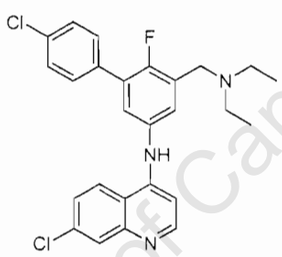

4

A comparison of nineteen aminoquinolines [1] to propose a structure-activity relationship for chloroquine (Table 1.1.) showed that 2- and 4-aminoquinolines are unique in their strong affinity for Fe(III)PPIX, and attachment of side chains to the amino group or the presence of the 7-chloro group has relatively little influence on the strength of quinoline-haematin complex formation. For example compounds 3-4 have roughly corresponding association constants with haematin (log K from 4.43 to 5.81), table 1.1. It was also shown that the 7-chloro group (**6** and **8**) is important for inhibition of β-haematin formation and that the side chain attached to the amino group had no effect

on this. Compounds **5** and **7**, for example, had no β-haematin inhibitory activity, table 1.1. The basic amino group in the side chain also appeared to be important for activity as the IC_{50} for compound **6** is approximately two orders of magnitude less than compound **8**. It is suggested that the basic amino group is responsible for vacuolar accumulation of the compound by means of pH trapping. Although this at first seems to contradict evidence [47, 73] that ~90% of observed drug accumulations occurs via specific binding to haematin, free drug in the parasite vacuole is in fact a critical requirement for this binding. Therefore the accumulation of drug through pH trapping is likely to be an essential requirement.[1]

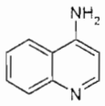

5

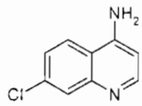

6

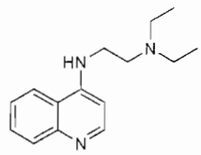

7

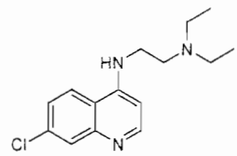

8

Compound	Log K (40% DMSO, pH 7.5, 25°C)	BHIA	IC_{50} (D10 strain of P.falciparum)/nM
Chloroquine	5.52 ± 0.03	+	38 ± 14
5	4.49 ± 0.01	-	>10000
6	4.43 ± 0.01	+	3800 ± 500
7	4.75 ± 0.03	-	799 ± 404
8	5.81 ± 0.01	+	49 ± 14

Table 1.1. Haematin association constants, β-haematin inhibitory activity (BHIA) and IC_{50} compared for compounds **5-8** and chloroquine.

On this basis, a structure-activity relationship has been proposed for chloroquine (Figure 1.6.).

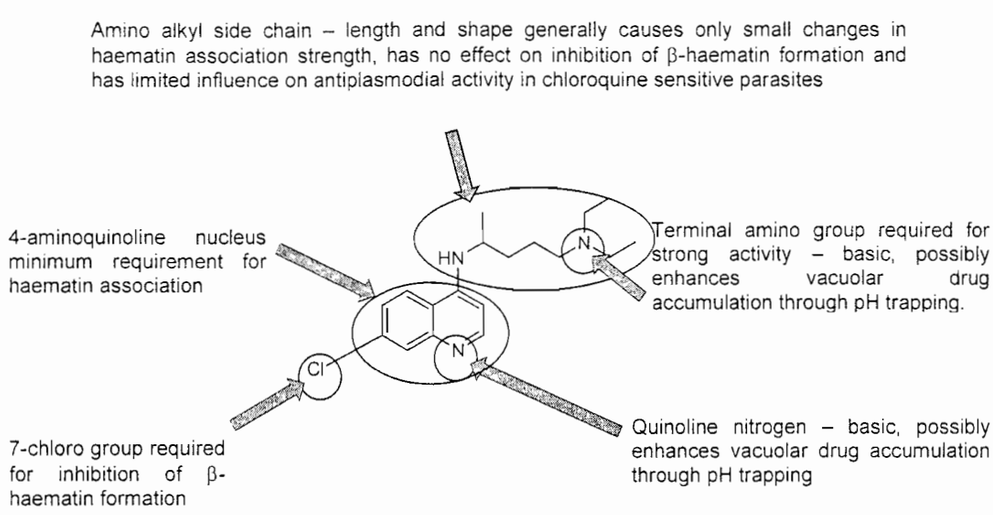

Figure 1.6. Proposed SARs in chloroquine based on a study of 19 quinolines.[1]

Several studies have investigated the effect of replacing the 7-chloro group on the quinoline ring with other groups.[2, 61, 74, 81] The strong electron withdrawing bromo, iodo, nitro and trifluoromethyl analogues (as characterized by their Hammet constants) retained strong activity while the weakly electron withdrawing or electron donating fluoro, hydroxyl, amino and methoxy derivatives showed reduced or strongly reduced activity. The nitro and bromo analogues of chloroquine showed strong β-haematin inhibitory activity while the 7-amino and 6-chloro analogues were unable to inhibit β-haematin formation. The 6-chloro analogue also associated poorly with haematin [61, 81] was reported. A modest but significant correlation between IC_{50} for β-haematin formation inhibition and that for inhibition of parasite growth normalized for β-haematin μ-oxo dimer binding affinities.[61] Another recent study [2] with different substituents at the 7-position on the quinoline ring showed that the group at the 7-position lowers the pK_a of both the quinolinium nitrogen and the tertiary amino nitrogen in the side chain of chloroquine analogues. The quinolinium nitrogen pK_a ranges from 6.28 in the strongly electron withdrawing nitro derivative to 8.36 in the electron donating amino derivative. For the tertiary amino nitrogen the pK_a ranged from 7.65 in the trifuoromethyl derivative to 10.02 in the amino derivative. Using these pK_a values the accumulation ratios (concentration of the compounds inside the food vacuole relative to that outside the food vacuole) were estimated using equation 1. This was then compared with chloroquine to obtain a relative accumulation ratio (α) used to normalize the IC_{50} for

each derivative with equation 2. This normalised antiplasmodial IC_{50} gave a good correlation with $BHIA_{50}$ (activity of compound which would inhibit 50% of β-haematin formation) values for the same derivatives (Figure 1.7.d). Graphs of log IC_{50} against log K (Fig. 1.7..a), log IC_{50} against log $BHIA_{50}$ (Fig. 1.7.b) and log ($IC_{50}\times\alpha$) against log K (Fig. 1.7.c) gave no or very poor correlation.

$$AR = \frac{[Q]_v}{[Q]_e} = \left\{ \frac{1 + \frac{[H^+]_v}{Ka_2} + \frac{[H^+]_v^2}{Ka_1 Ka_2}}{1 + \frac{[H^+]_e}{Ka_2} + \frac{[H^+]_e^2}{Ka_1 Ka_2}} \right\} \qquad (1)$$

$$\alpha = \frac{AR_{QUINOLINE}}{AR_{CHLOROQUIN}} \qquad (2)$$

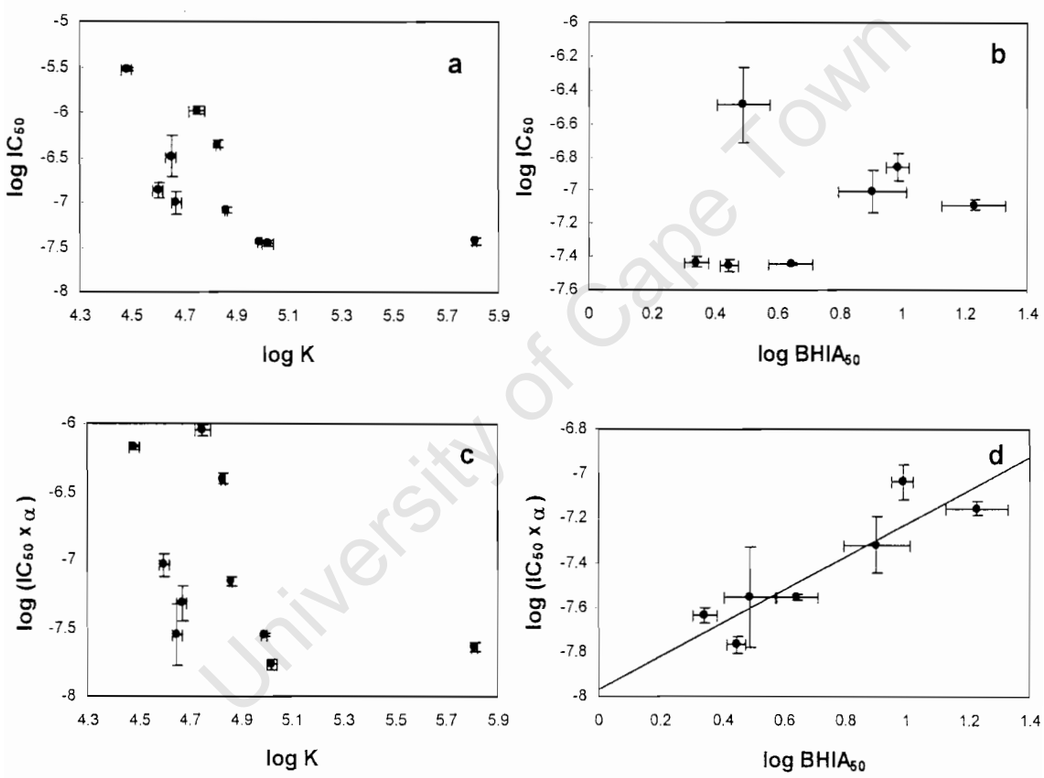

Figure 1.7. Correlation of log IC_{50} values against log K (a); log IC_{50} against log $BHIA_{50}$ (b); log IC_{50}, corrected for the extent of vacuolar accumulation, against log K (c); log IC_{50}, corrected for the extent of vacuolar accumulation against log $BHIA_{50}$ (d).[2]

A further set of formulae (equations 3-7) was proposed in this study [2] to describe the quantitative structure activity relationships of the 4 aminoquinolines and to make predictions for new compounds.

$$pKa_1 = -1.90\sigma_m + 8.2 \quad (3)$$

pKa_1 is the acid dissociation constant for quinolinium nitrogen and can be predicted by equation 3 using the Hammett meta-substituent constant for the group in the 7 position of the quinoline,

$$pKa_2 = -3.19\sigma_m + 9.5 \quad (4)$$

pKa_2 is the acid dissociation constant for tertiary amino group in the lateral chain and can be predicted by equation 4 using the Hammett meta-substituent constant for the group in the 7 position of the quinoline,

$$\log K = 0.29\pi + 4.71 \quad (5)$$

The log K value for the 7-substituted-4-aminoquinoline-haematin association can be predicted using equation 5 which incorporates the substituent lipophilicity constant (π),

$$\log BHIA_{50} = -0.519 \times \log K - 1.06 \times \sigma_m + 3.67 \quad (6)$$

The log $BHIA_{50}$ value is predicted using the log K value calculated with equation 5 and the Hammett meta-substituent constant for the group in the 7 position of the quinoline,

$$\log (IC_{50} x\alpha) = 0.741 \times \log BHIA_{50} - 7.97 \quad (7)$$

Equation 7 relates the for normalized the IC_{50} value to the $BHIA_{50}$ value.

Using this set of formulae, the predicted values for the thesis targets, *N*^{1},*N*^{2}-Diethyl-*N*^{2}-(7-trifuoromethylthio-4-quinolinyl)-1,2-ethanediamine **11** and *N*^{1},*N*^{2}-Diethyl-*N*^{2}-(7-trifuoromethoxy-4-quinolinyl)-1,2-ethanediamine **12** were calculated (Table 1.2.).

Property	11	12
AR	3110	3271
α	0.53	0.56
pKa_1	7.44	7.48
pKa_2	8.22	8.28
log K	5.13	5.01
log $BHIA_{50}$	0.58	0.66
log ($IC_{50}\times\alpha$)	-7.54	-7.48

Table 1.2. The predicted values for **11** and **12** calculated using equations 1-7.

1.8. Alternative structure template for quinoline antimalarials

Benzimidazoles are known to show a variety of biological activities.[82, 83] The mesomeric effect in the imidazole ring system possibly results in a very similar electron density profile for the benzimidazole nucleus compared to the 4-aminoquinoline nucleus. This makes the benzimidazoles an attractive alternative template for investigation as potential antimalarials.

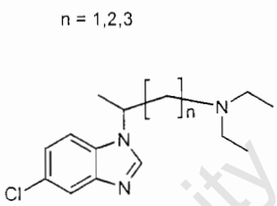

9

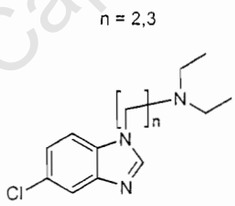

10

Since the 1920's a number of publications reported on benzimidazoles. Synthesis of 2-β-aminoethylethoxybenzimidazoles were reported in 1929.[84] In 1940 synthesis of methoxylated 1-diethylaminoalkylbenzimidazoles was described.[85, 86] In 1944 Clemo and Swan also published work on a number of benzimidazoles substituted in position 1 with the chloroquine side chain.[87] Where biological data had been reported it showed that none of the above compounds had any activity in avian malaria. Important synthetic work was done in 1962 by Knobloch *et al.* [88] and in 1969 by Heindel *et al.* [89]

which forms the bases for our synthetic approach to benzimidazoles as a new structure template. Both these groups made benzimidazole analogues (e.g. **9** [88] and **10** [89]) of chloroquine which were tested for neuropharmacological action.[88, 89]

1.9. Objectives

The objectives of this work are the following:

- Synthesis and characterization of two novel 7-substituted-4-aminoalkylated quinolines, N^1,N^1-diethyl-N^2-(7-trifuoromethylthio-4-quinolinyl)-1,2-ethanediamine **11** and N^1,N^1-diethyl-N^2-(7-trifuoromethoxy-4-quinolinyl)-1,2-ethanediamine **12** for antimalarial activity.

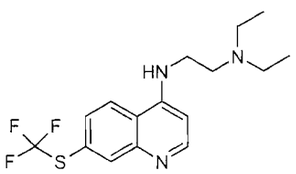

11

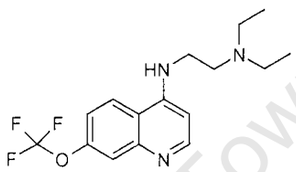

12

- Investigation, synthesize and characterization of novel benzimidazole analogues of 7-substituted-4-aminoalkylated quinolines for antimalarial activity. (**13-15**)

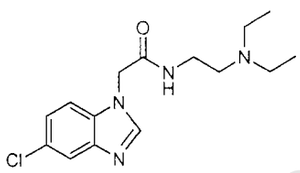

13

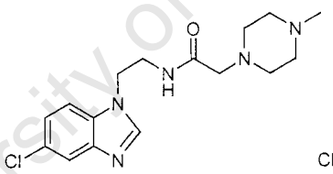

14

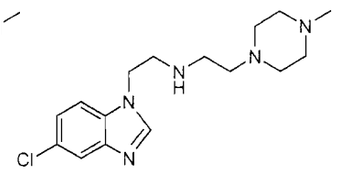

15

- Synthesize and characterization of the corresponding quinoline analogues of the benzimidazole targets. (**16** and **17**)

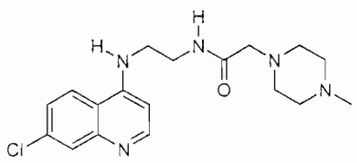

16

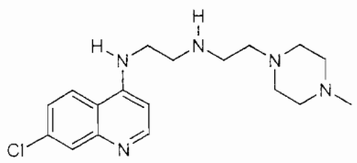

17

- The comparison of the biological activity of the structurally analogous benzimidazoles and quinolines to determine the effect of the benzimidazole nucleus versus the 4-aminoquinoline nucleus.

- Measurement of pKa values of the basic nitrogens of the targets.

- Measurement of the log K association constant for each target for association with haematin.

- Measurement of both quantitative β-haematin inhibitory activity ($BHIA_{50}$) and qualitative β-Haematin inhibitory activity (BHIA) for each target, in order to investigate the predictive utility of the QSARs obtained in our laboratory.

2. Synthesis

2.1. Background

Chloroquine has been the most widely used anti-malarial agent for almost half a century in the prophylaxis and treatment of malaria. The spread of chloroquine resistance has virtually voided it of therapeutic value, and this has stimulated great interest in the understanding of structure-activity relationships in chloroquine, which may contribute to the rational design of superior quinoline antimalarials.

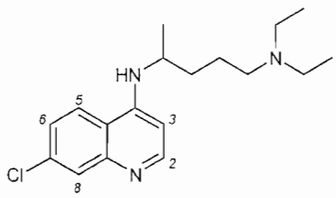

chloroquine

In the introduction, a number of analogues of chloroquine were reviewed where either or both the side chain and substituent in the 7-positions were altered in an attempt to improve particular aspects of the antimalarial activity. In this study, four aspects in the rational design of novel antimalarials were addressed.

1. Testing of a hypothesis

It was firstly decided to test the hypothesis of structure-activity relationships made by Kaschula *et al.* [90] in which the 7-substituent was varied, and the commercially available *N,N*-diethylethylenediamine side chain was used as the 4-substituent to overcome resistance by *P. falciparum*. The trifluoromethylthio **11** and trifluoromethoxy **12** derivatives were selected since they involve a level of electron-withdrawing character (Figure 2.1.). These substituents are also attractive in the design of novel pharmaceuticals owing to their lipophilicity and activity-enhancing capability.

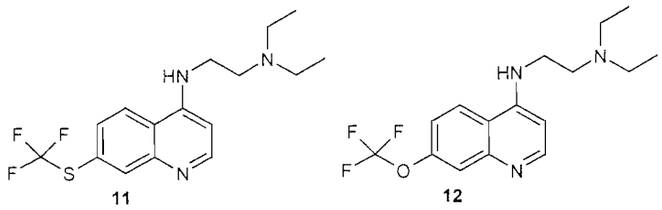

Figure 2.1. 4-aminoquinolines selected to test hypothesis.

2. *A new template*

The benzimidazole nucleus is a possible alternative template for the 4-aminoquinoline nucleus since from a resonance point of view the benzimidazole mimics the dipolar character of the pyridine ring of quinoline (Figure 2.2.). Sterically, however, the benzimidazole nucleus is smaller, containing a five-membered ring in place of the pyridine ring. As reviewed in chapter 1, benzimidazole was used by Knobloch *et al.* [88] and Heindel *et al.* [89] to replace the 4-aminoquinoline nucleus in chloroquine analogues which were unsuccessful as antimalarial agents.[82] Structure-activity relationships for these analogues were unresolved and further work was necessary to conclude that this template was ineffective.

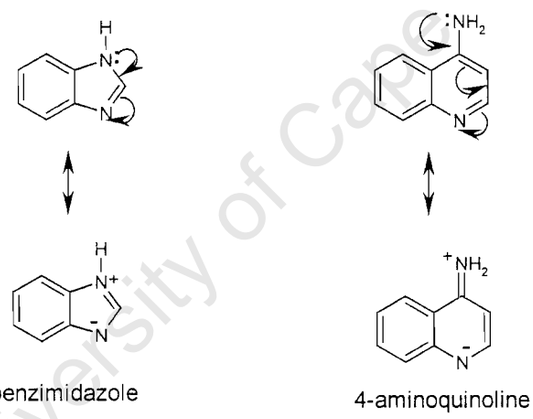

Figure 2.2. Illustration of the similar resonance characteristics of benzimidazole and 4-aminoquinoline.

Derivatives **13**,**14** and **15** were therefore synthesized to explore the structure-activity relationships of chloroquine-like benzimidazoles (Figure 2.3.).

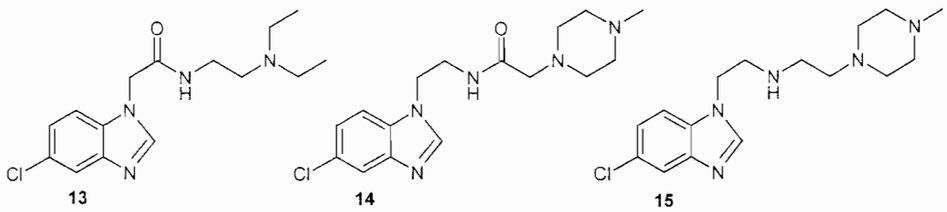

Figure 2.3. Target benzimidazoles.

3. Synthesis of a novel side-chain

N-(2-Aminoethyl)-2-(4-methylpiperazin-1-yl)ethanamide (Figure 2.4.) **14b** was designed and synthesized, in a short but difficult synthesis. The primary intention was to eventually reduce the secondary amide to a secondary amine to yield a compound with a third basic nitrogen capable of increasing vacuolar accumulation of the 5-chlorobenzimidazoles in the parasite, and also to fine-tune the activity of 7-chloro-4-aminoquinoline analogues.

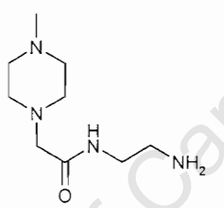

14b

Figure 2.4. The side-chain chosen for the regioselective synthesis of **14** and **15**.

4. Benzimidazole nucleus versus the 4-aminoquinoline nucleus.

In an attempt to establish the efficacy of the benzimidazole nucleus combined with the *N*-(2-Aminoethyl)-2-(4-methylpiperazin-1-yl)ethanamide side chain, the 7-chloroquinoline analogue with both this side chain and its reduced form (Figure 2.5.) were targeted for synthesis for comparison purposes.

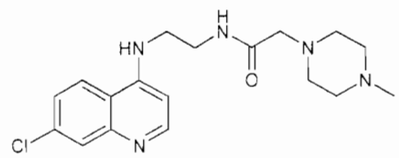

16

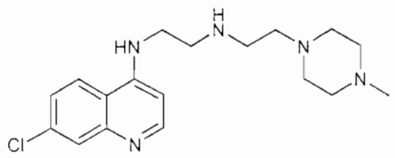

17

Figure 2.5. Quinoline analogues **16** and **17**, targeted to compare with benzimidazoles **14** and **15**.

2.2. 7-Substituted-4-N^1,N^1-diethylethylendiaminequinolines

2.2.1. Synthesis of 7-X-4-chloroquinolines

2.2.1.1. Route of Price and Roberts

The 7-X-4-aminoquinolines, (X = SCF_3, OCF_3) were synthesized according to methodology developed in the synthesis and derivatisation of chloroquine. These routes will be briefly discussed, in order to give the background for this method.

Chloroquine was produced in the United States just after WW II, following the route developed by Surrey and Hammer (Scheme 2.1.).[31, 91]

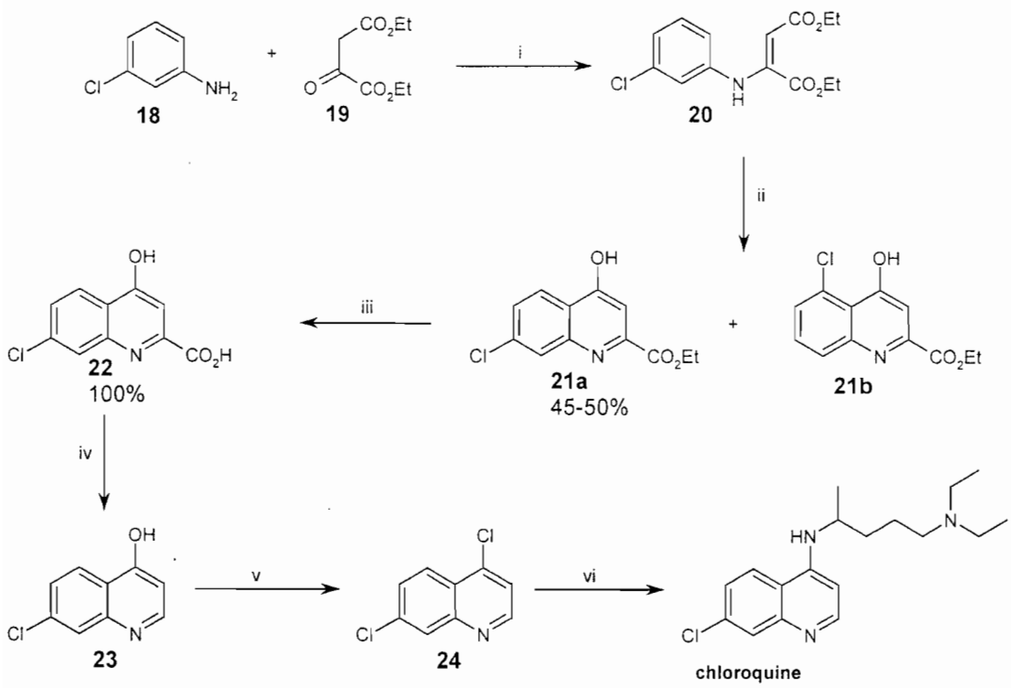

Scheme 2.1. Commercial route to chloroquine developed by Surrey and Hammer in 1946. Reagents and conditions: i. CH_3COOH (aq), 40–50°C, 15–18 hrs; ii. mineral oil, 250°C, 20 min; iii. 35% NaOH, reflux, 2 hrs; iv. mineral oil, 270°C, 5 min; v. $POCl_3$, reflux, 2 hrs; vi. 4-amino-1-diethylaminopentane, 160–180°C, 7 hrs.[91]

In the case of chloroquine, *m*-chloroaniline **18** was condensed with diethyl 2-oxo-succinate **19** to form enamine **20**. Thermal cyclization of **20** gave a 1:1 mixture of 2-(ethoxycarbonyl)-4-hydroxy-7-chloroquinoline **21a** and its 5-chloroisomer **21b** from which the desired **21a** was isolated by selective crystallization. Hydrolysis to the acid followed by decarboxylation and chlorination of the resultant 7-chloro-4-hydroxyquinoline **23** gave 4.7-dichloroquinoline **24**, which underwent 4-substitution with excess 4-amino-1-diethylaminopentane (novol diamine, NDA) for 3–5 hrs at 160–170°C to yield chloroquine as the free base which was then treated with phosphoric acid and isolated as the diphosphate salt.

Interesting alterations from Surrey and Hammer's laboratory synthesis to plant production of chloroquine were reviewed by Kenyon in 1949. One improvement was the use of Dowtherm instead of mineral oil for the cyclization and decarboxylation steps ii and iv respectively as the mineral oil was difficult to remove owing to its high viscosity and tendency to carbonize. The addition of phenol to **24** prior to coupling with NDA (step vi), was another improvement. The phenol reacts with **24** to form 7-

chloro-4-phenoxyquinoline **25** [92] (Scheme 2.2.) which then couples more readily with NDA enabling the use of stoichiometric amounts of NDA and lower reaction temperatures. This then eliminated the need to isolate chloroquine as its free base prior to formation of the diphosphate salt.

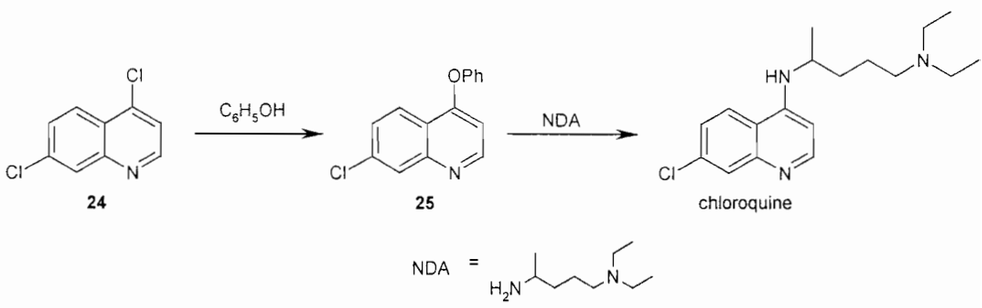

Scheme 2.2. Improved preparation of chloroquine from **24.**

Johnson and Buell provided another route, which gave only the desired 7-chloroisomer upon cyclization. In this route, methyl acrylate and *m*-chloroaniline were condensed to give **26** [93] (Scheme 2.3.). Tosylation and saponification of **26** gave the acid **27** which was cyclized and detosylated to give **28**. Condensation with NDA in the presence of an oxidising agent then gave chloroquine. The authors claimed that an overall 25% yield from the *m*-chloroaniline was obtained which compares well to the Surrey and Hammer method.

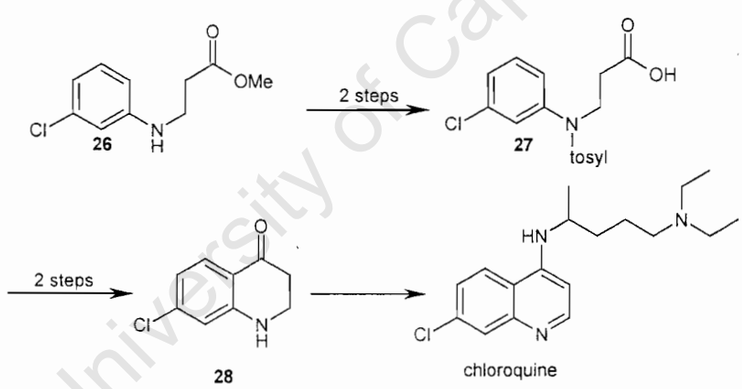

Scheme 2.3. Synthesis of chloroquine as developed by Johnson and Buell.[93]

Price and Roberts [94] developed a superior route to 4,7-dichloroquinoline in 1946 that involved condensation of diethyl ethoxymethylenemalonate (EMME) **29** with *m*-chloroaniline **18** (Scheme 2.4.). In this method, cyclization of **30** formed

predominantly the 7-chloroisomer **31** (80-90%) with only traces of the undesired 5-chloroisomer. The cyclization and decarboxylation steps ii and iv were both carried out using Dowtherm A.

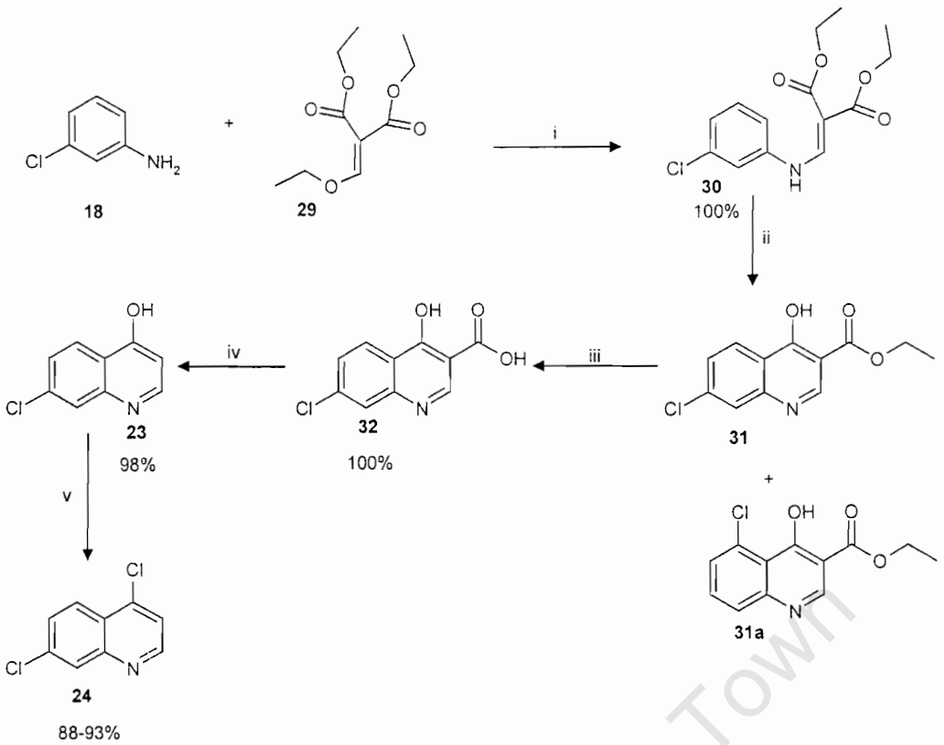

Scheme 2.4. Improved route to 4,7 dichloroquinoline [94]. Reagents and conditions: i. 100°C, 1 hr; ii. diphenyl ether, reflux, 45 min; iii. 10% NaOH (aq), reflux, 1 hr; iv. 240-270°C; v. $POCl_3$, reflux, 2 hrs.

The Price and Roberts' method was used to synthesize the 7-X-4-aminoquinolines required for this study, where X= SCF_3 and OCF_3 (Scheme 2.6.).

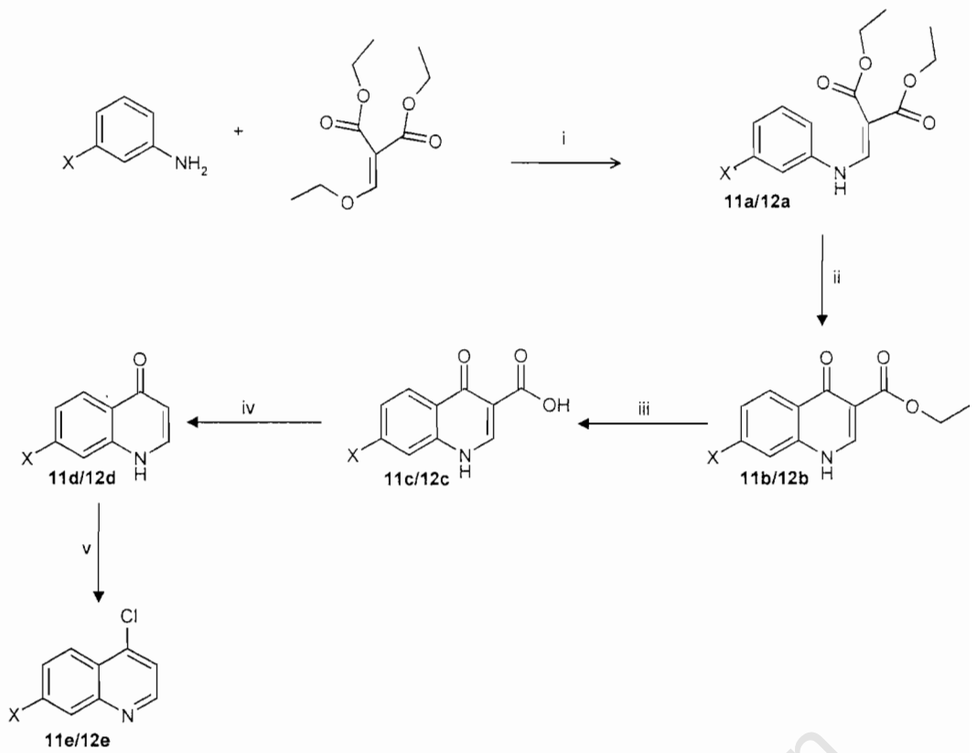

Scheme 2.6. Route to 7-X-4chloroquinolines, X= SCF_3 for **11a-f** and **11**; OCF_3 for **12a-f** and **12**. Reagents and conditions. I. 78°C, 3 hrs; ii. diphenyl ether, reflux, 20-30 minutes; iii. 10% NaOH (aq), reflux, 2 hrs; iv. diphenyl ether, reflux, 30 min; v. $POCl_3$, 115°, 30 minutes.

In this dissertation the synthesis started with the appropriate *m*-substituted aniline and EMME **29,** which were heated at 100°C for 3 hrs to afford the acrylates **11a/12a.** These were purified by crystallization from ethanol in 93-99% yield. Each purified **11a/12a** was then refluxed in diphenyl ether for 15-30 minutes to give the desired 7-substituted quinoline products **11b/12b** regioselectively in 73-75% yields. Because of poor solubility characteristics, the regioselectivity was only confirmed by NMR in the next step.

Saponification of **11b/12b** by refluxing in 10% NaOH (aq) for 2 hours gave the sodium salts of **11c/12c** which were precipitated out of solution by carefully adjusting the pH to neutral with 10% H_2SO_4 to avoid the formation of the water-soluble quinolinium ion. The white sludge that formed was filtered off and washed extensively with water. The formation of the 7-chloro-regioisomer as **11c/12c** in stead of the 5-chloro-regioisomer was confirmed by the ^1H NMR splitting patterns and coupling constants of the quinoline benzene ring. H-5 and H-8 appeared as

doublets and H-6 as a doublet of doublets with ortho and meta coupling constants of 8.4-8.7 and 1.2-1.5 Hz respectively. The analogous 5-regioisomers would have revealed a completely different coupling pattern,[90] since the three aromatic protons of the A-ring are next to each other.

11c/12c were decarboxylated in refluxing diphenyl ether for 30 minutes to give the respective 7-X-4-quinolones **11d/12d** in quantitative yields. The 7-X-4-quinolones **11d/12d** showed the characteristic ortho and meta couplings between the protons of the quinoline benzene ring as well as a pair of AB doublets with a coupling constant of 4.7 Hz corresponding to H-2 and H-3 in the quinolone pyridine ring (Figure 2.6.), thus proving that decarboxylation had taken place. H-2 resonated at a higher chemical shift owing to the deshielding effect of the adjacent nitrogen of the [90] quinoline pyridine ring.

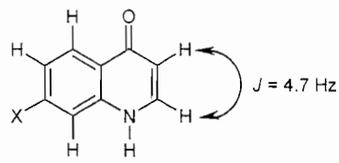

Figure 2.6. Characteristic ^{1}H NMR multiplicities and coupling constants for 7-X-4-quinolones **11d/12d**.

Chlorination of **11d/12d** in phosphorus oxychloride and phosphorus pentachloride at 120°C for 30 minutes gave 7-X-4-chloroquinolines **11e/12e** in yields of 88%. Infrared spectroscopy revealed the absence of a broad OH band at 3600-3200cm^{-1}.

It was noted that C-7 in the analogous 7-methoxy derivative studied by Kaschula *et al.* [90] resonated at 161.7 ppm in the ^{13}C NMR spectrum, whereas the for X = OCF_3 in the present case, it appeared at 171.1 ppm. This deshielding downfield shift of nearly 10 ppm, going from OCH_3 to OCF_3, can be attributed to the inductive effect of F_3 versus H_3.

The ^{13}C and Infra-red data of compounds **11/12b-d** agreed with literature data for analogous compounds, and was consistent with these compounds existing predominantly in the 4-quinolone tautomeric form (**B**) rather than as the 4-hydroxyquinoline tautomer (**A**), (Scheme 2.5). The prototropic tautomerism of 4-quinolones, in particular those bearing an ester or carboxyl function at the 3-position has been studied. Typical ^{13}C chemical shifts for a series of 4-quinolones analogous

to those in this dissertation have been reported by Lubomir *et al.*[95] to be in the range of 172.8-178.4 ppm. Compounds **11/12b-d** all had their C-4 chemical shifts in the range 176.1-177.8 ppm. The carbonyl Infra-red stretching frequencies for compounds **11/12b-d** appeared in the range 1640-1620 cm^{-1} consistent with values reported in the literature for 4-quinolinones in the range 1650-1620 cm^{-1}.[96, 97] Furthermore, compounds **11/12b-d** showed no hydroxyl stretch at around 3600-3200 cm^{-1}.[98]

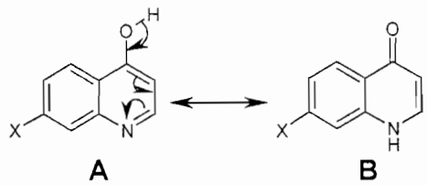

Scheme 2.5. Tautomerization of 7-X-4-hydroxyquinoline to 7-X-4-quinolone.

FAB High Resolution Mass Spectrometry (HRMS) returned accurate masses to five decimal places for all compounds.

2.2.1.3. ^{13}C-F Coupling

Carbon signals were assigned by HSQC where possible and by analogy to assignments made by Kaschula *et al.*[2, 90]

In all ^{13}C spectra obtained for **11a-e**, **11**, **12a-e** and **12**, a quartet (Figure 2.7.) due to C-F coupling was found at 129.3-129.8 ppm and 119.3-123.0 ppm for the SCF_3 and OCF_3 derivatives respectively. This confirmed that fluorine was present as three fluorine atoms in accordance with the multiplicity = 2nI + 1 (n = 3, I = ½) = **4** in which fluorine has a spin moment of a ½. These quartets were spread over ≈ 8 ppm, and their coupling constants were 308.1-308.6 Hz and 253.4-258.7 Hz for the SCF_3 and OCF_3 derivatives respectively, which are typical geminal coupling constants for C-F coupling.[98]

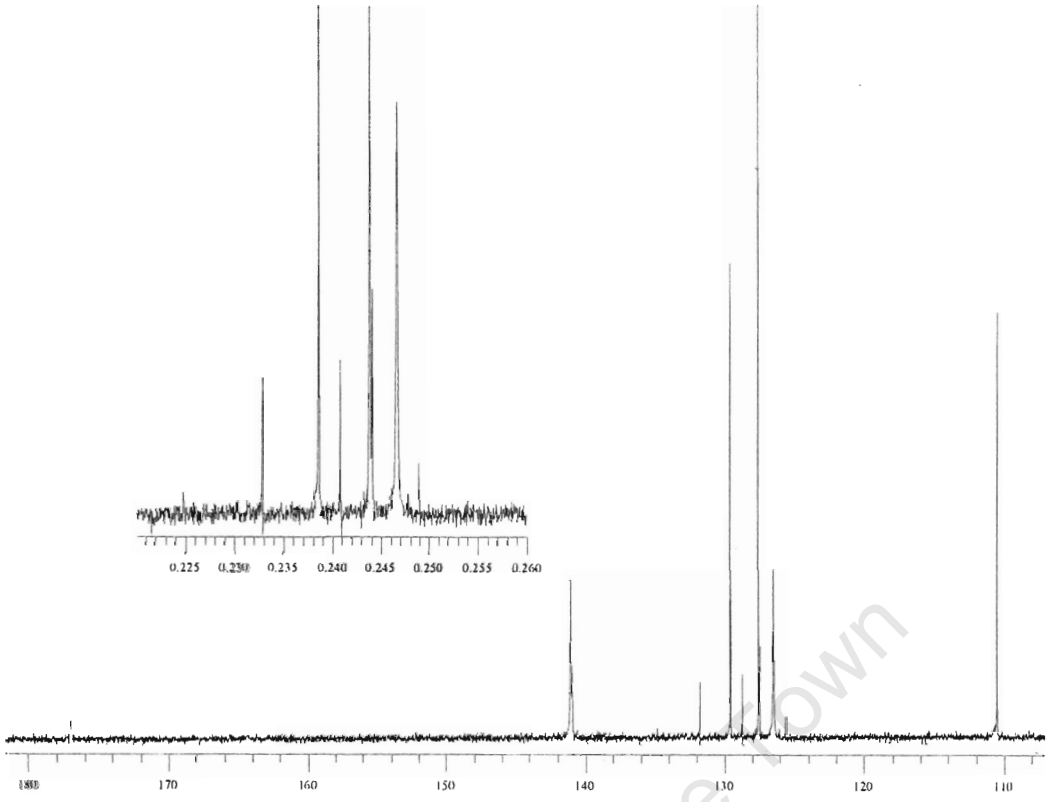

Figure 2.7. ^{13}C NMR spectrum of **11d** with an expansion of the quartet observed for SCF_3.

2.2.1.2. Mechanistic comments

The mechanism for thermal conversion of **11a/12a** to **11b/12b** has not been studied in detail before. Kaschula *et al.* [90] made the hypothesis that either a polar intramolecular nucleophilic substitution mechanism or a 6π-electrocyclic mechanism can be considered.[90]

The nucleophilic substitution mechanism (Scheme 2.7.) involves the attack of the aromatic ring on the carbonyl group to produce the polar intermediate (**A**) in the rate-determining step. Subsequent expulsion of ethanol followed by rapid tautomerism would lead to products **11b/12b**.

Mechanism 1.

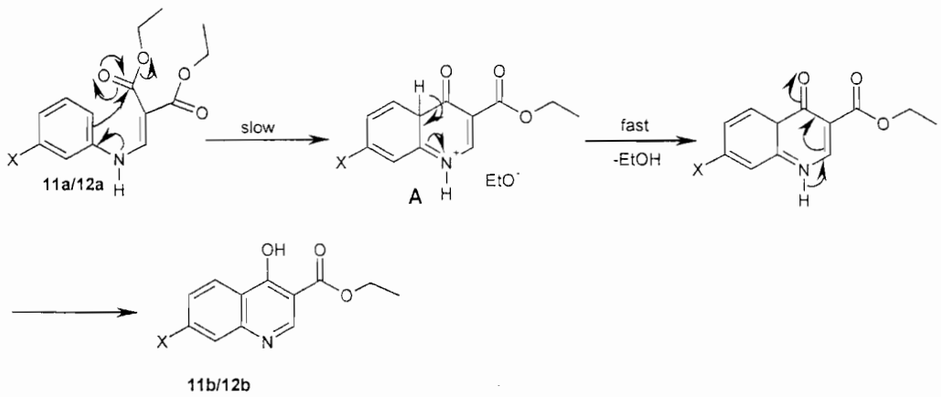

Scheme 2.7. The proposed cyclization mechanism 1 via a polar intermediate **A**.

In contrast, the 6π-electrocyclic mechanism would proceed via the formation of a reactive ketene intermediate (**C**), formed by an entropically driven (favoured by a high temperature) expulsion of ethanol. A subsequent disrotatory 6π-electrocyclic thermal rearrangement followed by tautomerism would give the products **11b/12b** (Scheme 2.8.).

Mechanism 2.

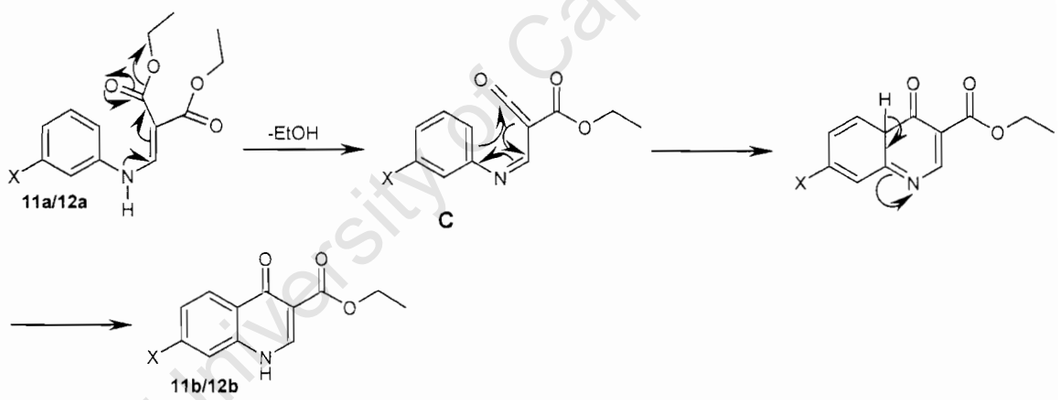

Scheme 2.8. The proposed cyclization mechanism 2 via a ketene intermediate **C**.

In an attempt to improve the yield of the cyclization reaction, **11a** was refluxed in different solvents (dichloromethane, tetrahydrofuran, and toluene) with boron

trifluoride etherate (Table 2.1.). Under these conditions no product formed. The normal reaction conditions were also altered by lowering the reaction temperature to 100-180°C and increasing the reaction times, which also gave poor conversion. The lack of any response to the Lewis acid activation, coupled with the high reaction temperature necessary for cyclization, appears to favour the proposed entropically-driven 6π-electrocyclic mechanism.

Solvent	Reagent	Temperature	Yield
Diphenyl ether		100°C	10%
Diphenyl ether		180°C	10%
Dichloromethane	$BF_3 \cdot Et_2O$	30°C	0%
Tetrahydrofurane	$BF_3 \cdot Et_2O$	66°C	0%
Toluene	$BF_3 \cdot Et_2O$	110°C	0%
Diphenyl ether		260°C	73-75%

Table 2.1. Different conditions applied to **11a** in an attempt to improve yields.

2.2.2. Synthesis of the 7-X-4-aminoquinolines

The 7-X-4-aminoquinoline analogues were synthesized from their respective 7-X-4-chloroquinolines **11e/12e** by nucleophilic substitution with commercially available *N,N*-diethylethylenediamine via heating together in a sealed thick-walled glass tube at 120-150°C for 4-5 hrs. Aqueous 10% NaOH was added to the product and the resulting yellow precipitate then extracted into dichloromethane, and the solvent dried and removed under reduced pressure. The residue was then chromatographed on silica gel using methanol and dichloromethane as eluent to give the free bases of **11**, **12** (Scheme 2.9.). Both compounds showed the expected signals for the 4-aminoethylated side chain in both the ^1H (Figures 2.8. and 2.9.) and ^{13}C NMR spectra confirming that substitution had taken place. All other data supported structures **11** and **12**.

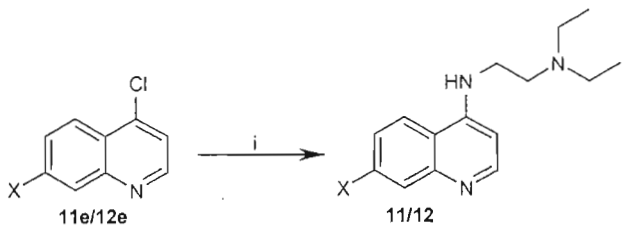

Scheme 2.9. Route to 7-X-4-aminoquinolines. Reagents and conditions. i. *N,N*-diethylethylenediamine, 120-150°C, 4-5 hrs.

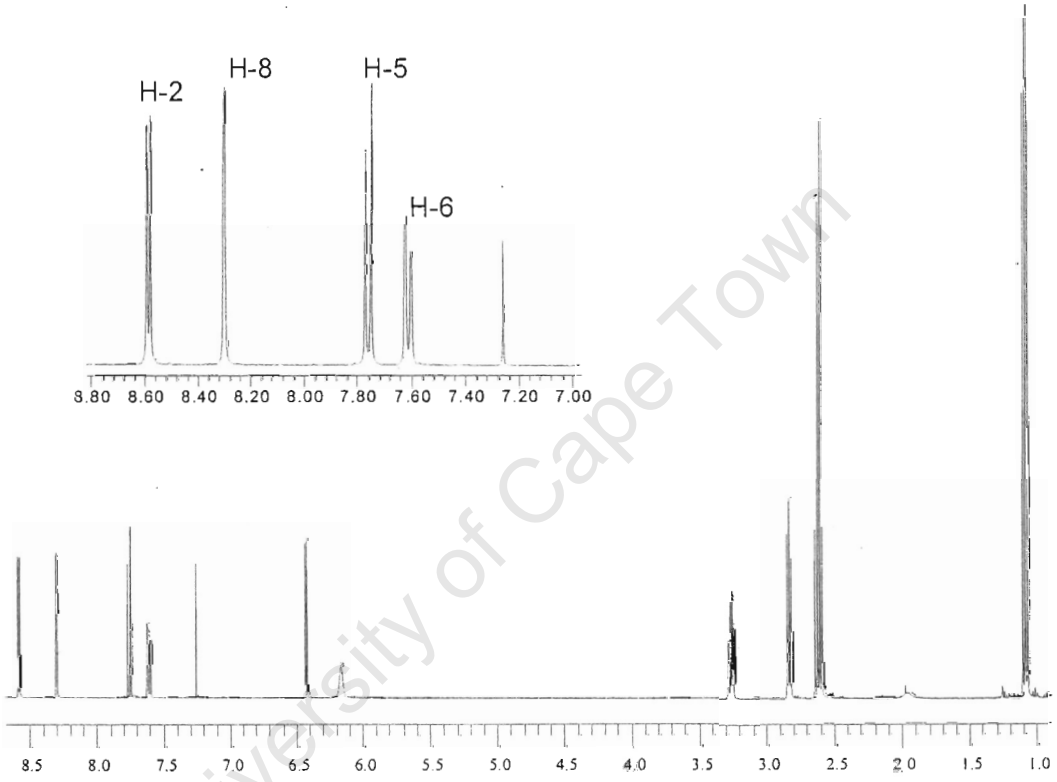

Figure 2.8. ^{1}H NMR spectrum of **11**. The expansion shows some aromatic protons.

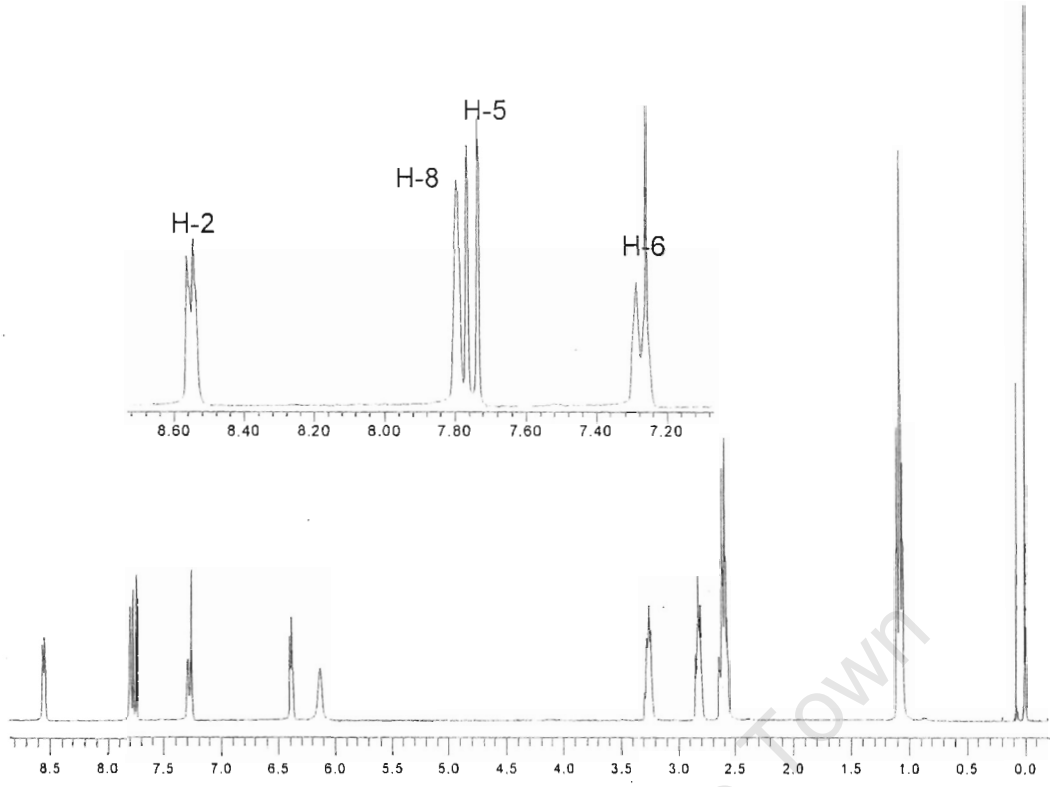

Figure 2.9. ^{1}H NMR spectrum of **12**. The expansion shows the aromatic and NH protons.

2.3. Aminoamidopiperazinyl side-chain

As discussed in the introduction of this chapter, part of the development plan was to work on both the 7-substituent as well as the 4-side chain. The design of a new side-chain was multi-faceted, having to take into account the number of nitrogens in the chain for improving accumulation as well as synthetic accessibility. In the event, a chain was identified incorporating a secondary amide as a connecting group as well as a piperazine ring in the view of the latter's well-known activity as a pharmacophore. As with chloroquine, a terminal primary amine group was identified as providing the connection to the heteroaromatic template. In the case of the benzimidazoles, this nitrogen would form part of the imidazole ring. Synthesis of the side-chain from simple building blocks is shown in scheme 2.10.

2.3.1. Synthesis

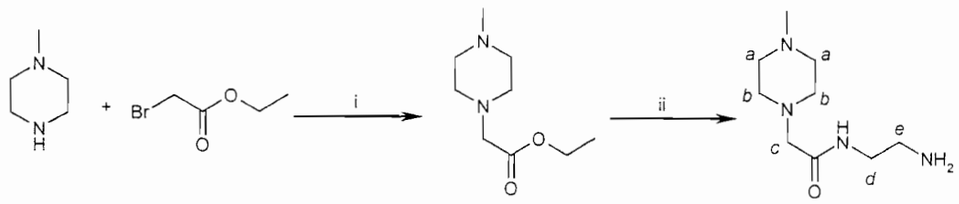

14a **14b**

Scheme 2.10. Synthesis route for the aminoamidopiperazinyl side-chain. Reagents and conditions: i. dichloromethane, , 0°-rt, 3 hrs; ii. ethylenediamine, 120°C, 4 hrs.

N-Methylpiperazine and diisopropylethylamine were added together with dichloromethane as solvent and cooled to 0°C. Ethyl bromoacetate was slowly added over 10 minutes. After 3 hrs the reaction mixture was filtered to remove the Hünig's base salt formed. The solvent was removed under reduced pressure and the crude product vacuum distilled to yield ester **14a**, as a colourless oil with a very low viscosity.

The ester **14a** and excess ethylenediamine were stirred at 120°C for 4 hrs, after which time TLC (dichloromethane, methanol and ammonia solution, 80:19:1) indicated the disappearance of starting material and the formation of a more polar product. The excess ethylenediamine was removed under reduced pressure and the resulting crude product was vacuum distilled to yield **14b** as a viscous yellow oil. Carbonization of the crude product at the high temperature made the distillation difficult and lowered the overall yield. An aqueous work-up and column chromatography of **14a** and **14b** was avoided because of the high polarity of these compounds. Rf values for **14a-b** were 0.4 and 0.05 respectively on TLC with dichloromethane, methanol and ammonia solution as the mobile phase (80:19:1).

The ^{1}H NMR spectra for **14a** and **14b** showed characteristic chemical shifts and splitting patterns for the piperazinyl region. The *N*-CH_3 singlet was observed at 2.21-2.23 ppm in the ^{1}H NMR spectra for **14a** and **14b**. The piperazinyl protons, assigned for positions *a* and *b*, were observed as two broad single peaks at 2.40-2.42 and 2.51-2.55 ppm respectively integrating for two sets of 4 protons. The *b*-position was more deshielded due to the electron withdrawing effect of the amide. This was

confirmed with an HSQC of **14d**. The ^{13}C NMR spectrum gave the correct number of resonances for **14b** (7).

2.4. Synthesis of 5-chloro-1-aminoalkylated benzimidazoles.

Two approaches were followed for the synthesis of the 5-chlorobenzimidazoles; approach 1, which yielded regioisomers, and approach 2 which was regioselective.

2.4.1. Approach 1.

The route followed by approach 1 yielded the 5-chloro regioisomer **13** and its 6-chloro regioisomer (Scheme 2.11.) which could not be separated.

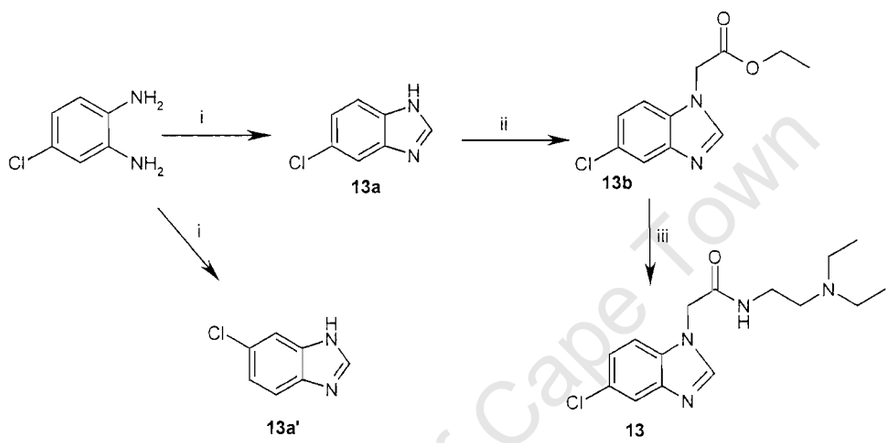

Scheme 2.11. Regioisomeric route to 5-chlorobenzimidazole **13**. *Reagents and conditions.* i. trimethylorthoformate, $BF_3.Et_2O$, dichloromethane, 0°C, 4 hrs; ii. ethyl bromoacetate, sodium hydride, tetrahydrofuran, -78°C, 30 minutes; iii. *N,N*-diethylethylenediamine, 100°, 45 minutes.

4-chloro-1,2-phenylenediamine was reacted with trimethyl orthoformate in dry dichloromethane, and the solution was cooled to 0°C before adding boron trifluoride etherate. After 4 hrs when TLC indicated complete conversion of starting material, the reaction mixture was poured into aqueous Na_2CO_3. The compound was then extracted into ethyl acetate followed by dichloromethane, and the organic extracts dried. The solvent was removed under reduced pressure and the oily residue chromatographed on silica gel using equal parts of petroleum ether and ethyl acetate as eluent to yield **13a** and **13a'** as a yellow solid, which formed amorphous crystals in

a mixture of ethyl acetate and petroleum ether. The formation of the imidazole ring was confirmed by the appearance of a singlet at 8.16 ppm in the ^{1}H NMR spectrum for H-2. The ^{1}H and ^{13}C NMR spectra of revealed two sets of resonances, which were tentatively assigned as the two regioisomers **13a** and **13a'** (scheme 2.11.). Interestingly, these appeared not to equilibrate to one thermodynamically more favoured form.

In the next step sodium hydride was added to a cooled solution (0°C) of **13a/13a'** in dry tetrahydrofuran. For clarity sake, Scheme 2.11. only shows the conversion of **13a**, although in practice both regioisomers were converted. The mixture was stirred for 1 hr during which a colour change of orange to green was observed. The mixture was then cooled to -78°C and ethyl bromoacetate was slowly added over 10 minutes. After 30 minutes the reaction mixture was quenched with saturated ammonium chloride solution. The product was then extracted with ethyl acetate and dried. All solvent was then removed under reduced pressure and the product recrystallized from ethyl acetate to yield **13b/13b'** (60%). The ^{1}H NMR spectrum for **13b/13b'** again showed a double set of signals, indicative once again of the regioisomers. A major to minor set of integrals were observed and the major set was picked out and assigned for one isomer **13b** (arbitrarily assigned).

The mixture of isomers **13b/13b'** was then stirred in *N,N*-diethylethylenediamine in a sealed vessel under N_2 at 100°C for 45 minutes. The excess *N,N*-diethylethylenediamine was removed under reduced pressure. The resulting oil was then column chromatographed on silica gel with a mixture of dichloromethane and methanol (80:20) as eluent. This yielded a non-crystalline solid, **13/13'** (73%). Once again, two sets of signals were observed in the ^{1}H NMR spectra, which further supported the presence of regioisomers. Only the set of signals for one of the isomers is recorded in the experimental section, and has been arbitrarily associated with **13** in the text, although a true assignment of individual isomers was not possible. The appearance of a singlet for H-2 at 7.90 ppm for the imidazole ring and the resonances for the aliphatic *N,N*-diethylethylenediamino side chain were noted in the ^{1}H NMR spectrum. The correct number of ^{13}C NMR resonances (13 for each isomer) together with an accurate mass from FAB High Resolution Mass Spectrometry (HRMS) was further evidence that structure **13** was obtained in the product mixture. At this point it was decided to develop a regioselective route, in view of the difficulty in developing an authentic structure-activity profile.

2.4.2. Approach 2.

A regioselective synthetic route was needed to overcome the difficulties associated with the regioisomeric route discussed in section 2.4.2. It would entail differentiating the two nitrogens of 4-chloro-1,2-phenylenediamine in order to N-substitute the nitrogen *para* to the chlorine. A survey of the literature revealed that in 1969, Heindel *et al.* reported the synthesis of chloroquine-analogous benzimidazoles (Scheme 2.12.) in which commercially available 2,5-dichloronitrobenzene was used for the above mentioned purpose.[89] The route involved nucleophilic monosubstitution of 2,5-dichloronitrobenzene at the 2-position followed by nitro group reduction and cyclization using EMME. This route yielded only the desired 5-chloroisomer in the benzimidazole class.

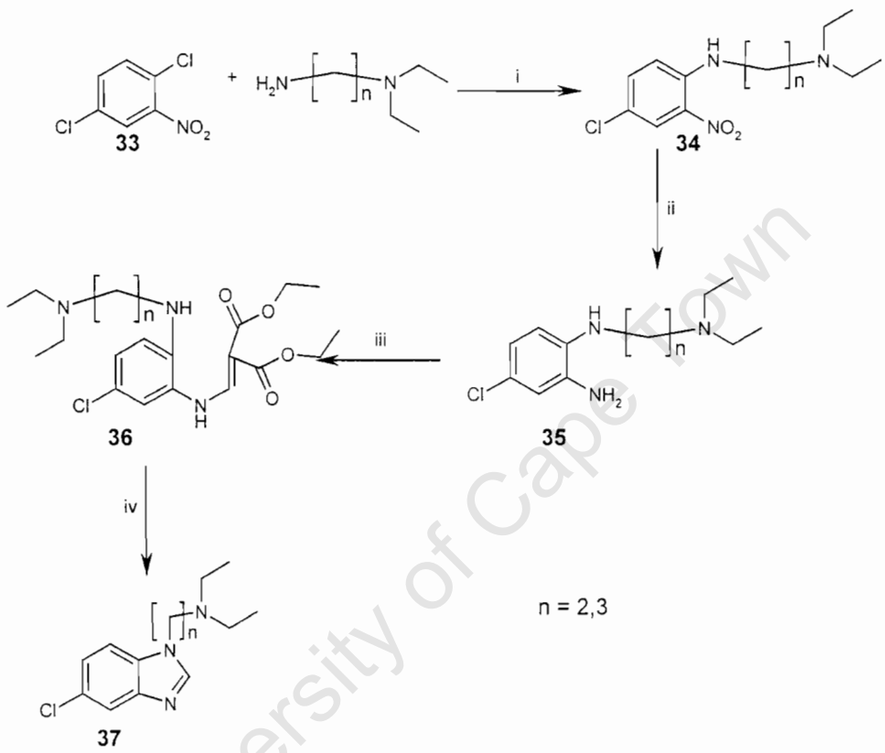

Scheme 2.12. Synthetic route to **37** as reported by Heindel *et al.*[89] *Reagents and conditions*. i. reflux, 3 hrs; ii. stannous chloride, HCl conc., 10°C-rt 2 hrs; iii. EMME, 100°C. iv. diphenyl ether, reflux, 20-30 minutes.

Heindel's route involved reacting equimolar amounts of the dialkylaminoalkylamine and 2,5-dichloronitrobenzene **33** under reflux for 3 hrs in a nucleophilic substitution reaction. The material was poured into water, basified with aqueous NaOH and

extracted thoroughly (diethyl ether). The residue from the concentrated ethereal phase was either vacuum distilled or recrystallized in the case of solids to yield **34** in 80-84%.

The coupled nitro derivative **34** was dissolved in HCl and slowly added to a chilled solution of stannous chloride over 5 minutes. The temperature was maintained at 10°C or lower. This was allowed to stir at room temperature for 2 hrs whereafter it was added to chilled aqueous NaOH and extracted into diethyl ether. The dried extract was evaporated *in vacuo* and the resultant oily diamine **35** used directly in the cycle-forming reaction.

The crude amine **35** was heated on a steam cone with EMME until the theoretical amount of ethanol had evolved. The oily adduct **36** was then added to refluxing diphenyl ether and heated for 20-30 minutes. The diphenyl ether was removed by distillation and the benzimidazole **37** was fractionated under vacuum in 52-64% yield [89].

A synthetic variation on the final (cyclization) step in the synthesis of **14** was provided by Knobloch *et al.* [88] (Scheme 2.13). Instead of forming the adduct **36** with EMME and performing a thermal cyclization to yield **37**, they used the method of Phillips [99] in which **38** was dissolved in HCl and added to a diluted solution of methanoic acid. The reaction mixture was heated to 120°C for 6 hrs whereafter the product was vacuum distilled to yield **39** in 84%.

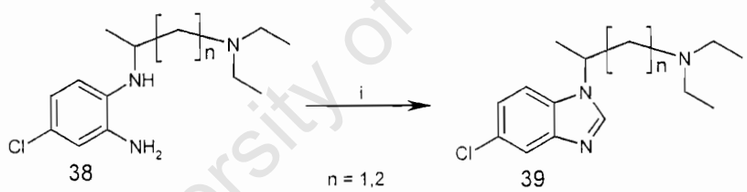

Scheme 2.13. Implementation of the Phillips' method by Knobloch *et al.* [88]. *Reagents and conditions.* i. methanoic acid, reflux, 6 hours.

Both these routes were reported to be regioselective and a combination of them were used in the synthesis of **14** (Scheme 2.14.).

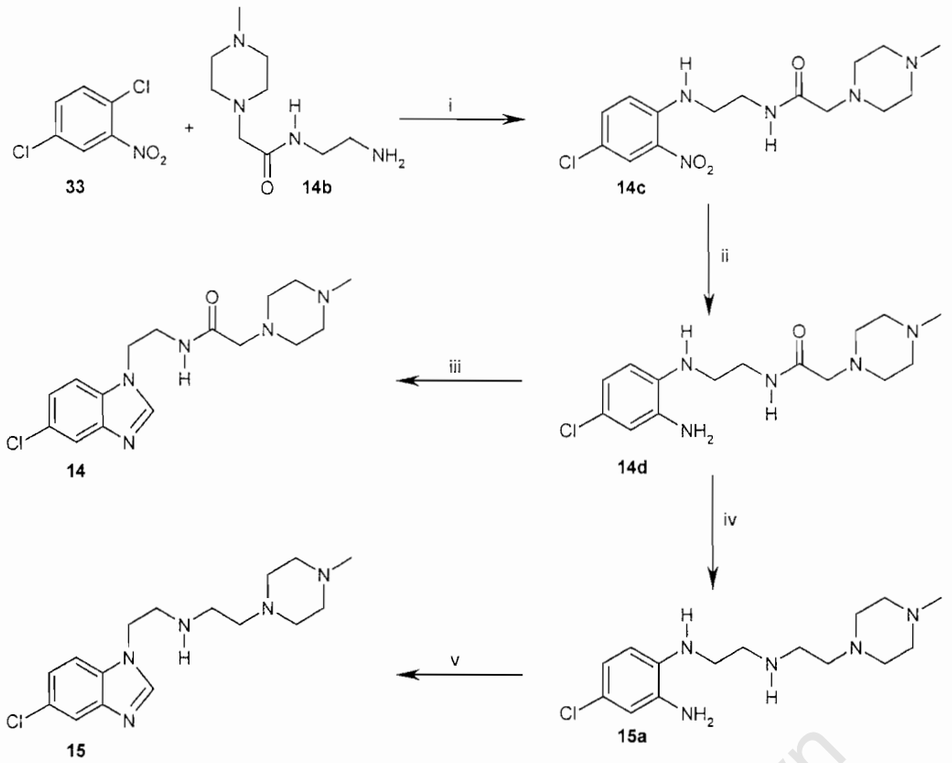

Scheme 2.14. Synthesis route to **14** and **15**. *Reagents and conditions*. i. dimethylformamide, reflux, 3 hrs; ii. stannous chloride, HCl conc., 0°-rt, 2hrs; iii. methanoic acid, HCl conc., 120°C, 2.5 hrs; iv. $LiAlH_4$, tetrahydrofuran, 70°C, 60 hrs; v. methanoic acid, HCl conc., 120°C, 1 hrs.

To this end a solution of **14b** and 2,5-dichloronitrobenzene in dimethylformamide was refluxed for 3 hrs whereafter the reaction mixture was cooled and basified with 10% NaOH. The product was then extracted into ethyl acetate. After a charcoal clean, the solvent was removed under reduced pressure and the solid recrystallized from ethyl acetate and petroleum ether to yield orange crystals of **14c**. Its infrared spectra showed the presence of a carbonyl group in the 1700 cm^{-1} region. Its ^1H NMR spectrum integrated for the correct number of protons and revealed two broad singlets at 7.44 ppm for the amide NH and 8.04 ppm for the aromatic NH. The correct number of resonances (13) were observed in the ^{13}C spectrum.

14c was dissolved in conc. HCl and added to a chilled solution of stannous chloride in conc. HCl. After 2 hrs the reaction mixture was poured into ice and basified by adding a stoichiometric amount of NaOH pellets to the solution. The product was extracted into ethyl acetate twice and once into dichloromethane and dried. The

solvent was removed under reduced pressure and the resultant solid recrystallized from ethyl acetate to yield purple crystals of **14d** in a yield of 94%. Three broad singlets were now observed for NH protons at 3.45 ppm (NH_2), 3.79 ppm (aromatic NH) and at 7.42 (amide NH) at a similar chemical shift to **14c**.

14d was added to a 10% solution of formic acid. The mixture was then acidified with conc. HCl and heated to 120°C for 2.5 hrs. On TLC (dichloromethane, methanol and ammonia solution, 80:19:1) **14** retained the same Rf value as **14d**. After cooling to room temperature, the product was extracted into ethyl acetate and dried. All solvent was removed by reduced pressure and the target product recrystallized from ethyl acetate to yield pink crystals of **14** (87%). Cyclization to the benzimidazole was evident from the appearance of a new singlet in both the ^{1}H (7.84 ppm) and proto-decoupled ^{13}C (144.1 ppm) NMR spectra for H-2 and C-2 respectively of the 5-membered ring.

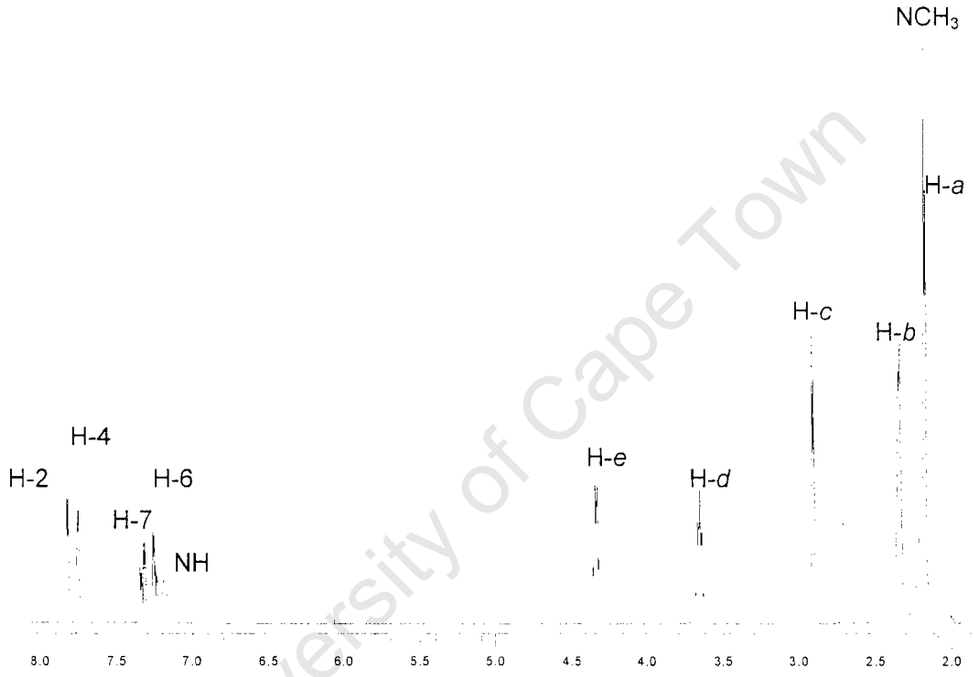

Figure 2.10. ^{1}H NMR spectrum of **14**.

It was then decided to reduce the amide in the side chain to introduce another basic nitrogen to potentially enhance biological activity. This could only be done by reduction of **14d** since the benzimidazole C=N double bond is more easily reduced than that of the amide C=O group and would therefore be reduced in an attempt to

reduce the amide in **14**. Although a number of reagents are available for reduction of secondary amides to secondary amines, lithium aluminium hydride ($LiAlH_4$) was selected for the task. Thus **14d** was heated at 70°C with $LiAlH_4$ in dry tetrahydrofuran in a thick-walled glass tube with a pressure seal in order to allow heating above the boiling point of the solvent (66°C). The mixture was first stirred at room temperature for 1 hr and then heated to 70°C for 60 hrs during which it was monitored by TLC (dichloromethane, methanol and ammonia solution, 80:19:1) at intervals until it appeared that no further reduction was achieved. On cooling, the product was slowly quenched with a chilled mixture of tetrahydrofuran, triethylamine and water (8:1:1). This mixture was stirred until the colourless aluminium salts had formed and then filtered through Celite. The organic solution was dried and removed under reduced pressure to yield a mixture of **14d** and the reduced amide, **15a** (scheme 2.14.), as a purple oily residue. Rather than purifying at this stage, **15a** was subjected to cyclization in view of its high polarity towards column chromatography.

Thus the crude product was added to a 10% solution of methanoic acid. The mixture was then acidified with HCl conc. and heated to 120°C for 1 hr. On cooling, the excess water was azeotropically removed with toluene under reduced pressure. The crude material was chromatographed with a mixture dichloromethane, methanol and ammonia solution (80:19:1) as eluent, to give **15**. The ^1H NMR spectrum showed the presence of four quartets in the region of 2.5-4.5 ppm accounting for the four methylene groups in the side chain. The H-2 singlet for the imidazole ring appeared slightly more downfield (8.12 ppm). FAB High Resolution Mass Spectrometry (HRMS) returned an accurate mass to five decimal places for **15**. The polar character of **15** prevented successful column chromatographic purification thereof and the crude product was submitted for biological assays.

2.5. 7-Chloro-4-aminoamidopiperazinylquinolines

With the aminoamidopiperazinyl side-chain successfully synthesized and introduced into the benzimidazoles, all that remained was to establish the effect of the benzimidazole template on biological activity. This was achieved by synthesizing and comparing the analogous 4-aminoquinoline **16** (Figure 2.11.) of the

benzimidazole target **14**, in which only the aromatic nucleus is structurally different to **14**.

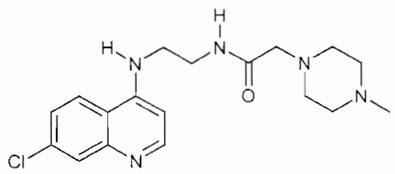

16

Figure 2.11. The 4-aminoquinoline **16** which is analogues of the benzimidazoles **14**.

The 7-chloro-4-aminoquinoline **16** was synthesized from 4,7-dichloroquinoline by nucleophilic substitution with the aminoamidopiperazinyl side chain **14b** with dimethylformamide as solvent in a sealed tube at 120-150°C for 4-5 hrs. The reaction was folowed by TLC (dichloromethane, methanol and ammonia solution, 90:10:0.1) in which **16** had a Rf value of 0.7. For the formation of **16**, potassium fluoride was added to promote coupling. The reaction mixture was poured into water to selectively extract the aminoamidopiperazinyl side chain. The pH was adjusted to basic with potassium hydroxide solution and the product extracted with ethyl acetate, dried and the solvent removed under reduced pressure. The product was then recrystallized to give the free base of **16** (Scheme 2.14.). A characteristic singlet in the ^{1}H NMR spectrum of **16** for the methylene group α to the amide carbonyl was observed at 2.82 ppm as well as a multiplet integrating for the 4 protons of the other two aliphatic methylene groups at 3.34 ppm. The ^{13}C NMR spectrum showed a C=O carbon resonance downfield at 169.9 ppm. Correct integration of the aliphatic and aromatic protons revealed substitution had successfully taken place.

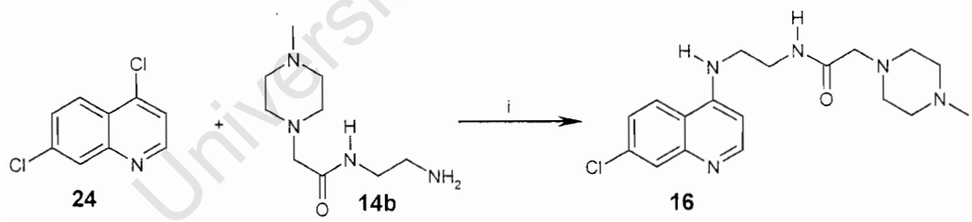

24 **14b** **16**

Scheme 2.14. Synthesis of the chloroquinoline substituted with aminoamidopiperazinyl side-chain. Reagents and conditions: i. dimethylformamide, potassium fluoride, 120-150°C, 4-5 hrs.

The attempt at the end of this project to reduce the amido side-chain of **16** with lithium aluminium hydride at 70°C in a sealed tube for 3 hours, failed. Mass Spectrometry of the product revealed that it did not form under these conditions.

3. Structure-activity relationships.

In this chapter the results of the structure-activity relationship (SAR) and quantitative structure-activity relationships (QSAR) studies of compounds **9** and **11-16** will be discussed.

3.1. QSAR of short chain 4-aminoquinolines.

QSAR studies were performed on a number of previously reported short-chain analogues of chloroquine [2] to which compounds **11** and **12** were compared (Figure 3.1.)

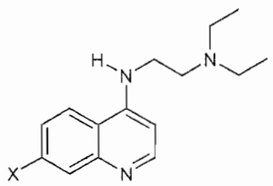

X = (a) NH_2,(b) OH, (c) OCH_3, (d) H, (e) CH_3, (f) F, (g)I, (h) Br, (i) Cl, (j) CF_3, (k) NO_2, (11) SCF_3, (12) OCF_3

Figure 3.1. The short-chain analogues of chloroquine where group X was varied.[2]

3.1.1. Acid dissociation constants

Results for pKa_1 (quinoline ring nitrogen) and pKa_2 (tertiary nitrogen of the side-chain) are shown in table 3.1.

7-position substituent	pKa_1 observed	pKa_2 observed	pKa_1 predicted*	pKa_2 predicted*
SCF_3	6.56 ± 0.06	8.28 ± 0.05	7.44	8.22
OCF_3	6.97 ± 0.1	8.41 ± 0.06	7.48	8.28

Table 3.1. Results for pKa_1 and pKa_2 compared with predicted values for SCF_3 and OCF_3 derivatives (* see table 1.2.). The observed pKa values are a mean of three determinations ± the standard error of the mean.

The observed pKa_1 values for SCF_3 and OCF_3 compare poorly with the predicted pKa_1 values whereas the observed pKa_2 values compared very well and in fact are identical for the SCF_3 value within experimental error.

The observed values for the SCF_3 and OCF_3 and other short chain analogues [2] were plotted against the para- and meta-Hammett (σ_p and σ_m) constants for the group in the 7-position of the quinoline ring respectively (Figure 3.2.). The improved p value and a similar r^2 value suggests that using the linear free energy equation with the σ_p constant gives a better predictive equation for the short chain analogues.

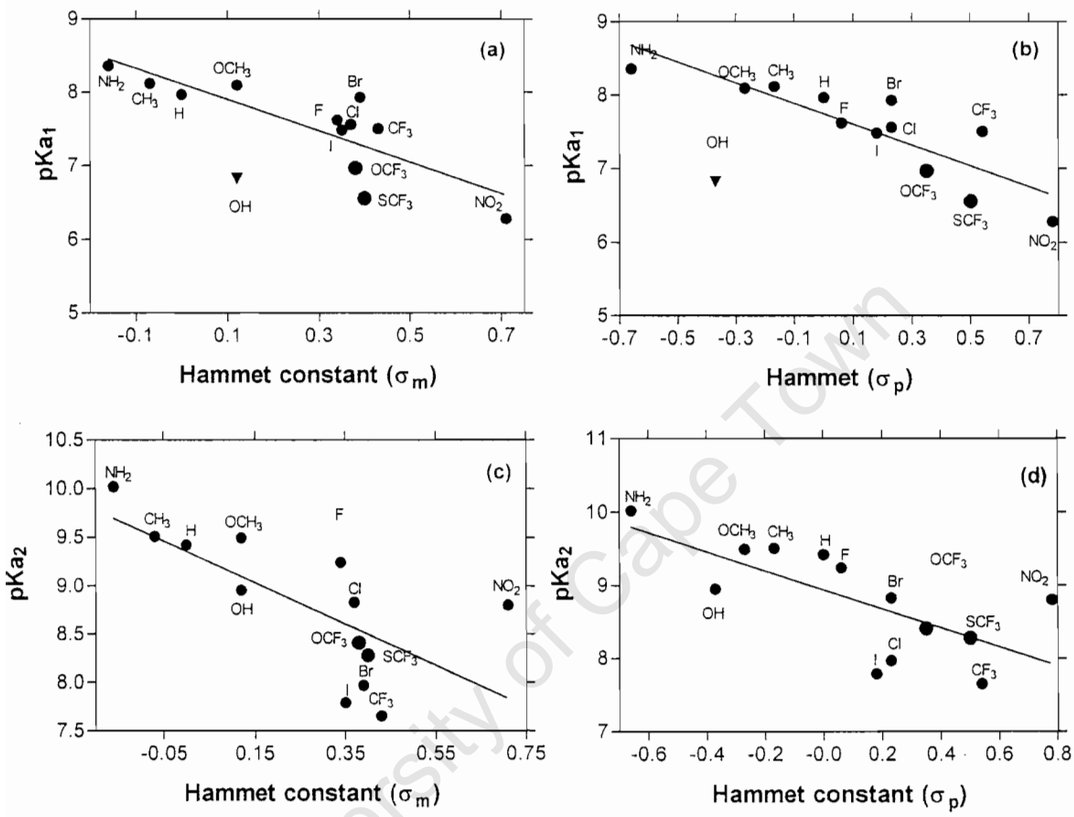

Figure 3.2. (a) Correlation between the quinoline nitrogen pKa (pKa_1) and the Hammett constant for the meta position (σ_m) of the group at the 7-position of the quinoline ring in compounds **a-k**, **11** and **12**. Without the OH derivative the data conform to the empirical equation $pKa_1 = -2.13\sigma_m + 8.1$ ($r^2 = 0.68$, $P = 0.001$). (b) Correlation between the quinoline nitrogen pKa (pKa_1) and the Hammett constant for the para position (σ_p) of the group at the 7-position of the quinoline ring. Without the OH derivative the correlation improves significantly [2] and the data conform to the empirical equation $pKa_1 = -1.41\sigma_p + 7.7$ ($r^2 = 0.745$, $P = 0.0003$). (c) Correlation between the pKa of the lateral chain terminal amino group (pKa_2) and Hammett constant for the meta position of the group at the 7-position on the quinoline ring.

Data conform to the empirical equation $pKa_2 = -2.06\sigma_m + 9.4$ (r^2 = 0.464, P 0.600). The NO_2 derivative appears to conform poorly to this correlation as identified in the original study.[2] Its omission leads to a significantly better correlation: $pKa_2 = -3.19\sigma_m + 9.5$ (r^2 = 0.697, P 0.0026) (d) Correlation between the pKa of the lateral chain terminal amino group (pKa_2) and Hammett constant for the para position (σ_p) of the group at the 7-position on the quinoline ring. Data conform to the empirical equation $pKa_2 = -1.29\sigma_p + 8.9$ (r^2 = 0.46, P = 0.021). The NO_2 derivative appears to conform poorly to this correlation. Its omission leads to a significantly better correlation: $pKa_2 = -1.91\sigma_p + 8.8$ (r^2 = 0.6694, P 0.0038).

In a previous study σ_m was proposed for the calculation of pKa values because the correlation was marginally better than that with the σ_p.[2] As can be seen in figure 3.2.d, the pKa_2 values show a good correlation with σ_p when SCF_3 and OCF_3 are included. Thus a better correlation is found with σ_p for both pK_a values.

3.1.2. Association constants

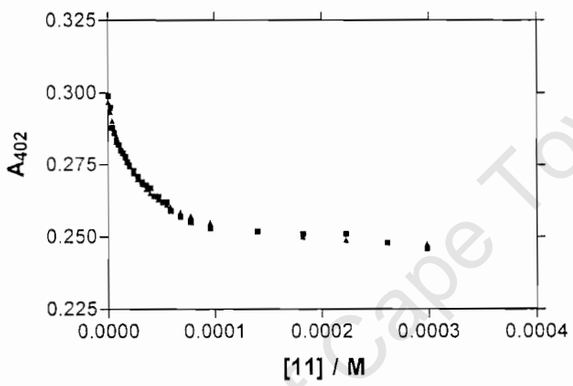

Figure 3.3. A typical spectrophotometric titration for log K determination (e.g. **11**)

The results for the association constant assay (log K) are shown in table 3.2 (e.g. **11**, Figure 3.3.).

X	Observed log K*	Predicted log K**
SCF_3	4.85 ± 0.03	5.13
OCF_3	4.66 ± 0.06	5.01

Table 3.2. Log K results compared with the predicted values for SCF_3 and OCF_3 derivatives. * log K was obtained using a 1:1 association model derived by Mavuso [100] and values are a mean of three determinations ± the standard error of the mean. ** See table 1.2.

Values for SCF_3 and OCF_3 were plotted on the same graph as values for derivatives **a-k** (Figure 3.4.). On this graph the SCF_3 and OCF_3 derivatives lie significantly below the line like the CF_3 derivative, possibly as suggested previously [2] because of their relatively large steric bulk. This would explain the poor agreement of observed log K values for SCF_3 and OCF_3 with predicted values. An almost parallel trend line can be fitted to these three points which may indicate a new family of compounds with their own linear free energy correlation (dotted line in Fig.3.4.), however owing to the fact that there are only three of these derivatives, a statistically significant correlation for these compounds cannot be extracted from the current data.

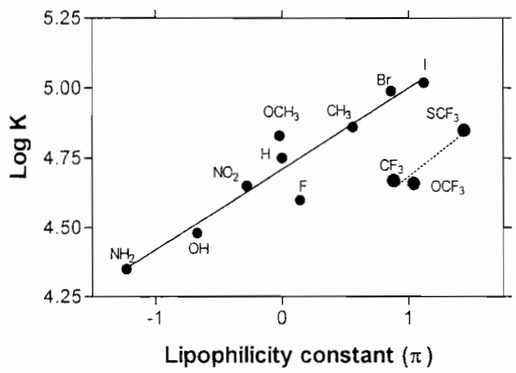

Figure 3.4. Correlation between haematin-aminoquinoline association constant (log K) and the lipophilicity constant (π) for the substituent at position-7 on the quinoline ring [2] to which data for the SCF_3 and OCF_3 derivatives have been added. The data for the Cl derivative (log K = 5.81) is not shown because it lies far above the remaining data. The data for CF_3, SCF_3 and OCF_3 were also not used in the correlation. The remaining points conform to the empirical equation $\log K = 0.290\pi + 4.71$ ($r^2 = 0.89$, $P = 0.0001$).[2] The CF_3, SCF_3 and OCF_3 derivatives may form their own new linear free energy relationship line (.....).

3.1.3. β-Haematin inhibitory activity (BHIA)

The qualitative infrared BHIA assay for SCF_3 and OCF_3 showed inhibitory activity for both compounds. The results of a typical infrared assay are shown in figure 3.5. The results for the quantitative $BHIA_{50}$ analysis are shown in table 3.3.

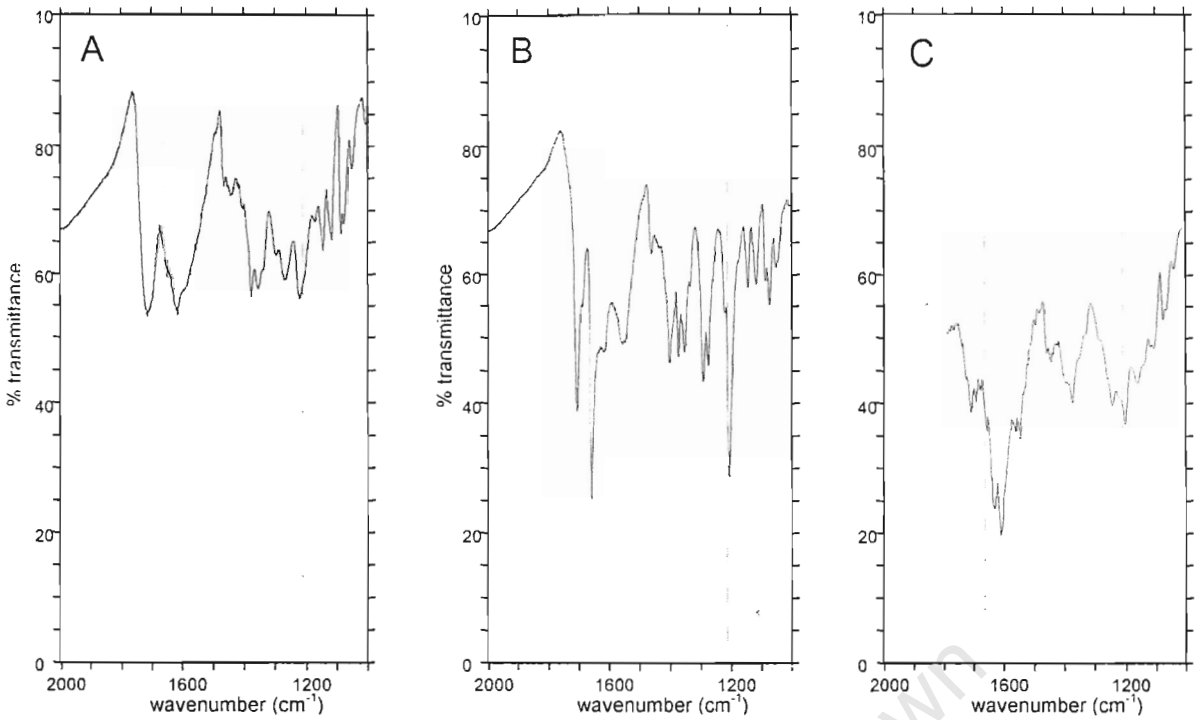

Figure 3.5. Infra-red spectra of (A) haematin, (B) β-haematin and (C) the product formed in the presence of 12 obtained as KBr discs in the region 2000 cm^{-1} – 1000 cm^{-1}. The dotted lines are at 1662 cm^{-1} and 1210 cm^{-1}. Absence of a peak at 1660 cm^{-1} in the presence of **12** indicates that it has inhibited β-haematin formation

X	Observed	Predicted*	New prediction **
SCF_3	2.1 ± 0.2	3.8	5.4
OCF_3	4.2 ± 0.2	4.6	7.1

Table 3.3. $BHIA_{50}$ results for SCF_3 and OCF_3 derivatives compared with predicted values. The observed values are a mean of two determinations done in triplicate ± the standard error of the mean.
* See table 1.2. ** Prediction based on observed log K value.

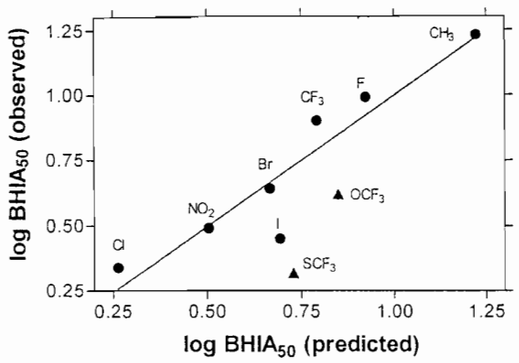

Figure 3.6. β-haematin inhibitory activity correlated with both the association constant for haematin-aminoquinoline association and the σ_m according to the empirical equation log $BHIA_{50}$ = -(0.519)(log K) – $1.06\sigma_m$ + 3.67. (r^2 = 0.87; and for both of the parameters log K and σ_m *P* lies in the range 0.01 – 0.02). SCF_3 and OCF_3 were not included in the linear relationship.

The observed $BHIA_{50}$ (Figure 3.6.) value for the SCF_3 derivative compares very poorly with the original predicted value (Table 1.2.), while that for the OCF_3 is better. However, if the observed log K values are used to predict the $BHIA_{50}$ values, there is a very poor correlation with the predicted values. This suggests that the correlation of the quantitative structure-activity relationship used to predict log $BHIA_{50}$ previously may indeed be fortuitous as originally suggested [2] or the SCF_3 and OCF_3 derivatives may be outliers and that they interact with haematin in a manner that is structurally quite distinct from the remaining compounds.

3.1.4. Correlation of IC_{50} with $BHIA_{50}$ and pKa

The results for the antiplasmodial test of the SCF_3 and OCF_3 derivatives are shown in table 3.4.

X	Observed IC_{50} (D10 CQ sensitive strain)	Observed IC_{50} (K1 CQ resistant strain)	Predicted IC_{50}
SCF_3	94 ± 22 nM	81 ± 5 nM	55 nM
OCF_3	164 ± 24 nM	103 ± 19 nM	60 nM

Table 3.4. IC_{50} values of SCF_3 and OCF_3 derivatives against the D10 chloroquine sensitive strain and K1 chloroquine resistant strain of *P. falciparum* compared with their predicted values. The observed values are a mean of two determinations done in triplicate ± the standard error of the mean.

The observed IC_{50} value for SCF_3 against the D10 strain falls within one standard deviation of the observed IC_{50} against the K1 strain, while for the OCF_3 it falls within three standard deviations. Thus there is no significant difference in activity against the chloroquine sensitive and resistant strains. This finding is probably to be expected for these short chain analogues, which have been shown to retain activity against chloroquine resistant *P. falciparum* in a previous study [81] of analogues containing other groups at the 7-position.

Kaschula *et al.* showed an excellent linear correlation between the log of the accumulation normalized antiplasmodial activity and the log of the β-haematin inhibitory activity (r^2 = 0.83, P = 0.0043). SCF_3 and OCF_3 were plotted on this correlation graph and agreed excellently with the linear relationship (Figure 3.7.).[2]

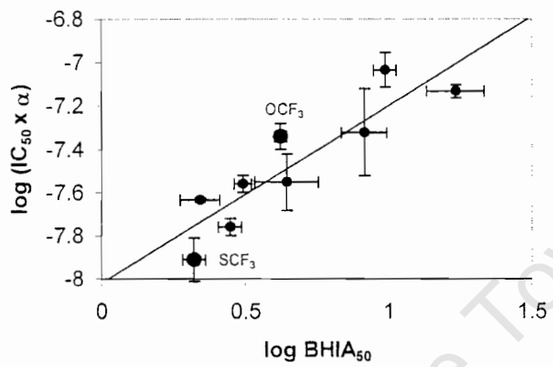

Figure 3.7. Linear correlation between the log of the normalized antiplasmodial activity and the log of the β-haematin inhibitory activity (r^2 = 0.80, P = 0.0011 compared to r^2 = 0.83, P = 0.0043 when SCF_3 and OCF_3 are omitted [2]).

The considerably decreased p value for the linear relationship when SCF_3 and OCF_3 are included indicates that statistically the data set improved even although the r^2 value decreased slightly. The y-intercept (-8.01 ± 0.1) and the coefficient of log $BHIA_{50}$ (0.82 ± 0.15) for the linear equation fall within 1 standard deviation of the previously reported equation [2] which shows that inclusion of SCF_3 and OCF_3 does not significantly alter the predictive equation for log $BHIA_{50}$. This finding suggests that the SCF_3 and OCF_3 derivatives have excellent activity at the proposed vacuolar site of action and that the poor observed activity against strains of *P. falciparum* is probably the result of the low pKa_1 for the SCF_3 and OCF_3 derivatives, which would cause less accumulation in the acidic food vacuole of the parasite.

Thus the findings for these new compounds strongly support the hypothesis that the activity of this class of compound depends on the ability to inhibit haemozoin formation and to accumulate in the food vacuole through pH trapping.

3.2. 5-Chlorobenzimidazoles

The results of SAR studies done on 5-chlorobenzimidazoles **13a**, **13-14** (Figure 3.8.) will be reported and discussed in this section.

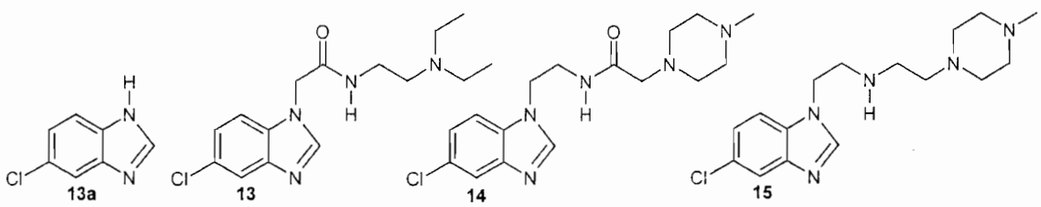

Figure. 3.8. Benzimidazole target compounds tested.

3.2.1. Acid dissociation constants

Results for determination of pKa_1 (benzimidazole ring nitrogen at 3-position) and pKa_2 (the tertiary amine nitrogen in the side-chain) compounds **13** and **14** are shown in table 3.5.

Compound	pKa_1	pKa_2
13	3.70 ± 0.2	8.90 ± 0.02
14	4.46 ± 0.04	8.30 ± 0.03

Table 3.5. Results of pKa_1 and pKa_2 determinations for **13** and **14**. The observed values are a mean of two determinations ± the standard error of the mean.

These values agree with pKa values (pKa_1 = 3.2-3.9 and pKa_2 = 8.1-9.9) determined by Knobloch *et al.*, for chloroquine-like benzimidazoles **9** [88] reviewed in section 1.8. From these values for **13** and **14** little vacuolar accumulation can be expected (AR **13** = 78, AR **14** = 77 and AR chloroquine = 5896).

3.2.2. Association constants

Association constants for interaction with haematin were determined by spectrophotometric determination. The observed log K values are reported in table 3.6.

Compound	log K*
13a	4.40 ± 0.09
13	4.78 ± 0.04
14	4.21 ± 0.14

Table 3.6. Results of log K determinations. * log K was obtained using a 1:1 association model derived by Mavuso [100] and values are a mean of three determinations ± the standard error of the mean.

The log K values for benzimidazoles **13a**, **13** and **14** are similar to previously published log K values for 4-aminoquinoline analogues [46].

3.2.3. BHIA by infrared

Infrared spectroscopy was used to determine whether these benzimidazoles were able to inhibit β-haematin formation. Results for the BHIA assay by infrared are shown in table 3.7.

Compound	BHIA (+/-)*
13a	+
13	-
14	-

Table 3.7. Results obtained from BHIA infrared assay. *(+) – active; (-) – inactive.

Previously unpublished studies in our laboratory showed that benzimidazole itself does not have β-haematin inhibitory activity. When a chlorine is introduced in the 5-position (**13a**), β-haematin inhibitory activity is observed, although introduction of the aminoamidopiperazinyl side-chain at the 1-position decreases this activity drastically so that it is not observed in either of the derivatives **13** and **14**.

The negative BHIA infrared assay results and the low biological activity for the benzimidazole targets made it unnecessary to perform the $BHIA_{50}$ assay on them.

3.2.4. Biological activity

The IC_{50} values for compounds **13** and **14** against both the D10 chloroquine sensitive strain and K1 chloroquine resistant strain of *P. falciparum* are reported in table 3.8.

Compound	Observed against D10 strain	Observed against K1 strain
13	4741 ± 794 nM	> 10 000 nM
14	> 10 000 nM	> 10 000 nM

Table 3.8. IC_{50} values against D10 chloroquine sensitive strain and K1 chloroquine resistant strain of *P. falciparum*. The observed values are a mean of two determinations done in triplicate ± the standard error of the mean. Values greater than 10 000 nM are not reported as this indicates insignificant activity.

The very weak or non-existent antiplasmodial activities of **13** and **14** are attributed to their lack of β-haematin inhibitory activity and their poor accumulation ratio (AR) in the food vacuole.

3.2.5. Preliminary study on the reduction of the side chain of benzimidazole 14

It was hypothesized that reduction of the secondary amide in the side-chain of **15** to a secondary amine would improve vacuolar accumulation via pH trapping. Results for compound **15** (Figure 3.8.) were obtained from an impure sample and results are shown in table 3.9.

Compound	Observed IC_{50} against D10 strain	Observed IC_{50} against K1 strain
15	6919 ± 1753 nM	9235 ± 1130 nM

Table 3.9. Preliminary SAR study IC_{50} results for compound **15**. The observed values are a mean of two determinations done in triplicate ± the standard error of the mean.

The IC_{50} results for **15** appear to show some improvement in activity against the D10 chloroquine sensitive strain and the K1 chloroquine resistant strain of *P. falciparum*, relative to **14**. This indicates that activity increased after the secondary amide in the side-chain was reduced to a secondary amine. A pure sample of **15** is needed to give a better indication of antiplasmodial activity.

3.3. Quinoline with the piperazinyl containing side-chain.

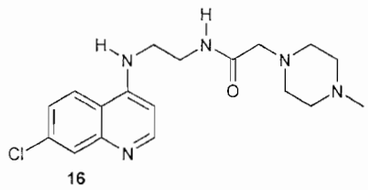

16

Figure 3.9. Quinoline **16** with the piperazinyl containing side-chains.

3.3.1. Target 16

Results for the SAR study performed on **16** (Figure 3.9.) are shown in table 3.10.

Compound	Log K	BHIA - IR	Observed against strain	IC_{50} D10	Observed against strain	IC_{50} K1
16	4.74 ± 0.07	+	104 ± 40 nM		1602 ± 448 nM	

Table 3.10. Results for **16**. The observed Log K values are a mean of two determinations ± the standard error of the mean and the observed IC_{50} values are a mean of two determinations done in triplicate ± the standard error of the mean.

In contrast to **14**, **16** was active, suggesting that the combination of the aminoamidopiperazinyl side-chain with the 5-chlorobenzimidazole nucleus has an influence that eliminates β-inhibitory activity while this activity is maintained in the 4-aminoquinoline analogue **16** (Figure 3.9.). This suggests that the relationship between the heteroaromatic nucleus and side chain and BHIA is a complicated one.

3.4. Conclusion

This dissertation has confirmed and extended some earlier proposed SAR for 7-substituted-4-aminoquinolines.[2, 101] The linear dependence of the log IC_{50} of **11** and **12**, corrected for vacuolar accumulation, on the β-haematin inhibitory activity in this family of compounds strongly supports the hypothesis that activity results from the inhibition of haemozoin formation in the parasite. It also supports the proposal that pH trapping, supposedly via the quinoline ring nitrogen and the tertiary side chain nitrogen, is essential for drug activity by ensuring that the compound is concentrated at the site of action. The latter is strengthened by the observation of a greater accumulation normalized log IC_{50} than predicted together with much lower observed pKa_1 values for both the SCF_3 and OCF_3 derivatives.

Where σ_m gave a marginally better correlation with pKa values in previous studies discussed, σ_p now gave a better correlation when pKa values for **11** and **12** are brought into account. A new equation can therefore be derived using σ_p, to predict pKa values.

The poor or no antiplasmodial activity of the 5-chlorobenzimidazoles can be attributed to the combination of two factors: their low pKa values and inability to inhibit β-haematin inhibitory activity once substituted in the 1-position.

The structure-activity data collected for target **15** need to be verified with analytically pure samples before the results can be accepted.

4. General conclusion and future studies

4.1. Conclusion

The objectives of this thesis as outlined in chapter 1 were:

i. The synthesis and characterization of two novel 7-substituted-4-aminoalkylated quinolines, N^1,N^1-diethyl-N^2-(7-trifuoromethylthio-4-quinolinyl)-1,2-ethanediamine **11** and N^1,N^1-diethyl-N^2-(7-trifuoromethoxy-4-quinolinyl)-1,2-ethanediamine **12** and to perform a quantitative structure activity analysis of them with respect to their pK_a values, association constants with haematin, β-haematin inhibitory activities and biological activities against *Plasmodium falciparum* ;

ii. The synthesis of the novel side chain *N*-(2-aminoethyl)-2-(4-methylpiperazin-1-yl)ethanamide **14b** for incorporation into a 5-chlorobenzimidazole template to fill the requirements for adequate vacuolar accumulation in *P. falciparum*;

iii. The investigation of the benzimidazole nucleus as an alternative template to the 4-aminoquinoline nucleus in chloroquine analogous anti-malarials by the synthesis and structure-activity studies of *N*-[2-(5-chlorobenzimidazol-1-yl)ethyl]-2-(4-methylpiperazin-1-yl)ethanamide **14** and [2-(5-chlorobenzimidazol-1-yl)ethyl]-[2-(4-methylpiperazin-1-yl)ethyl]amine **15**;

iv. Establishment of the effect of the benzimidazole nucleus relative to the quinoline nucleus by the synthesis of *N*-[2-(7-chloro-4-quinolinyl)ethyl]-2-(4-methylpiperazin-1-yl)ethanamide **16** and *N*-(7-chloroquinolin-4-yl)-*N'*-[2-(4-methylpiperazin-1-yl)ethyl]-ethane-1,2-diamine **17** to compare the bioloical results with **14** and **15**.

The 4-aminoquinolines **11** and **12** were successfully synthesized and characterized via a versatile 6-step route which allows for the introduction of a wide variety of groups in the 7-position and side chains in the 4-position. The targets **11** and **12** behaved in a chemically similar manner to the other short-chain analogues studied

by Kaschula et al.[2] The QSAR compiled on **11** and **12**, consisted of determining the acid dissociation constants (pKa_1 and pKa_2) of their basic nitrogens ; their associations constant (log K) for interaction with haematin; the β-haematin inhibitory activity (BHIA) by both the infrared assay and qualitative assay and the inhibitory concentration (IC_{50}) in both the D10 and K1 strain of *P. falciparum*. Lower than expected pKa_1 values for **11** and **12** were reflected in the lower than expected observed IC_{50} against the parasite, which supports the hypothesis that biological activity of 4-aminoquinolines proceeds via pH trapping in the acidic food vacuole of the parasite. An excellent correlation between the IC_{50} normalized for vacuolar accumulation and the log $BHIA_{50}$ of this class compound was demonstrated. This further supports the hypothesis that inhibition of β-haematin formation is the basis of biological activity in the food vacuole of the parasite. Biological activity can thus be predicted well based on a knowledge of the pK_a values and β-haematin inhibitory activities of these compounds. These two compounds were also found to be active against chloroquine resistant parasites.

The pK_a values were found to correlate well with the Hammett constant σ_p. By contrast, the QSAR for predicting β-haematin inhibitory activity was not useful. Prediction of log K for association with haematin was also poor, possibly due to the steric bulk of the groups at the 7-position (similar to CF_3). Thus the overall ability to predict biological activity in this group of compounds is hampered by a lack of understanding of factors controlling association with haematin and inhibition of β-haematin formation.

Synthesis of 5-chlorobenzimidazoles via 4-chloro-1,2-phenylenediamine (approach 1, section 2.4.1.) gave regioisomers which were difficult to characterize and purify. This led to the use of the route via 2,5-dichloronitrobenzene – a regioselective route. The results of the assays performed on the benzimidazole targets **14** and **15** showed that they were not useful as antimalarials because of their low pK_a values which causes decreased vacuolar accumulation in the parasite. It was also found that introduction of the *N*-(2-aminoethyl)-2-(4-methylpiperazin-1-yl)ethanamide **14b** side chain destabilized the β-haematin inhibitory activity since 5-chlorobenzimidazole showed β-haematin inhibitory activity as determined by the infrared assay contrary to any of the 5-chlorobenzimidazoles **13**,**14** and **15** with a side-chain in the 1-position. It was therefore concluded that the 1-substituted-5-chlorobenzimidazoles are inactive against malaria parasites. Nonetheless, the β-haematin inhibitory activity of 5-

chlorobenzimidazole does suggest that 5-chlorobenzimidazoles with alternative sites of substitution for the side chain may potentially be active.

The aminoamidopiperazinyl side-chain **14b** was designed for the regioselective benzimidazole targets **14** and **15** and was successfully synthesized and characterized in a two step synthesis which involved characteristically difficult work-up of amines. These properties were carried over to all intermediates in the regioslective 5-chlorobenzimidazole synthesis route.

The 5-chlorobenzimidazole analogous to 4-aminoquinoline **16** was successfully synthesized and characterized. Reduction of the aminoamidopiperazinyl sidechain to produce **17** however, was unsucessfull. Compound **16** retained biological activity against malaria parasites, but showed strong chloroquine cross-resistance between the D10 strain and K1 strain of *P. falciparum*. The weak anti-plasmodial activity of **16** could be attributed to the long side chain as with other long side-chain analogues reviewed in the introduction of this thesis.

4.2. Future work

Extensive studies have been performed on 7-substituted 4-aminoquinolines as reviewed in the *Chapter 1*. There is now considerable understanding of the relationship between structure and activity in this specific class of compound. Nonetheless, the origin of the β-haematin inhibitory activity of these compounds is still poorly understood and requires further investigation. Application of both experimental and computational methods to this problem need to be undertaken. In addition to this, the focus should shift towards a QSAR study on the 4-aminoalkyl side chain and its relationship to cross-resistance with chloroquine. This may permit a more rational selection of side chains for circumventing such cross-resistance.

Since [2-(5-Chlorobenzimidazol-1-yl)ethyl]-[2-(4-methylpiperazin-1-yl)ethyl]amine **15** was not purified before testing owing to its polar character, the results from its biological testing is only about 70% accurate judged by ^{1}H NMR spectra. Further attempts must therefore be made to purify this compound, possibly via tosylation of the secondary amine in the diaminopiperazinyl side-chain which would yield a less polar product. This will permit a better evaluation of this compound.

The 5-chlorobenzimidazoles in this study proved to be inactive against *P. falciparum*. There are however many other analogues to be studied before the benzimidazole nucleus can be abandoned as an alternative template to the 4-aminoquinoline nucleus. Possible analogues to be studied includes benzimidazoles with chlorine in the 4, 6 or 7-position. Analogues with the side-chain in the 2-position should also be targeted.

5. Experimental

5.1. Synthetic methods

5.1.1. General procedures

Thin layer chromatography (TLC) was used to monitor reactions using Merck F_{2554} aluminium-backed precoated silica gel plates and these were visualized with a combination of ultraviolet light, iodine staining, ceric ammonium sulphate spray and anisaldehyde spray. Column chromatography was performed using Merck kieselgel 60: 70-230 mesh. Melting points were obtained with a Reichert-Jung Thermovar hot stage microscope. Infrared spectra were recorded as dichloromethane solutions or as KBr discs using a Perkin Elmer Paragon 1000 FT-IR spectrophotometer. ^{1}H and ^{13}C NMR spectra were recorded on a Varian VXR-200 spectrometer at 200 MHz or a Varian Mercury spectrometer at 300 MHz or a Varian Unity spectrometer at 400 MHz. Spectra were recorded in deuterochloroform ($CDCl_3$) or deuterodimethylsulfoxide (d_6 DMSO) using internal standards for ^{1}H of δ_H = 7.26 ppm and 2.50 ppm respectivily and for ^{13}C of δ_c = 77.16 ppm and 39.52 ppm. All chemical shifts are reported in ppm and all coupling constants in Hz. Elemental analysis were performed using a Fison's Instruments Elemental Analyser EA1108. Mass spectrometry was performed externally by Dr. Philip Boshoff at Cape Technicon on a VG Micromass instrument.

5.1.2 Synthesis, purification and characterisation

Ethyl 2-ethoxycarbonyl-3-(3-trifluoromethylthioanilino)propenoate (11a)

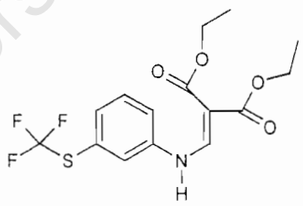

A mixture of 3-trifluoromethylthioaniline (1.0 g, 5.3 mmol) and diethyl methoxymethylene malonate (1.3 g, 5.8 mmol) was refluxed in ethanol (100 ml) for 3 hours after which the solvent was removed *in vacuo*. The resulting solid was

recrystallized from ethanol and dried to give **11a** (1.9 g, 99%), mp 69°C; δ_H(400 MHz, $CDCl_3$) 1.29 (3H, t, *J* 7.0, CH_3), 1.32 (3H, t, *J* 7.0, CH_3), 4.22 (2H, q, *J* 7.0, CH_2), 7.15 (1H, m, Ar-H), 7.32 (3H, m, Ar-H), 8.38 (1H, d, *J* 13.6, vinylic H), 10.97 (1H, bd, *J* 13.2, NH); δ_C (100.6 MHz, $CDCl_3$) 14.2 (CH_3), 14.4 (CH_3), 60.3 (CH_2), 60.6 (CH_2), 95.1 (C=CH), 119.2 (C-6), 124.4 (C-4), 126.4 (C-3), 129.3 (q, J_{C-F} 308.2, SCF_3), 130.8 (C-5), 132.0 (C-2), 140.4 (C-1), 151.2 (C=CH), 165.5 (C=O), 168.9 (C=O); (Found: MS (HRMS) *m/z* 363.07429. Requires: 363.07521); (Found: C, 49.40; H, 4.82; N, 3.87; S, 8.8%. Requires for $C_{15}H_{16}F_3NO_4S$: C, 49.5; H, 4.4; N, 3.8; S, 8.8%)

Ethyl 1,4-dihydro-4-oxo-7-(trifluoromethylthio)quinoline-3-carboxylate (11b)

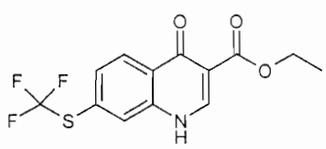

11a (1.0 g, 2.7 mmol) was refluxed in diphenyl ether (10 ml) for 30 minutes. The flask was opened during the first 10 minutes of the reaction to allow the ethanol formed to escape. When the reaction mixture cooled to room temperature, a white precipitate formed. This was filtered and washed with petroleum ether, ethyl acetate and methanol to remove all diphenyl ether and other impurities to give **11b** (0.6 g, 75%) after drying, mp 265-266°C; ν_{max}/cm^{-1} (KBr) 3150, 1637 (CO); δ_H (200 MHz, d_6 DMSO) 1.30 (3H, t, *J* 7.2, CH_3), 4.25 (2H, q, *J* 7.2, CH_2), 7.60 (1H, d, *J* 4.6, H-6), 7.98 (1H, s, H-8), 8.25 (1H, d, *J* 4.6, H-5), 8.67 (4H, s, H-2); (Found: MS *m/z* 317. Requires: M^+, 317); (Found C, 49.1; H, 3.1; N, 4.4; S, 9.7%. Requires for $C_{13}H_{10}F_3NO_3S$: C, 49.2; H, 3.1; N, 4.4; S 10.1%).

Ethyl 1,4-dihydro-4-oxo-7-(trifluoromethylthio)quinoline-3-carboxylate (11b)

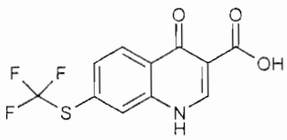

A mixture of **11b** (0.9 g, 2.8 mmol) and 10% NaOH (10 ml) was heated at 120°C for 2 hours. During this period all of the solid dissolved. The aq.ueous phase was then carefully neutralised with 10% H_2SO_4 to avoid formation of the water-soluble quinolinium ion, and a white solid precipitated which was filtered off and washed with cold water. The solid was dried over P_2O_5 under vacuum to yield **11c** (0.5 g, 70%), mp 233-236°C; ν_{max}/cm^{-1} (KBr) 2900, 1620; δ_H (300 MHz, d_6 DMSO) 7.80 (1H, dd, *J* 8.4, 1.5, H-6), 8.16 (1H, d, *J* 1.5, H-8), 8.37 (1H, d,*J* 8.4, H-5), 8.98 (1H, s, H-2), 13.44 (1H, bs, COOH), 14.85 (1H, bs, Ar-OH); δ_C (75.5 MHz, d_6 DMSO) 108.5 (C-3), 125.6 (Ar-CH), 126.3 (C-5), 126.8 (C-8), 129.3 (q, J_{C-F} 308.3, SCF_3), 129.5 (C-4a), 131.3 (C-6) , 139.5 (C-8a), 146.3 (C-2), 165.7 (COOH), 177.8 (C-4); (Found: MS (HRMS) *m/z* 289.00182. Requires for $C_{10}H_6F_3NO_3S$: 289.00205).

7-(Trifluoromethylthio)quinolin-4-one (11d)

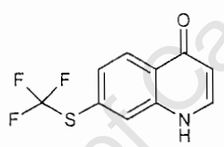

11c (0.8 g, 2.9 mmol) was added to diphenyl ether (8 ml) and the mixture refluxed in a preheated oil bath. After 30 minutes the reaction was allowed to cool when all the solid had dissolved. A precipitate formed which was filtered, and washed with petroleum ether and cold ethyl acetate to remove all diphenyl ether to yield **11d** (0.4 g, 68%), which was recrystallized from methanol and ethyl acetate, mp 214-215°C; ν_{max}/cm^{-1} (KBr) 2943, 1630; δ_H (300 MHz, d_6 DMSO) 6.12 (1H, d, *J* 7.2, H-3), 7.52 (1H, dd, *J* 8.4, 1.2, H-6), 7.92 (1H, d, *J* 1.2, H-8), 7.99 (1H, d, *J* 7.2, H-2), 8.19 (1H, d, *J* 8.4, H-5), 11.89 (1H, bs, Ar-OH); δ_C (100.6 MHz, d_6 DMSO) 109.6 (C-3), 125.6 (C-6), 126.6 (C-7/C-4a), 126.6 (C-7/C-4a), 126.7 (C-5), 128.7 (C-8), 129.4 (q, J_{C-F} 308.2,

SCF_3), 140.1 (C-8a), 140.2 (C-2), 176.06 (C-4); (Found: MS (HRMS) *m/z* 245.01228. Requires for $C_{10}H_6F_3NOS$: 245.01222).

4-Chloro-7-trifluoromethylthioquinoline (11e)

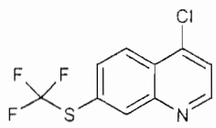

A mixture of **11d** (0.4 g, 1.4 mmol), phosphorus oxychloride (1 ml, 11.4 mmol) and phosphorus pentachloride (0.3 g, 1.6 mmol) was refluxed under N_2 at 120°C for 30 minutes. The reaction mixture was then poured into cold aq. 10% NaOH (1 M, 50 ml) and the white precipitate was filtered and washed with water. The solid was then dissolved in ethyl acetate (100 ml), dried ($MgSO_4$) and the solvent removed *in vacuo*. Recrystallization from petroleum ether gave **11e** (0.3 g, 88%), mp 69°C; δ_H (400 MHz, $CDCl_3$) 7.57 (1H, d, *J* 4.7, H-3), 7.83 (1H, dd, *J* 9.0, 1.7, H-6), 8.28 (1H, d, *J* 9.0, H-5), 8.48 (1H, d, *J* 1.7, H-8), 8.85 (1H, d, *J* 4.7, H-2); δ_C (75.5 MHz, $CDCl_3$) 122.8 (C-3), 122.9 (C-7), 125.7 (C-5), 127.6 (C-4a), 129.6 (q, J_{C-F} 308.6, SCF_3), 133.2 (C-6), 138.0 (C-8), 142.9 (C-4), 149.0 (C-8a), 151.3 (C-2); (Found: MS (HRMS) *m/z* 262.97808. Requires for $C_{10}H_5ClF_3NS$: 262.97833).

N^2-(7-Trifluoromethylthio-4-quinolinyl)-N^1,N^1-diethyl-1,2-ethanediamine (11)

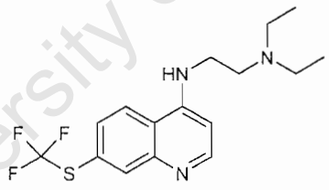

11e (0.2 g, 1.0 mmol) and *N*,*N*-diethylethylenediamine (3 ml) were heated together in a sealed tube under N_2 at 140°C for 4 hrs. Aq. 10% NaOH (2 ml) was added to the product and the resulting yellow precipitate was then extracted into dichloromethane (3 × 100 ml). The solvent was dried ($MgSO_4$) and removed under reduced pressure to furnish a residue which was chromatographed on silica gel using methanol and

dichloromethane (2:8) as eluent to give **11** (0.4, 80%), mp 110-111°C; δ_H (400 MHz, $CDCl_3$) 1.08 (6H, t, *J* 7.3, 2×CH_3), 2.61 (4H, q, *J* 7.3, 2×CH_2), 2.83 (2H, t, *J* 6.2, CH_2-β), 3.28 (2H, q, *J* 6.2, CH_2-α), 6.21 (1H, bs, NH), 6.43 (1H, d, *J* 5.1, H-3), 7.61 (1H, dd, *J* 9.0, 1.8, H-6), 7.72 (1H, d, *J* 9.0, H-5), 8.30 (1H, d, *J* 1.8, H-8), 8.58 (1H, d, *J* 5.1, H-2); δ_C (100.6 MHz, $CDCl_3$) 12.3 ($CH_2\underline{C}H_3$), 39.9 (CH_2-α), 46.7 ($\underline{C}H_2CH_3$), 50.8 (CH_2-β), 100.3 (C-3), 120.3 (C-7), 121.2 (C-5), 125.2 (C-4a), 129.8 (q, $J_{C\text{-}F}$ 308.1, SFC_3), 130.3 (C-6), 138.5 (C-8), 148.7 (C-4), 149.9 (C-8a), 152.5 (C-2); (Found: MS *m/z* (HRMS) 344.14095 (M+H). Requires for $C_{16}H_{21}F_3N_3S$ (M+H): 344.14082).

Ethyl 2-ethoxycarbonyl-3-(3-trifluoromethoxyanilino)propenoate (12a)

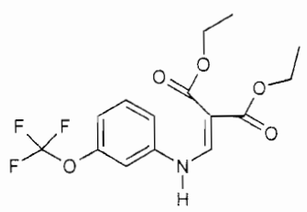

A mixture of 3-trifluoromethoxyaniline (1.0 g, 5.6 mmol) and diethyl methoxymethylene malonate (1.3 g, 6.2 mmol) was refluxed in ethanol for 3 hours after which the solvent was removed *in vacuo*. The resulting solid was recrystallized from ethanol and dried to give **12a** (1.8 g, 93 %), mp 42-43°C; δ_H (400 MHz, $CDCl_3$) 1.30 (3H, t, *J* 7.3, CH_3) 1.30 (3H, t, *J* 7.3, CH_3), 4.24 (2H, q, *J* 7.3, CH_2), 4.24 (2H, q, *J* 7.3, CH_2), 6.95 (2H, m, H-2 and H-4), 7.35 (1H, t, *J* 7.5, H-6), 7.33 (1H, m, H-5), 8.40 (1H, dd, *J* 13.2, 7.7, C=$\underline{C}$H), (1H, d, *J* 13.2, NH); δ_C (100.6 MHz, $CDCl_3$) 14.2 (CH_3), 14.3 (CH_3), 60.3 (CH_2), 60.6 (CH_2), 95.0 ($\underline{C}$=CH), 109.9 (C-5), 115.2 (C-6), 116.6 (C-4), 120.4 (q, $J_{C\text{-}F}$ 257.9, OCF_3), 131.1 (C-2), 140.9 (C-1), 150.3 (C-3), 151.2 (C=$\underline{C}$H), 165.4 (C=O), 168.9 (C=O); (Found: MS (HRMS) *m/z* 347.09786. Requires for $C_{15}H_{16}F_3NO_5$: 347.09805).

Ethyl 1,4-dihydro-4-oxo-7-(trifluoromethoxy)quinoline-3-carboxylate (12b)

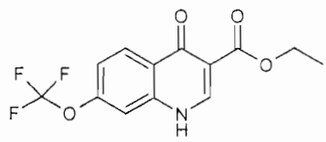

12a (1.0 g, 2.8 mmol) was refluxed in diphenyl ether (10 ml) for 15-30 minutes. The flask was opened during the first 10 minutes of the reaction to allow the ethanol formed to escape. When the reaction mixture cooled to room temperature, a white precipitate formed. This was filtered and washed with petroleum ether, ethyl acetate and methanol to remove all diphenyl ether and other impurities, to give **12b** after drying, (0.6 g, 73 %), mp 234-235°C; ν_{max}/cm^{-1} (KBr) 2918, 1622; δ_H(400 MHz, d_6 DMSO) 1.26 (3H, t, *J* 6.5, CH_3), 4.25 (2H, q, *J* 7.3, CH_2), 7.32 (1H, d, *J* 8.7, H-5), 7.53 (1H, s, H-8) 8.27 (1H, d, H-6), 8.50 (1H, s, H-2); (Found: MS (HRMS) *m/z* 301.05637. Requires for $C_{13}H_{10}F_3NO_4$: 301.05619).

1,4-Dihydro-4-oxo-7-(trifluoromethoxy)quinoline-3-carboxylic acid (12c)

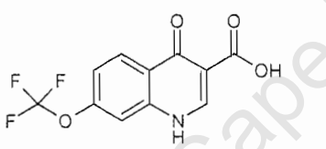

A mixture of **12b** (1.1 g, 3.6 mmol) and 10% NaOH (10 ml) was heated at 120°C for 2 hours. During this period, all of the solid dissolved. On cooling, the organic impurities were extracted into ethyl acetate (3 × 100 ml). The aq.ueous phase was then carefully neutralised with 10% H_2SO_4 to avoid formation of the water-soluble quinolinium ion, and a white solid precipitated which was filtered and washed with cold water. The white solid was dried over P_2O_5 under vacuum to yield **12c** (0.8 g ,84%), mp 274-279°C; ν_{max}/cm^{-1} (KBr) 2930, 1634; δ_H (300 MHz, d_6 DMSO) 7.46 (1H, dd, *J* 8.7, 1.2, H-6), 7.73 (1H, d, *J* 1.2, H-8), 8.41 (1H, d, *J* 8.7, H-5), 8.87 (1H, s, H-2); δ_C (75.5 MHz, d_6 DMSO) 108.2 (C-3), 110.6 (C-8), 118.4 (C-6), 119.8 (q, J_{C-F} 258.7 , OCF_3),123.1 (C-4a), 128.2 (C-5), 141.1 (C-8a), 146.8 (C-2), 151.3 (C-7), 166.1 (COOH), 177.3 (C-4); (Found: MS (HRMS) *m/z* 273.02454. Requires for $C_{11}H_6F_3NO_4$: 273.02489).

7-(Trifluoromethoxy)quinolin-4-one (12d)

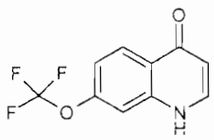

12c (0.8 g, 3.0 mmol) was added to diphenyl ether (8 ml) and the mixture refluxed in a preheated oil bath. After 30 minutes the reaction was allowed to cool when all the solid had dissolved. A precipitate formed which was filtered, and washed with petroleum ether and cold ethyl acetate to remove all diphenyl ether to yield **12d** (0.6 g, 86%), which was recrystallized from methanol and ethyl acetate, mp 224-227°C; ν_{max}/cm^{-1} (KBr) 2930, 1639; δ_H (400 MHz, d_6 DMSO) 6.04 (1H, d, *J* 7.6, H-3), 7.27 (1H, d, *J* 9.1, H-5), 7.47 (1H, d, *J* 1.4, H-8), 7.92 (1H, dd, *J* 9.1, 1.4, H-6), 8.16 (1H, d, *J* 7.6, H-2), 11.79 (1H, bs, Ar-OH); δ_C (75.5 MHz, d_6 DMSO) 109.8 (C-3), 110.1 (C-8), 116.5 (C-6), 120.6 (q, J_{C-F} 256.7 , OCF_3) 125.1 (C-4a), 128.8 (C-5), 140.9 (C-8a), 141.6 (C-2), 151.0 (C-7) , 176.8 (C-4); (Found: MS (HRMS) *m/z* 229.03509. Requires for $C_{10}H_6F_3NO_2$: 229.03506).

4-Chloro-7-trifluoromethoxyquinoline (12e)

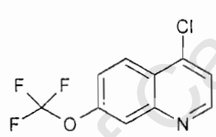

A mixture of **12d** (0.5 g, 2.1 mmol), phosphorus oxychloride (1.6 ml, 16.8 mmol) and phosphorus pentachloride (0.5 g, 2.5 mmol) was refluxed under N_2 at 120°C for 30 minutes. The reaction mixture was then poured into cold aq. 10% NaOH (1 M, 50 ml) and the white precipitate filtered and washed with water. The solid was then dissolved in ethyl acetate (100 ml), dried ($MgSO_4$) and the solvent removed *in vacuo*. Recrystallization from petroleum ether gave **12e** (0.5 g, 89%), mp 37°C; δ_H (400 MHz, $CDCl_3$) 7.50 (1H, dd, *J* 9.0, 2.6, H-6), 7.51 (1H, d, *J* 4.7, H-3), 7.97 (1H, d, *J* 2.6, H-8), 8.28 (1H, d, *J* 9.0, H-5), 8.81 (1H, d, *J* 4.7, H-2); δ_C (100.6 MHz, $CDCl_3$) 111.2 (C-8), 119.7 (C-3), 121.7 (C-4a), 121.7 (C-6), 123.0 (q, J_{C-F} 253.4, OCF_3),

126.5 (C-5), 149.8 (C-4), 150.6 (C-8a), 151.4 (C-2), 171.1 (C-7); (Found: MS (HRMS) *m/z* 247.00101. Requires for $C_{10}H_5F_3ClNO$: 247.00117).

N^2-(7-Trifluoromethoxy-4-quinolinyl)-N^1,N^1-diethyl-1,2-ethanediamine (12)

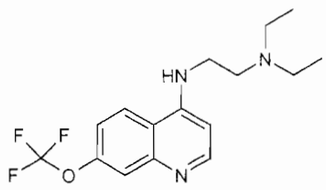

12e (0.2 g, 1.0 mmol) and *N*,*N*-diethylethylenediamine (3 ml) were heated together in a sealed tube under N_2 at 140°C for 4 hrs. Aq. 10% NaOH (2 ml) was added to the product and the resulting yellow precipitate was then extracted into dichloromethane (3 × 100 ml). The solvent was dried ($MgSO_4$), removed under reduced pressure and the residue chromatographed on silica gel using methanol and dichloromethane (10-20:90-80) as eluent to give **12** (0.4 g, 80%), mp 110-111°C; δ_H (300 MHz, CDC_3) 1.08 (6H, t, *J* 6.9, CH_3), 2.61 (4H, q, *J* 6.9, CH_2), 2.83 (2H, t, *J* 5.4, CH_2-β), 3.24 (2H, q, *J* 5.4, CH_2-α), 6.13 (1H, bs, NH), 6.38 (1H, , *J* 5.1, H-3), 7.27 (1H, , *J* 9.0, H-6), 7.75 (1H, d, *J* 9.0, H-5), 7.98 (1H, d, *J* 0.6, H-8), 8.59 (1H,d , *J* 5.1, H-2); δ_C (100.6 MHz, $CDCl_3$) 12.3 ($CH_2\underline{C}H_3$), 39.9 (CH_2-β), 46.7 ($\underline{C}H_2CH_3$), 50.8 (CH_2-α), 99.5 (C-3), 117.6 (C-8), 118.2 (C-6), 120.1 (q, $J_{C\text{-}F}$ 258.0, OCF_3), 121.8 (C-5), 149.4 (C-8a), 150.0 (C-4), 152.6 (C-2), 158.5 (C-7); (Found: MS (HRMS) *m/z* 328.16392. Requires for $C_{16}H_{20}F_3N_3O$ (M+H): 328.16366).

5-Chloro-1H-benzimidazole (13a)

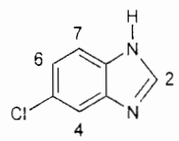

4-chloro-1,2-phenylenediamine (4.8 g, 33 mmol) was dissolved in dry dichloromethane (50 ml). Trimethylorthoformate (8.5 ml, 66 mmol) was added and the solution cooled to 0°C before adding boron trifluoride etherate (9.2 ml, 83 mmol).

After 4 hrs the reaction mixture was poured into aq. Na_2CO_3 (50 ml, 1 M). The compound was then extracted into ethyl actetate (3 × 100 ml) followed by dichloromethane (1 × 100 ml), and the organic extracts dried ($MgSO_4$). The solvent was removed under reduced pressure and the oily residue chromatographed on silica gel using equal parts of petroleum ether and ethyl acetate as eluent to yield **13a** (4.8 g, 94%) as a yellow solid which was recrystallized from ethyl acetate and petroleum ether, mp 122°C; δ_H (400 MHz, $CDCl_3$) 7.26 (1H, dd, *J* 8.8, 1.8, H-6), 7.55 (1H, d, *J* 8.8, H-7), 7.63 (1H, d, *J* 1.8, H-4), 8.16 (1H, s, H-2), 10.40 (1H, bs, NH); δ_C (75.5 MHz, $CDCl_3$) 115.3 (C-7), 116.2 (C-4), 123.6 (C-6), 128.7 (C-5), 136.1 (C-3a/C-7a), 138.2 (C-3a/C-7a), 141.7 (C-2); (Found: MS (HRMS) *m/z* 152.01374. Requires for $C_7H_5ClN_2$: 152.01412).

(5-Chlorobenzoimidazol-1-yl)ethanoic acid ethyl ester (13b)

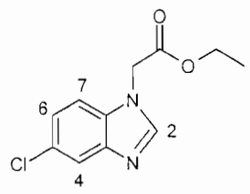

NaH (1.3 g, 32 mmol) was added to a cooled solution (0°C) of **13a** (3.2 g, 21.3 mmol) in dry tetrahydrofuran (100 ml). The mixture was stirred for 1 hr during which a colour change of orange to green was observed. The mixture was then cooled to -78°C and ethyl bromoacetate (4.3 g, 25.6 mmol) was slowly added over 10 minutes. After 30 minutes the reaction mixture was quenched with saturated ammonium chloride solution. The product was then extracted with ethyl acetate (3 × 100 ml) and the extracts dried ($MgSO_4$). All solvent was then removed under reduced pressure and the product recrystallized from ethyl actetate to yield **13b** (3.0 g, 60%); δ_H (400 MHz, $CDCl_3$) 1.24 (3H, t, *J* 7.3, CH_3), 4.20 (2H, q, *J* 7.3, OCH_2), 4.83 (2H, s, NCH_2), 7.20 (1H, d, *J* 9.0, H-7), 7.24 (1H, dd, *J* 9.0, 2.1, H-6), 7.77 (1H, d, *J* 2.1, H-4), 7.90 (1H, s, H-2); δ_C (100.6 MHz, $CDCl_3$) 14.0 (CH_3), 46.2 (NCH_2), 62.4 (OCH_2), 110.2 (C-7), 120.2 (C-4), 121.7 (C-3a), 124.0 (C-6), 128.3 (C-5), 132.7 (C-7a), 144.7 (C-2), 167.0 (C=O); (Found: MS *m/z* 238.05073. Requires for $C_{11}H_{11}ClN_2O_2$: 238.05090).

2-(5-Chlorobenzoimidazol-1-yl)-*N*-(2-diethylaminoethylethanamide (13)

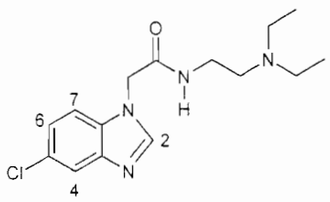

13b (0.5 g, 2.1 mmol) was stirred in *N*,*N*-diethylethylenediamine (10ml) in a sealed vessel under N_2 at 100°C for 45 minutes. The excess N,*N*-diethylethylenediamine was removed under reduced presure. The resulting oil was then subjected column chromatography on silica gel with a mixture of dichloromethane and methanol (80:20) as eluent. This yielded a non-crystalline solid, **13** (0.5 g, 73%); δ_H (400 MHz, $CDCl_3$) 0.71 (6H, t, *J* 7.2, CH_3), 2.28 (4H, q, *J* 7.2, $\underline{C}H_2CH_3$), 2.40 (2H, t, CH_2), 3.24 (2H, m, $NHCH_2$), 4.79 (2H, s), 6.60 (1H, bs, NH), 7.24 (1H, dd, *J* 8.6, 2.0, H-6), 7.36 (1H, d, *J* 2.0, H-4), 7.68 (1H, d, *J* 8.6, H-7), 7.90 (1H, s, H-2); (Found: MS (HRMS) *m/z* 309.14838. Requires for $C_{15}H_{22}ClN_4O$: 309.14821 (M+H)).

(4-Methylpiperazin-1-yl)ethanoic acid ethyl ester (14a)

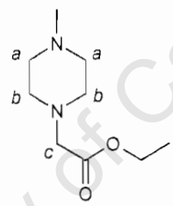

N-methylpiperazine (10 ml, 90 mmol) and triethylamine (15 ml) were added together with dichloromethane as solvent and cooled to 0°C. Ethyl bromoacetate (11 ml, 99 mmol) was slowly added over 10 minutes. Formation of the white hydrobromide salt of Hünig's base was immediately observed. After 3 hrs the reaction mixture was filtered to remove the salt formed. The solvent was removed under reduced pressure and the crude product vacuum distilled (b.p. 89°C, 0.05 mm Hg) to yield, a colourless oil, **14a** (12 g, 75%); δ_H (400 MHz, $CDCl_3$) 1.19 (3H, t, *J* 7.3, CH_3), 2.21 (3H, s, NCH_3), 2.42 (4H, bs, 2×CH_2-*a*), 2.55 (4H, bs, 2×CH_2-*b*), 3.13 (2H, s, CH_2-c), 4.14 (2H, q, *J* 7.3, OCH_2); δ_C (75.5 MHz, $CDCl_3$) 14.1 (CH_3), 45.9 (NCH_3), 52.9 (2×CH_2-*a*),

54.7 (2×CH_2-*b*), 59.4 (CH_2-*c*), 60.4 (OCH_2), 170.1 (C=O); (Found: MS (HRMS) *m/z* 186.13694. Requires for $C_9H_{18}N_2O_2$:186.13682).

_N_-(2-Aminoethyl)-2-(4-methylpiperazin-1-yl)ethanamide (14b)

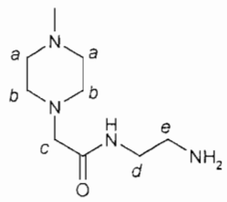

14a (11.5 g, 61 mmol) and excess ethylenediamine (12 ml) were stirred in a sealed tube under N_2 at 120°C for 4 hrs. The excess ethylenediamine was removed under reduced pressure and the resulting crude product was vacuum distilled (b.p. 67°C, 0.05 mm Hg) to yield a yellow oil, **14b** (8.8 g, 70%); δ_H (400 MHz, $CDCl_3$) 1.75 (2H, bs, NH_2), 2.23 (3H, s, NCH_3), 2.40 (4H, bs, 2×CH_2-*a*), 2.51 (4H, bs, 2×CH_2-*b*), 2.77 (2H, t, *J* 5.8, CH_2-*e*), 2.96 (2H, s, CH_2-*c*), 3.26 (2H, q, *J* 5.8, CH_2-*d*), 7.36 (1H, bs, NH); δ_C (75.5 MHz, $CDCl_3$) 38.8 (CH_2-*d*), 45.9 (NCH_3), 53.3 (2×CH_2-*a*), 53.5 (2×CH_2-*b*), 55.1 (CH_2-*e*), 61.3 (CH_2-*c*), 142.0 (C=O); (Found: MS (HRMS) *m/z* 200.16368. Requires for $C_9H_{20}N_4O$: 200.16370).

_N_-[2-(4-Chloro-2-nitrophenylamino)ethyl]-2-(4-methylpiperazin-1-yl)ethanamide (14c)

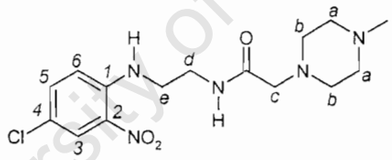

A solution of **14b** (12 g, 63 mmol) and 2,5-dichloronitrobenzene (13 g, 69 mmol) in dimethylformamide were refluxed. After 3 hrs the reaction mixture was cooled and basified with 10% NaOH (1 M, 80 ml). The product was then extracted into ethyl acetate (3 × 100 ml). After a charcoal clean the solvent was removed under reduced pressure and the solid recrystallized from ethyl acetate and petroleum ether to yield orange crystals of **14c** (8.9 g, 40%), mp 86-88°C; δ_H (400 MHz, $CDCl_3$) 2.27 (3H, s, NCH_3), 2.35 (4H, bs, 2×CH_2-*a*), 2.53 (4H, m, 2×CH_2-*b*), 3.01 (2H, s, CH_2-*c*), 3.41 (4H,

m, 2×CH_2-*d*,*e*), 6.94 (1H, d, *J* 9.5, H-6), 7.33 (1H, dd, *J* 9.5, 2.9, H-5), 7.44 (1H, bs, NH), 8.04 (1H, bs, NH-Ar) 8.14 (1H, d, *J* 2.9, H-3); δ_C (100.6 MHz, $CDCl_3$) 38.1 (CH_2-*d*), 42.4 (CH_2-*e*), 45.8 (NCH_3), 53.4 (CH_2-*b*), 55.0 (CH_2-*a*), 61.2 (CH_2-*c*), 115.1(C-3), 120.5 (C-6), 125.9 (C-5), 132.0 (C-4), 136.3 (C-2), 143.8 (C-1), 171.0 (C=O); (Found: MS (HRMS) *m/z* 356.14854 (M+H). Requires for $C_{15}H_{23}ClN_5O_3$ (M+H): 356.14893).

_N_-[2-(2-Amino-4-chlorophenylamino)ethyl]-2-(4-methylpiperazin-1-yl)ethanamide (14d)

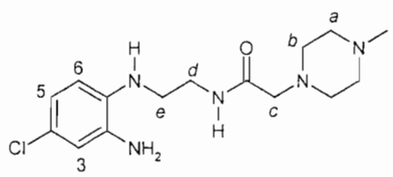

14c (2.9 g, 8.3 mmol) was dissolved in conc. HCl (8 M, 2 ml) and added to a chilled solution of stannous chloride (7.5 g, 33 mmol) in conc.HCl (8 M, 5 ml). After 2 hrs the reaction mixture was poured onto ice and basified by adding NaOH (2.4 g, 6 mmol) pellets to the solution. The product was extracted into ethyl acetate (2 × 100 ml) followed by dichloromethane (1 × 100 ml) and the organic extract dried ($MgSO_4$). The solvent was removed under reduced pressure and the solid recrystallized from ethyl acetate to yield purple crystals of **14d** (2.5 g, 94%), mp 123-124°C; δ_H (400 MHz, $CDCl_3$) 2.26 (3H, s, NCH_3), 2.38 (4H, bs, 2×CH_2-*a*), 2.53 (4H, m, 2×CH_2-*b*), 2.99 (2H, s, CH_2-*c*), 3.24(4H, m, CH_2-*e*), 3.45 (1H, bs, NH_2), 3.56 (2H, t, *J* 6.24, CH_2-*d*), 3.79 (1H, bs, NH-Ar), 6.49 (1H, d, *J* 8.3, H-6), 6.65 (1H, d, *J* 2.4, H-3) 6.69 (1H, dd, *J* 8.3, 2.4, H-5), 7.42 (1H, bs, NH); δ_C (100.6 MHz, $CDCl_3$) 38.8 (CH_2-*d*), 44.9 (CH_2-*e*), 45.9 (NCH_3), 53.5 (CH_2-*b*), 55.1 (CH_2-*a*), 61.4 (CH_2-*c*), 112.1 (C-3), 115.8 (C-6), 119.6 (C-5), 123.3 (C-4), 135.6 (C-2), 150.1 (C-1), 171.4 (C=O); (Found: MS (HRMS) *m/z* 325.16662. Requires for $C_{15}H_{24}ClN_5O$: 325.16693).

***N*-[2-(5-Chlorobenzoimidazol-1-yl)ethyl]-2-(4-methylpiperazin-1-yl)ethanamide (14)**

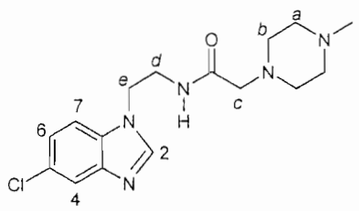

14d was added to a 10% solution in water of formic acid (3.7 mmol). The mixture was then acidified with conc. HCl (8 M, 1 ml) and heated to 120°C for 2.5 hrs. After cooling to room temperature, the product was extracted into ethyl acetate (3 × 100 ml) and the organic extracts dried ($MgSO_4$). All solvent was removed by reduced pressure and the product recrystallized from ethyl acetate to yield pink crystals of **14** (0.9 g, 87%), mp 156-157°C; δ_H (300 MHz, $CDCl_3$) 2.19 (3H, s, NCH_3), 2.19 (4H, bs, CH_2-*a*), 2.36 (4H, t, CH_2-*b*), 2.93 (2H, s, CH_2-*c*), 3.67 (2H, q, *J* 5.9, CH_2-*d*), 4.36 (2H, t, *J* 5.9, CH_2-*e*), 7.19 (1H, bs, NH), 7.26 (1H, dd, *J* 8.8, 1.8, H-6), 7.33 (1H, d, *J* 8.8, H-7), 7.78 (1H, d, *J* 1.8, H-4), 7.84 (1H, s, H-2) ; δ_C (100.6 MHz, $CDCl_3$) 39.2 (C-*d*), 44.2 (C-*e*), 46.0 (NCH_3), 53.6 (C-*b*), 55.0 (C-*a*), 61.3 (C-*c*), 110.4 (C-7), 120.5 (C-4), 123.8 (C-6), 128.2 (C-5), 132.7 (C-7a), 144.1 (C-2), 144.8 (C-3a), 171.3 (C=O); (Found: MS (HRMS) *m/z* 336.1594 (M+H). Requires for $C_{16}H_{23}ClN_5O$ (M+H): 336.1591).

***N*-[2-(5-Chlorobenzoimidazol-1-yl)ethyl]-*N*-[2-(4-methylpiperazin-1-yl)ethyl]amine (15)**

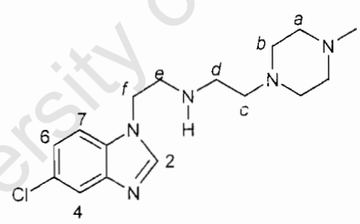

A solution of **14c** (0.9 g, 2.6 mmol) in anhydrous tetrahydrofuran was slowly added to a chilled suspension of lithium aluminium hydride (0.5 g, 13 mmol) in anhydrous tetrahydrofuran under N_2 in a cyclization tube. The mixture was stirred at room temperature for 1 hr and then heated to 70°C for 60 hrs. On cooling, the product was slowly poured onto a mixture of tetrahydrofuran, triethylamine and water (8:1:1, 50

ml) cooled in an ice-water bath. This mixture was stirred untill the suspension turned white and then filtered through Celite to remove the salts. The solvent was dried ($MgSO_4$) and removed under reduced pressure to yield a mixture of **14c** and the reduced form of the amide **14e** (0.8 g) as a purple oily residue, which could not be purified owing to its very polar character. The crude product was added to methanoic acid (0.2 g, 3.7 mmol). The mixture was then acidified with conc. HCl (8 M, 1 ml) and heated to 120°C for 1 hr. On cooling the excess water and methanoic acid were azeotropically removed with toluene under reduced pressure. The crude material was chromatographed with a mixture of dichloromethane, methanol and ammonia solution (80:19:1) as eluent, to give **15** (0.2 g, 49%); δ_H (400 MHz, $CDCl_3$) 2.49 (3H, s, NCH_3), 2.59 (2H, *J* 6.0, CH_2), 2.63 (4H, bs, H-*a*), 2.71 (4H, bs, H-*b*), 2.79 (2H, t, *J* 6.0, CH_2), 3.17 (2H, t, *J* 6.0, CH_2), 4.44 (2H, t, *J* 6.0, CH_2), 5.70 (1H,m bs, NH), 7.23 (1H, dd, *J* 8.8, 2.0, H-6), 7.42 (1H, d, *J* 8.8, H-7), 7.61 (1H, d, *J* 2.0, H-4), 8.12 (1H, s, H-2); (Found: MS (HRMS) *m/z* 322.17987 (M+H). Requires for $C_{16}H_{25}ClN_5$ (M+H): 322.17984).

N-[2-(7-Chloro-4-quinolinyl)ethyl]-2-(4-methylpiperazin-1-yl)ethanamide (16)

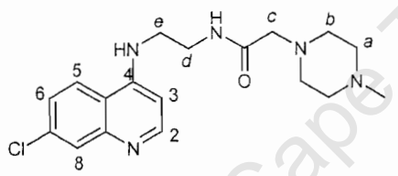

A mixture of 4,7-dichloroquinoline (0.5 g, 2.6 mmol), **14b** (0.5 g, 2.6 mmol) and potassium fluoride (0.2 g, 3.3 mmol) were dissolved in dimethylformamide in a sealed tube under N_2 and heated to 150°C for 5 hrs. On cooling, the reaction mixture was poured into water, basified with potassium hydroxide solution (5 ml, 1 M) and the product extracted into ethyl acetate (3 × 100 ml). The solvent was removed under reduced pressure and the solid recrystallized from ethyl acetate to yield **16** (0.5 g, 58%) as a crystalline solid, mp 197-199°; δ_H (400MHz, d_6 DMSO) 2.08 (3H, s, NCH_3), 2.23 (4H, bs, H-*a*), 2.35 (4H, bs, H-*b*), 2.82 (2H, s, H-*c*), 3.34 (4H, H-*d/e*), 6.55 (1H, d, *J* 5.6, H-3), 7.32 (1H, t, NH-Ar), 7.43 (1H, dd, *J* 8.8, 2.0, H-6), 7.77 (1H, d, *J* 2.0, H-8), 7.91 (1H, t, NH), 8.17 (1H, d, *J* 8.8, H-5), 8.39 (1H, d, *J* 5.6, H-2); δ_C (100.6 MHz, d_6 DMSO) 37.0 (C-*d*), 42.2 (C-*e*), 45.6 (NCH_3), 52.8 (C-*b*), 54.4 (C-*a*), 61.3 (C-*c*), 98.6 (C-3), 117.4 (C-4a), 123.8 (C-5), 124.0 (C-6), 127.5 (C-8), 133.3 (C-7), 149.0

(C-8a), 150.0 (C-4), 151.8 (C-2), 169.9 (C=O); (Found: MS (HRMS) *m/z* 362.17468 (M+H). Requires for $C_{18}H_{25}ClN_5O$ (M+H): 362.17475).

_N_-(7-Chloroquinolin-4-yl)-_N'_-[2-(4-methylpiperazin-1-yl)ethyl]ethane-1,2-diamine (17)

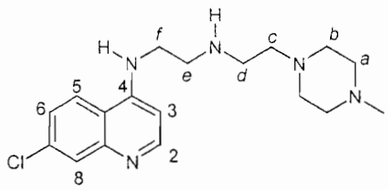

A solution of **16** (0.6 g, 1.6 mmol) in anhydrous tetrahydrofuran was slowly added to a suspension of lithium aluminium hydride (0.3 g, 8 mmol) in anhydrous tetrahydrofuran cooled in an ice-water bath under N_2 in a cyclization tube. The mixture was stirred at room temperature for 1 hr and then heated to 70°C for 3hrs. On cooling, the product was slowly poured onto a mixture of tetrahydrofuran, triethylamine and water (8:1:1) cooled in an ice-water bath. This mixture was stirred until the aluminium salts formed and then filtered through Celite. The organic extracts were dried ($MgSO_4$) and the solvent removed under reduced pressure to yield (0.3 g) a colourless oily residue. The spectral data for this compound did not correspond with that expected for the
target structure.

5.2. Experimental – Physical methods

5.2.1. β-Haematin inhibitory Activity

The formation of β-haematin can be induced by non-biological conditions in the laboratory, i.e. in the absence of proteins, peptides etc. The formation is found to occur spontaneously at 60-65°C in a 0.1-8.0 M acetate solution and pH 4.2-5.0. Quinolines such as quinine, chloroquine and amodiaquine with antimalarial activity block β-haematin formation.[45]

Two assays were used to determine the β-haematin inhibitory activity (BHIA) of the target compounds synthesized for the purpose of this dissertation. First a qualitative assay was performed to establish whether the novel antiplasmodial target compounds have β-haematin inhibitory activity. Thereafter a quantitative assay was performed to establish at how many equivilants of the compounds 50% of β-haematin formation was inhibited.

5.2.1.1. Qualitative β-haematin formation inhibition assay

For this assay described by Egan *et al* [45] haematin was obtained dissolving 15 mg of haemin in 3 ml of 0.1 M NaOH. This solution was stirred in a glass titration cell connected to a bath, thermostatted at 60°C. To the solution was added 0.30 ml of 1.0 M HCl and 1.71ml of 12.9 M acetate (pH 5) pre-incubated at 60°C. The reaction mixture was removed from the cell after 30 minutes, cooled on ice for 5 minutes and filtered on an 8 μm cellulose acetate Millipore filter type SC and extensively washed with water. The solid was removed and dried over silica gel and phosphorous pentoxide for 48 hours at room temperature. This served as the blank for the experiment. In separate experiments, all compounds tested for β-haematin inhibitory activity were each added at three equivalents to haematin to the solution under the same conditions as described above. The compound was added to the reaction mixture prior to acidification. Chloroquine was used as a control in a separate experiment. Infrared spectra were obtained form discs of each dried solid (2mg) in a KBr matrix (200mg).

Infrared spectroscopy is used for the characterization of β-haematin because it discriminates clearly between haematin and β-haematin and because little material is necessary for this unlike the alternative method of x-ray powder defraction which requires approximately 200mg of sample for the equipment available. This is impractical, as the scale of synthesis of the compounds synthesized is frequently small.

Two dominant sharp peaks are observed in the infrared spectra of β-haematin in the 1700-1200 cm^{-1} region in contrast to the corresponding region in haematin spectra. The peak at 1662 ± 2 cm^{-1} is due to C=O while the C-O bond gives rise to the other peak at 1210 ± 1 cm^{-1}. These are both from the iron coordinated carboxylate group.[102]

5.2.1.2. Quantitative β-haematin inhibitory activity assay

The quantitative β-haematin inhibitory activity assay determines the number of equivalents of a compound required to inhibit 50% of β-haematin formation.

An assay recently developed by Egan and Ncokazi was used where the method described in section 1 for β-haematin formation was adapted for a small-scale reaction. The assay was kindly conducted by Mr Kanyile Ncokazi. The reaction was performed in an Eppendorf tube and the total reaction volume was kept at 50 μl. The content consisted of 30.059 μl of a 1.66×10^{-3} M haematin stock solution, 3.05 μl of a particular drug stock solution and 17.74 μl 12.9 M acetate solution, which was pre-incubated in a thermostatted bath. In this new assay 19.950 ml of pyridine solution is added to the reaction mixture after 1 hour of incubation at 60°C in a thermostatted bath. This was followed by the addition of HCl (200 μl, 0.1 M) and 500 μl chloroform to aid the extraction of haematin. The pyridine coordinates with the iron of any free haematin present in the reaction mixture and forms a pink colored complex. The concentration of this coordinated complex was measured using colorimetric visible spectrophotometry at a wavelength of 405 nm. The pyridine cannot coordinate with the iron in β-haematin. The assay was done in triplicate for compounds **11**, **12** and chloroquine which served as a control.

Instruments that were used include Crison micropH 2000 pH-meter to determine pH for which standard buffer solutions were used at pH 4.00 ± 0.02 and 7.00 ± 0.02, to

calibrate the meter before use. Eppendorf Research micropipettes were used to transfer accurate volumes. Weighing was done either with a Precisa 400 M or Sartorius scale. A Varian Cary 100 Conc UV-vis spectrophotometer was used to collect the spectral data.

The 1.66×10^{-3} M haematin stock solution was prepared by weighing Sigma-Aldrich haematin (10.845 mg, 1.66×10^{-2} mol) and dissolving it in a 0.1 M solution of NaOH, which was made up volumetrically in a 10 ml volumetric flask.

The 0.2 M HEPES buffer solution was made by dissolving Sigma-Aldrich HEPES salt (11.915 g, 0.05 mole) in less than 250 ml distilled water and adjusting the pH with a concentrated solution of NaOH to 7.50. The solution was then carried over to a 250 ml volumetric flask and made up volumetrically with distilled water.

Compounds **1**(5.6 mg, 0.01mmole), **2** (5.3 mg, 0.01mmole) and chloroquine diphosphate (8.4 mg, 0.01 mmole) were weighed and dissolved in 1.0 M HCl to yield 0.1 M solutions. Dilutions were made with 1.0 M HCl to give ten different equivalents relative to haematin in the reaction mixture, ranging from 0.5 to 10 equivalents.

Finally a pyridine solution was made by adding 50 ml of HEPES buffer solution to 100 ml of pyridine and making it up volumetrically to 1 L with distilled water.

5.2.2. pK_a determination

pK_as were determined in duplicate for compounds **1-7** by potentiometric titration [103]. Distilled water, boiled to remove any CO_2, was used to make all solutions for the titration. A 0.1003 M NaOH solution was prepared from Merck Titrisol ampoules and stored under an atmosphere of N_2 (g) in high-density glass bottles. The solution was standardized against recrystallized potassium hydrogenphthalate and used within one week of preparation or discarded. A 0.1005 M HCl solution was also prepared from ampoules and standardized against recrystallized sodium tetraborate. The compounds were weighed directly into the titration vessel (0.01-0.03 mmole) and protonated with HCl. The volume of the solution in the vessel was then made up to 20 ml with 0.15 M NaCl to ensure a constant ionic background. The titration vessel was kept under N_2 (g) and thermostatted at 25°C by means of a heated bath. The

potential of the mixture was measured by a Metrohm 6.0222.100 combined electrode. The electrode was calibrated before use by buffer solutions with pH 4.00, 6.85 and 9.18. Titration with the NaOH solution was then performed by addition of 100 increments with a Dosimat automatic burette to a total volume sufficient to pass equivalence point. The 100 data points were then analyzed using the ESTA program.[104]

5.2.3. Drug-haematin association constants

Association constants was measured by titration of a haematin solution in HEPES buffer (pH 7.5) and DMSO (40% v/v) with drug stock solutions also in HEPES buffer and DMSO. The data were fitted to a model [100] based on a 1:1 haematin drug stoichiometry.

The haematin (8 mg, 0.01mmol) stock solution was prepared in a DMSO (10 ml). Hepes buffer (pH7.5) was prepared as described in section (1). This solution was kept away from light to prevent photodegradation. A stock solution (2 mM) was prepared in eppendorf tubes for each of compounds **10-12**, **12b** and **13-16** by dissolving them in 800 μl of DMSO adding 200 μl of HEPES buffer solution and making this up in a 2 ml volumetric flask. The analyte in each cuvet before titration consisted of 4 μl of haematin stock solution, 200 μl of HEPES buffer solution, 796 μl of DMSO and 1000 μl distilled water.

The absorbance was read on a Varian Cary 100 Conc UV spectrometer at 402 nm. A stable reading was taken for the analyte before adding between twenty six and thirty three increments of increasing volume of the drug stock solution and taking a stable reading after each increment.

Instruments that were used include Crison micropH 2000 pH-meter to determine pH for which standard buffer solutions were used at pH 4.00 ± 0.02 and 7.00 ± 0.02, to calibrate the meter before use. Eppendorf Research micropipettes were used to transfer accurate volumes. Weighing was done either with a Precisa 400 M or Sartorius scale.

The data points were then analyzed using a non-linear least squares fitting program. Each titration was performed in triplicate.

5.2.4. Antiplasmodial activity

All compounds **11**,**12**,**13**,**14**,**15** and **16** were tested for antiplasmodial activity against the chloroquine sensitive D10 strain and the chloroquine resistant K1 strain of P. falciparum. Testing was done by Mr. Donnelly van Schalkwyk at the department of Pharmacology, University of Cape Town. The parasites were cultured continuously by the method of Trager and Jensen.[105] The compounds were dissolved either in methanol or ethanol and the diluted with medium to final concentrations which contained less than 1% methanol/ethanol which were found to be non toxic to the parasites. Chloroquine diphosphate was dissolved in water. Parasite lactate dehydrogenase was measured to assess antiplasmodial activity. This was done by a modified method of Makler *et al*.[106] The antiplasmodial testing was performed at 1% hematocrit and 2% parasitemia. Compounds were added at a late trophozoite stage and parasites cultured in their presence for a period of 48 Hours before lactate dehydrogenase was measured. Each IC50 value was determined in triplicate in two independent experiments.

[1] T. J. Egan, *Minirev. Med. Chem.* **2001**, *1*, 114.

[2] C. H. Kaschula, T. J. Egan, R. Hunter, N. Basilico, S. Parapini, D. Taramelli, E. Pasini, D. Monti, *J. Med. Chem.* **2002**, *45*, 3531.

[3] TDR Malaria Data Base, World Health Organisation, Geneva, **2003**. (available at http://www.wehi.edu.au/MalDB-www/intro.html

[4] Weekly epidemiological record, **1996**.

[5] W. H. Wernsdorfer, I. McGregor, *Malaria: principles and practice of malariology*, Churchill-Livingstone, Edinburgh, **1988**.

[6] M. A. Rudzinska, W. Trager, R. S. Bray, *J. Protozool.* **1965**, *12*, 563.

[7] S. E. Francis, D. J. Sullivan, D. E. Goldberg, *Annu. Rev. Microbiol.* **1997**, *51*, 97.

[8] L. Tyas, R. P. Moon, H. Loetscher, *Adv. Exp. Med. Biol.* **1998**, *436*, 407.

[9] A. U. Orjih, H. S. Banyal, R. Chevli, C. D. Fitch, *Science* **1981**, *214*, 667.

[10] H. Ladan, Y. Nitzan, Z. Malik, *FEMS Microbiol. Lett.* **1993**, *112*, 173.

[11] A. L. Tappel, *Arch. Biochem. Biophys.* **1953**, *44*, 378.

[12] T. Yasuhara, Mori, M., Wakamatsu, K., Kubo, K., *Biochem. Biophys. Res. Commun.* **1991**, *81*, 95.

[13] S. Pagola, P. W. Stephens, D. S. Bohle, A. D. Kosar, S. K. Madsen, *Nature* **2000**, *404*, 307.

[14] D. S. Bohle, P. Debrunner, P. A. Jordan, S. K. Madsen, C. E. Schulz, *J. Am. Chem. Soc.* **1998**, *120*, 8255.

[15] A. F. G. Slater, A. Cerami, *Nature* **1992**, *355*, 167.

[16] A. Dorn, R. Stoffel, H. Matile, A. Bubendorf, R. G. Ridley, *Nature* **1995**, *374*, 269.

[17] A. Dorn, S. R. Vippagunta, H. Matile, A. Bubendorf, J. L. Vennerstrom, R. G. Ridley, *Biochem. Pharmacol.* **1998**, *55*, 737.

[18] K. Bendrat, B. J. Berger, A. Cerami, *Nature* **1995**, *378*, 138.

[19] R. G. Ridley, A. Dorn, H. Matile, M. Kansy, *Nature* **1995**, *378*, 138.

[20] D. J. Sullivan, I. Y. Gluzman, D. E. Goldberg, *Science* **1996**, *271*, 219.

[21] A. Lynn, S. Chandra, P. Malhotra, V. S. Chauhan, *FEBS Lett.* **1999**, *459*, 267.

[22] C. Y. H. Choi, J. F. Cerda, H.-A. Chu, G. T. Babcock, M. A. Marletta, *Biochemistry* **1999**, *38*, 16916.

[23] T. J. Egan, W. W. Mavuso, K. K. Ncokazi, *Biochemistry* **2001**, *40*, 204.

[24] A. D. Wright, G. M. König, C. K. Angerhofer, P. Greenridge, A. Linden, R. Desqueyroux-Faúndez, *J. Nat. Prod.* **1996**, *59*, 710.

[25] T. J. Egan, H. M. Marques, *Coord. Chem. Rev.* **1999**, *190-192*, 493.

[26] L. J. Bruce-Chwatt, *Chemotherapy of malaria*, 2nd ed., World Health Organisation, Geneva, **1981**.

[27] R. G. Coatney, *Am. J. Trop. Med. Hyg.* **1963**, *12*, 121.

[28] P. Winstanley, G. Edwards, M. Orme, A. Breckenridge, *Brit. J. Clin. Pharmacol.* **1987**, *23*, 1.

[29] N. J. White, S. Looareesuwan, D. A. Warrell, T. Chongsuphajaisiddhi, D. Bunnag, T. Harinasuta, *Lancet* **1981**, 1069.

[30] R. H. Black, C. J. Canfield, D. F. Clyde, W. Peters, W. H. Wernsdorfer, in *Chemotherapy of malaria* (Ed.: L. J. Bruce-Chwatt), WHO, Geneva, **1981**.

[31] R. L. Kenyon, *Ind. Chem. Eng* **1949**, *41*, 654.

[32] A. F. G. Slater, *Pharmac. Ther.* **1993**, *57*, 203.

[33] C. A. Homewood, D. C. Warhurst, V. C. Baggaley, *Trans R. Soc. Trop. Med. Hyg.* **1971**, *65*, 10.

[34] I. W. Sherman, *Comp. Biochem. Physiol.* **1976**, *53B*, 447.

[35] G. C. Kirby, M. J. O' Neill, D. Phillipson, D. C. Warhurst, *Biochem. Pharmacol.* **1989**, *38*, 4367.

[36] P. H. Schlesinger, D. J. Krogstad, B. L. Herwaldt, *Antimicr. Agents Chemother.* **1988**, *32*, 793.

[37] C. A. Homewood, Warhurst, D.C., Peters, W., Baggaley, V.C., *Nature* **1972**, *235*, 50.

[38] A. Yayon, Z. I. Cabantchik, H. Ginsburg, *Proc. Natl. Acad. Sci. USA* **1985**, *82*, 2784.

[39] H. Ginsburg, E. Nissani, M. Krugliak, *Biochem. Pharmacol.* **1989**, *38*, 2645.

[40] D. J. Krogstad, P. H. Schlesinger, I. Y. Gluzman, *J. Cell Biol.* **1985**, *101*, 2302.

[41] F. N. Gyang, B. Poole, W. Trager, *Mol. Biochem. Parasitol.* **1982**, *5*, 263.

[42] H. Ginsburg, O. Famin, F. Zhang, M. Krugliak, *Biochem. Pharmacol.* **1998**, *56*, 1305.

[43] P. Loria, S. Miller, M. Foley, L. Tilley, *Biochem. J.* **1999**, *339*, 363.

[44] T. J. Egan, J. M. Combrinck, J. Egan, G. R. Hearne, H. M. Marques, S. Ntenteni, B. T. Sewell, P. J. Smith, D. Taylor, D. A. van Schalkwyk, J. C. Walden, *Biochem. J.* **2002**, *365*, 343.

[45] T. J. Egan, D. C. Ross, P. A. Adams, *FEBS Lett.* **1994**, *352*, 54.

[46] T. J. Egan, W. W. Mavuso, D. C. Ross, H. M. Marques, *J. Inorg. Biochem.* **1997**, *68*, 137.

[47] P. G. Bray, O. Janneh, K. Raynes, M. Mungthin, H. Ginsburg, S. A. Ward, *J. Cell Biol.* **1999**, *145*, 363.

[48] D. C. Warhurst, *Biochem. Pharmacol.* **1981**, *30*, 3323.

[49] D. C. Warhurst, *Ann. Trop. Med. Parasitol.* **1987**, *81*, 65.

[50] J. Shack, W. M. Clarke, *J. Biol. Chem.* **1947**, *171*, 143.

[51] T. H. Davies, *J. Biol. Chem.* **1940**, *135*, 597.

[52] K. Bachawat, Thomas, C.J., Surolina, N., Surolina, A., *Biochem. Biophys. Res. Commun.* **2000**, *276*, 1075.

[53] J. B. Cannon, *J. Pharm. Sci.* **1993**, *82*, 435.

[54] S. B. Brown, T. C. Dean, P. Jones, *Biochem. J.* **1970**, *117*, 733.

[55] S. R. Vippagunta, A. Dorn, R. G. Ridley, J. L. Vennerstrom, *Biochim. Biophys. Acta* **2000**, *1475*, 133.

[56] S. Moreau, B. Perly, C. Chachaty, C. Deleuze, *Biochim. Biophys. Acta* **1985**, *840*, 107.

[57] I. Constantinidis, J. D. Satterlee, *J. Am. Chem. Soc.* **1988**, *110*, 4391.

[58] H. M. Marques, K. Voster, T. J. Egan, *J. Inorg. Biochem.* **1996**, *64*, 7.

[59] I. Constantinidis, J. D. Satterlee, *J. Am. Chem. Soc.* **1988**, *110*, 927.

[60] A. Dorn, S. R. Vippagunta, H. Matile, C. Jaquet, J. L. Vennerstrom, R. G. Ridley, *Biochem. Pharmacol.* **1998**, *55*, 727.

[61] S. R. Vippagunta, A. Dorn, H. Matile, A. K. Bhattacharjee, J. M. Karle, W. Y. Ellis, R. G. Ridley, J. L. Vennerstrom, *J. Med. Chem.* **1999**, *42*, 4630.

[62] P. M. O' Neill, D. J. Willock, S. R. Hawley, P. G. Bray, R. C. Storr, S. A. Ward, B. K. Park, *J. Med. Chem.* **1997**, *40*, 437.

[63] S. J. Foote, Cowman, A.F., *Acta Trop* **1994**, *56*, 157.

[64] T. E. Wellems, *Nature* **1992**, *355*, 108.

[65] D. A. Fidock, T. Nomura, A. K. Talley, R. A. Cooper, S. M. Dzekunov, M. T. Ferdig, L. M. B. Ursos, A. b. S. Sidhu, B. Naudé, K. W. Deitsch, X.-z. Su, J. C. Wootton, P. D. Roepe, T. E. Wellems, *Molec. Cell* **2000**, *6*, 861.

[66] P. B. Macomber, H. Sprinz, A. J. Tousimis, *Nature* **1967**, *214*, 937.

[67] C. D. Fitch, *Proc. Natl. Acad. Sci. USA* **1969**, *64*, 1181.

[68] D. J. Krogstad, I. Y. Gluzman, D. E. Kyle, A. M. J. Oduola, S. K. Martin, W. K. Milhous, P. H. Schlesinger, *Science* **1987**, *238*, 1283.

[69] C. P. Sanchez, S. Wünsch, M. Lanzer, *J. Biol. Chem.* **1997**, *272*, 2652.

[70] S. Wünsch, C. P. Sanchez, M. Gekle, L. Grosse-Wortmann, J. Wiesner, M. Lanzer, *J. Cell Biol.* **1998**, *140*, 335.

[71] J. A. Martiney, A. S. Ferrer, A. Cerami, S. M. Dzekunov, P. D. Roepe, *Novartis Found. Symp.* **1999**, *226*, 265.

[72] T. G. Geary, J. B. Jensen, H. Ginsburg, *Biochem. Pharmacol.* **1986**, *35*, 3805.

[73] P. G. Bray, M. Mungthin, R. G. Ridley, S. A. Ward, *Mol. Pharmacol.* **1998**, *54*, 170.

[74] D. De, F. M. Krogstad, F. B. Cogswell, D. J. Krogstad, *Am. J. Trop. Med. Hyg.* **1996**, *55*, 579.

[75] C. Biot, G. Glorian, L. A. Maciejewski, J. S. Brocard, *J. Med. Chem.* **1997**, *40*, 3715.

[76] M. Navarro, H. Pérez, R. A. Sánchez-Delgado, *J. Med. Chem.* **1997**, *40*, 1937.

[77] S. R. Hawley, P. G. Bray, M. Mungthin, J. D. Atkinson, P. M. O' Neill, S. A. Ward, *Antimicr. Agents Chemother.* **1998**, *42*, 682.

[78] R. G. Ridley, A. T. Hudson, *Exp. Opin. Ther. Patents* **1998**, *8*, 121.

[79] K. Raynes, *Int. J. Parasitol.* **1999**, *29*, 367.

[80] K. Raynes, D. Galatis, A. F. Cowman, L. Tilley, L. W. Deady, *J. Med. Chem.* **1995**, *38*, 204.

[81] D. De, F. M. Krogstad, L. D. Byers, D. J. Krogstad, *J. Med. Chem.* **1998**, *41*, 4918.

[82] M. R. Grimmett, *Int. Rev. Sci* **1973**, *4*, 4.

[83] P. N. Preston, *Chem. Rev.* **1974**, *74*, 279.

[84] B. Chatterjee, *J. Chem. Soc.* **1929**, 2965.

[85] E. Ochiai, Katada, M., *J. Pharm. Soc. Japan* **1940**, *60*, 543.

[86] A.M. Simonov, *J. Gen. Chem. Russia* **1940**, *10*, 1588.

[87] G. R. Clemo, Swan, G.A, *J. Chem. Soc.* **1944**, 274.

[88] W. Knobloch, Schafer, H., *Journal fur practische Chemie* **1962**, *17*, 187.

[89] N. D. Heindel, Orloff, J.E., Cyrus, J.O., *J. Med. Chem.* **1969**, *12*.

[90] C. H. Kaschula, *Ph.D Thesis*, University of Cape Town, **2002**, 1.

[91] A. R. Surrey, Hammer, H.F., *J. Am. Chem. Soc.* **1946**, *68*, 113.

[92] A. R. Surrey, Cutler, R.A., *J. Am. Chem. Soc.* **1951**, *73*, 2623.

[93] W. S. Johnson, Buell, B.G., *J. Am. Chem. Soc.* **1952**, *74*, 4513.

[94] C. C. Price, R. M. Roberts, *J. Am. Chem. Soc.* **1946**, *68*, 1204.

[95] Z. Lubomir, V. Milata, D. Ilavsky, *Magnetic Resonance in Chemistry* **1998**, *36*, 681.

[96] J. R. Price, J. B. Willis, *Aust. J. Chem.* **1959**, *12*, 589.

[97] N. J. McCorkindale, *Tetrahedron* **1960**, *14*, 223.

[98] D. H. Wiliams, I. Fleming, *Spectroscopic methods in organic chemistry*, second edition ed., McGrawHill, London, **1978**.

[99] M. A. Phillips, Barlow, R.B., *J. Chem. Soc.* **1928**, 2393.

[100] W. W. Mavuso, Ph.D. thesis, University of Cape Town (Cape Town), **2001**.

[101] T. J. Egan, R. Hunter, C. H. Kaschula, H. M. Marques, A. Misplon, J. C. Walden, *J. Med. Chem.* **2000**, *43*, 283.

[102] A. F. G. Slater, W. J. Swiggard, B. R. Orton, W. D. Flitter, D. E. Goldberg, A. Cerami, G. B. Henderson, *Proc. Natl. Acad. Sci. USA* **1991**, *88*, 325.

[103] G. E. Jackson, P. W. Linder, A. Voyé, *J. Chem. Soc. Dalton Trans.* **1996**, 4605.

[104] P. M. May, Murray, K., Williams, D.R., *Talanta* **1988**, *35*, 825.

[105] W. Trager, J. B. Jensen, *Science* **1976**, *193*, 673.

[106] M. T. e. a. Makler, *Am. J. Trop. Med. Hyg.* **1993**, *48*, 739.